The Use of Remote Sensing for the Characterization of Large River Basins Issues Pertaining to Challenge Program Benchmark Basins

Prasad S. Thenkabail

Challenge Program on Water and Food

The author: Dr. Prasad S. Thenkabail is an internationally recognized expert in the area of remote sensing. He has 20 years experience in the areas of remote sensing, natural resources assessment, water resources, hydrology, agricultural engineering, GIS, and agriculture. Prasad has worked globally in East Asia (China), the Middle East (Syria), North America (United States), South Asia (Bangladesh, India, Myanmar, Nepal, and Sri Lanka), and Western Africa (Rep. of Benin, Burkina Faso, Cameroon, Cote d'Ivoire, Gambia, Ghana, Mali, Niger, Nigeria, Senegal, and Togo). He has lead many scientific investigations that include: (1) estimating carbon from biomass in African savannas and rainforests using the satellite sensor data of three eras, (2) determining optimal hyperspectral wavebands for agriculture and vegetation through studies in the semi-arid agriculture of Syria and in the African savannas, (3) inland valley characterization and mapping across West and Central Africa using Landsat and SPOT images, (4) The characterization and mapping of the alternative to the slash-and-burn benchmark research area for Africa, located in the Congo basin rainforests of southern Cameroon, and (5) modeling soybean and corn crop growth and yield using Landsat TM data in northern Ohio. He was also a member of the Indian National Drought Monitoring Mission using NOAA AVHRR data to provide near-real-time drought assessments at Nation, State, District, Taluck, and Village level.

Prasad has over 38 publications, mostly in the major international journals on remote sensing. Part of his Ph.D. research, published in the American Society of Photogrammetry and Remote Sensing, won the 1994 Autometric Award (given annually) for an outstanding publication. His research on hyperspectral remote sensing for agriculture and optimal hyperspectral wavebands for an agricultural sensor is widely recognized.

Prasad is on a scientific advisory board of Rapideye, a private German Company planning to launch advanced sensors for agricultural assessments globally. He has been a principal investigator of a major NASA funded research project. Prasad has lead the remote sensing program/activities of two International centers (International Institute of Tropical Agriculture based in Nigeria and International Center for Integrated Mountain Development based in Katmandu, Nepal). Prasad obtained a Ph.D. from the Ohio State University and has a Master's in Water Resources and Hydraulics, and a Bachelor in Civil Engineering, both from Mysore University (India). Till recently, for 6 years, he worked for a leading center of excellence in remote sensing—Center for Earth Observation, Yale University.

Currently, Prasad is employed as a senior researcher (remote sensing) with the International Water Management Institute (IWM), based in Colombo, Sri Lanka, where he leads the remote sensing efforts. This working paper is part of his work at IWMI for the Challenge Program on Water and Food.

Thenkabail, P.S. 2003. *The use of remote sensing for the characterization of large river basins issues pertaining to Challenge Program Benchmark Basins*. Colombo, Sri Lanka: IWMI. Challenge Program. CD 1

/ river basins / ecology / hydrology / irrigated farming / environment / crop yield / climate / land use / remote sensing / satellites / sensors / land cover / indicators / biomass / leaf area index / primary data / secondary data / data banks / knowledge banks / science applications / watersheds / forests / drought / benchmark basins /

ISBN

Please send inquiries and comments to: p.thenkabail@cgiar.org

Acknowledgement

I am grateful to Dr. Ania Grobicki and Dr. Jonathan Woolley, the two CPWF coordinators (one former and one present) for commissioning and providing support to work on this working paper. At various stages Dr. Hugh Turral, Dr. Francis Gichuki, and Dr. Woulfgang Flugel provided useful comments. Secretarial support from Ms. Samanmali Jayathilake is acknowledged. Special thanks to all CP benchmark basin coordinators form the nine CP basins and their RS/GIS experts in providing comments or inputs. Finally, I want to give special acknowledgement to Prof. Frank Rijesberman, Director General, IWMI, whose vision for data banks and knowledge banks is creating a framework and making this kind of work possible.

Contents

Acronyms

ALI	Advanced Land Imager
ASTER	Advanced
AVHRR	Advanced Very High Resolution Radiometer
BB	Benchmark Basins
CGIAR	Consultative Group on International Agricultural Research
CP	Challenge Program
CP BBs	Challenge Program Benchmark Basins
CPWF	Challenge Program for Water and Food
DAAC	Distributed Active Archive Center
DEM	Digital Elevation Model
EO-1	Earth Observing-1
EOS	Earth Observing System
EOS-DIS	Earth Observing System-Data Information System
EROS	Earth Resources Observation System
ET	Evapotranspiration
ETM+	Enhanced Thematic Mapper+
EVI	Enhanced Vegetation Index
FCC	False Color Composite
GB	Giga Bytes
GIS	Geographic Information System
HRV	High Resolution Visible
IRS	Indian Remote Sensing Satellite
IWMI	International Water Management Institute
LAI	Leaf Area Index
Landsat	Land Satellite
LISS	Linear Imaging Self Scanning
LP	Land Processes
LP DAAC	Land Processes Distributed Active Archive Center
LULC	Land use/ Land cover
MB	Mega Bytes
MODIS	Moderate Imaging Spectrometer
MSS	Multi Spectral Scanner
NASA	National Atmospheric and Space Agency
NIR	Near-infrared
NOAA	National Oceanic and Atmospheric Agency
RGB	Red, Green, Blue color redention
RS	Remote Sensing
RS/GIS	Remote Sensing/Geographic Information System
SPOT	System Pour l'Observation de la Terre
TB	Terra-bytes
TCI	Temperature Condition Index

TM	Thematic Mapper
TIR	Thermal Infrared
NDVI	Normalized Difference Vegetation Index
NM	New Mellennium
NPOESS	National Ploar Operational Environmental Satellite System
SAS	Statistical Analysis System
SeaWIFS	Sea wide-field Infrared Spectrometer
SRTM	Shuttle Radar Topography Mission
USGS	United States Geological Survey
UTM	Universal Transverse Mercator
VCI	Vegetation Condition Index
VIIRS	Visible and Infrared Imaging Radiometer Suite

Foreword

The Challenge Program for Water and Food (CPWF) will require high quality, large datasets, consistently over time for the 9 CPWF benchmark basins. Given the advances in modern day remote sensing, we commissioned a review to explore the possibilities of using remote sensing in CPWF river basins. As a result, we have the present working paper entitled: "The Use of Remote Sensing for the Characterization of Large River Basins: Issues Pertaining to Challenge Program Benchmark Basins."

We hope that it will be a useful contribution to work on this subject.

Dr. Jonathan Woolley
Coordinator, Challenge Program on Water and Food

The Use of Remote Sensing for the Characterization of Large River Basins

Overview

The challenge program offers a rich scope for interdisciplinary research in areas that include large river basin water resources and hydrology, ecology, change analysis related to natural and anthropogenic perturbations, agriculture, economics, inter annual land use and climate change, land degradation, and policy issues related to water use. Nine large river basins in the developing world representing a wide range of biophysical, hydrological, ecological, climatological, and socioeconomical conditions, have been selected as hot spots for a sustained research activity over the next 5 years. These river basins are (see Figure on cover page, Figures 1, 6, 8, and 9; and Table 1) Sao Francisco, Volta, Limpopo, Nile, Karkeh, Indus, Ganges, Yellow River, and Mekong.

A study of these river basins offers many great challenges that include the vastness and complexity of river basins, and the critical need for consistent sets of quantitative data on a wide range of characteristics within and across basins obtainable repetitively over space and time and at various spatial scales. Such a challenge to obtain a consistent set of dataset over time periods is only possible through satellite based remote sensing.

The needs of remote sensing data in the Challenge Program (CP) will be met by a two-fold strategy that takes into consideration issues: (1) specific to individual basins: in which datasets, methods, and approaches will be in-built to achieve science goals of thematic research arising from the proposals, and (2) common to all basins: in which stand alone research will be conducted in a manner that cuts across all basins to produce products that are of uniform standards, apply advanced and uniform methods, and produce products that are of high value to all researchers and managers working in and for the basins.

Currently, we are in an exciting era of advanced sensors, providing repeated coverage and producing high quality data products and standards using sophisticated algorithms that meet the highest scientific standards (Table 2, 6, and 7). In addition, the pathfinder projects are making historical sensor data available to today's scientific community. These data are available in primary and secondary formats. The availability of well-calibrated primary data will facilitate the production of products of specific interest to basin researchers. Much of these data are free and are available for all basins at frequent time scales and in a wide range of spatial scales (Table 3). The plans within the CP will be to use satellite sensor data from three distinct eras: (1) The Earth Observing System (EOS) era of MODIS-Terra/Aqua and Landsat-7, (2) The New Millennium era of the test of concept satellites such as Earth Observing-1 (EO-1), and (3) the older generation Landsat era. A comprehensive list of URLs for data access over Internet for basins, subbasins, and watersheds are provided in a Netscape bookmark file named bookmarks-for-basin-remote-sensing-1a.html and discussed in detail in section 4.

The primary goal of this working paper is to outline a strategy for the use of satellite sensor data for the CP Benchmark Basins (BBs) throughout the project period. The paper outlines the datasets available at different levels (basin, subbasin and watersheds), discusses data standards, addresses the capacity available in the basins and at the centers, provides an overview of data characteristics, highlights the critical applications and their implications for understanding the basins, addresses some of the technical issues, points to data sources, discusses data access, and provides a comprehensive framework for handling, analyzing, and conducting scientific research using these datasets.

1.0 Challenge Program Benchmark Basins

The challenge program (CP) currently has eight benchmark basins (Figure 1) spread across Asia, Africa, Middle East, and South America. There are seven main basins (Sao Francisco, Limpopo, Nile, Karkeh, Indus-Gangetic, Mekong, and Yellow River) and one associated basin (Volta). The CP basins are selected to specifically address the critical water and food issues of the developing world using basins, subbasins, and watersheds as a study unit.

Figure 1. The challenge program basins shown on coarsest resolution image available to us. The NOAA AVHRR 8-km data in 5 spectral bands and in NDVI (shown above) are available for 1981-2001 periods at every 10-day interval. The data of this type can play a great role in generating the historical information on river basins and for any other terrestrial applications.

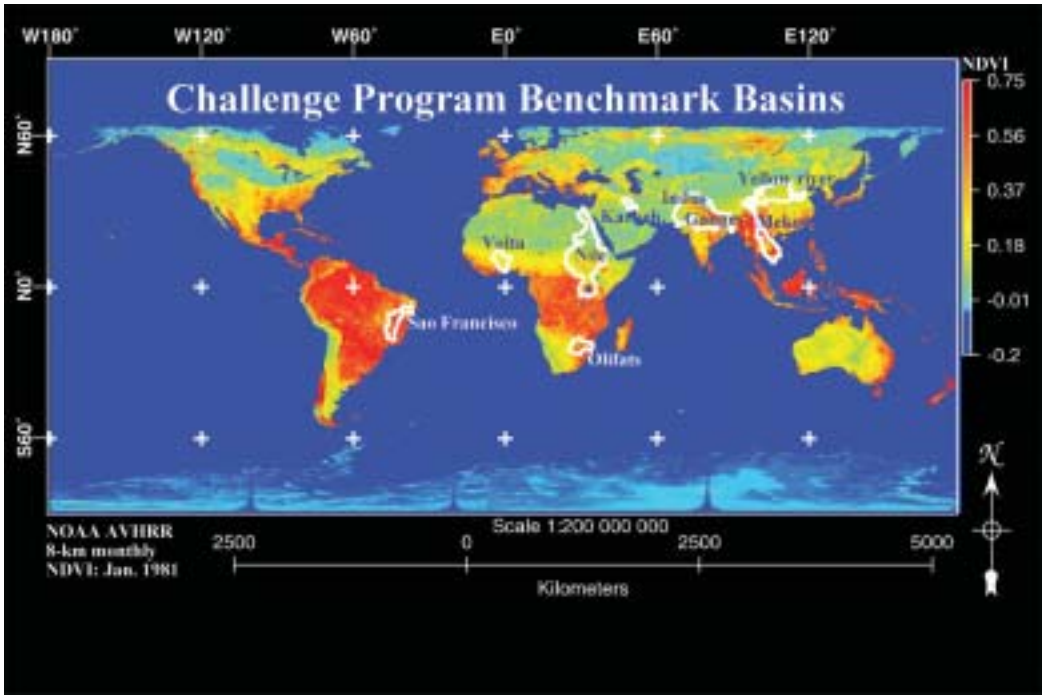

Several approaches in deriving basin boundaries were evaluated: (a) IWMI approach (GTOPO30), (b) WRI approach (ETOPO5, GTOPO30, and some digitizing from detailed Atlas), and (c) same and/or other different approaches in the basins (e.g., digitized from the topographic maps, GTOPO30). Other approaches (e.g., topographic maps, stereopair derived DEM) exist. Our outlook has been to keep basin boundaries least controversial and most consistent. An evaluation of different sources suggests that there is no one best approach (even if there is one, there are many dissenting voices). Given the above background, the final CP basin boundaries (see Figure 1 and the cover page) were selected based on: (1) boundaries provided by the basin coordinators (Virtual Andes, Mekong, Nile, Karkeh, and Sao Francisco), and (b) in absence of any basin boundary from the basin coordinators, the CP secretariat provided its own basin boundary based on GTOPO30 data (Indus, Ganges, Yellow River, Limpopo, and Volta).

2.0 The Need for Satellite Sensor Data in CP Research

2.1 General Need

The CP BBs (Figure 1 and Table 1) are spread across the globe, and the only form of data that can be consistently, timely, and repeatedly acquired and affordable for all the basins is through remote sensing from spaceborne sensors. Any other forms of data will be costly, time consuming, and are generally inconsistent. The satellite sensor data constitutes the single major source of any type of data that is currently acquired on a consistent, timely, and repeated basis for every part of the globe. Each and every CP BB is imaged every day by one satellite or the other. The present state-of-the-art of remote sensing guarantees data for every basin every 8-16 days (e.g., 8-day reflectance MODIS images shown in Figure 2 and 3) in a wide range of scales (or pixel resolutions), radiometry, bad numbers, band widths, advanced optics, and advances in algorithms and processing that lead to unprecedented quality (e.g., Figure 4). Added to this is the long-time series of archives and pathfinder datasets now becoming globally available. Much of this data is also free and accessible over Internet. Also, much of the secondary data (e.g., land use, biomass, LAI) currently

Table A1. AVHRR 8-km products

Data Product	Description	Begin Date	End Date	Preview
Tiled_8 km	Tiled time series products of the global daily composited data at 8 km x 8 km resolution.	1981-07-13 01:28:07	2000-12-31 01:45:06	Preview
Global_8 km	Global products of 10-day and monthly composited data at 8 km x 8 km resolution.	1981-07-13 01:28:07	2001-10-01 01:45:06	Preview
Global_1deg	Global 10-day and monthly composited data at 1 degree x 1 degree resolution.	1981-07-13 01:28:07	2001-10-01 01:45:06	Preview
Continental data	Continental and regional subset products of 10-day and monthly composited data at 8 km x 8 km resolutions.	1981-07-13 01:28:07	2001-10-01 01:45:06	Preview
FTP user subsets	User specified subset products of 10-day and monthly composited data at 8 km x 8 km resolutions.	1981-07-13 01:28:07	2001-10-01 01:45:06	
Reprojection Tool	Convert 10-day and monthly composited data at 8 Km x 8 Km resolution from Goodes to Equi-Angular Projection.	1981-07-13 01:28:07	2001-10-01 01:45:06	

Figure 2. MODIS 500-m data showing a subarea of Indus River basin. The Indus River command area (in red on either side of the meandering river) is a rich irrigated agricultural area seen on Day 97, 2001. The data of this type are available every 8-16 days in 2, 7, and 28 spectral bands associated with 250-m, 500-m, and 1000-m resolution for the entire globe. This is guaranteed data that has historical data going back to 1981 from its family of satellites in AVHRR to NPOESS, going into 2118.

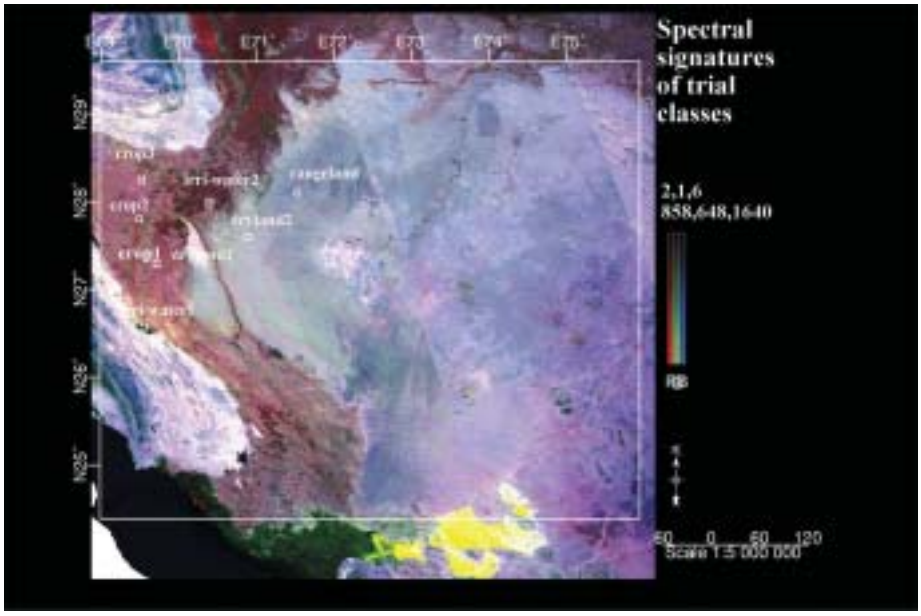

Figure 3. MODIS 500-m data shows a very small subarea of Indus River basin. This image was taken on day 265, 2002 when the kharif crop was at its peak. The data are time-composited, processed to highest level using algorithms for cloud and haze removal, and are available for download free of cost for any basin in a near-real-time basins. Further, the CP work needs datasets that facilitate comparison of results over time periods within and across basins. This is best done through the use of satellite sensor data from different eras.

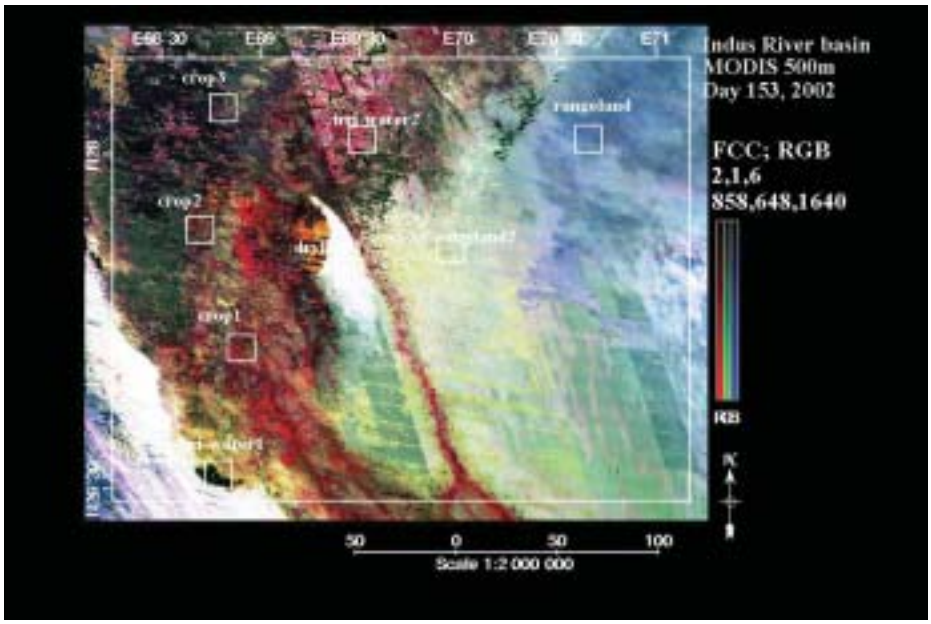

Figure 4. MODIS data highlighting great spectral detail. MODIS is acquired in 36 bands, mostly with narrow band widths providing unprecedented spectral, radiometric, and temporal resolutions with quality of production enhanced multifold as a result of high levels of processing for cloud and haze removal, and normalization for topographic, radiometric, and atmospheric effects. The image here demonstrates the quality of MODIS product by clearly showing the land link that existed between Sri Lanka and India millions of years back. The circled area is under water, but the MODIS sensor can penetrate and look through. Color key: RGB (FCC): 858 nm, 645 nm, and 1640 nm.

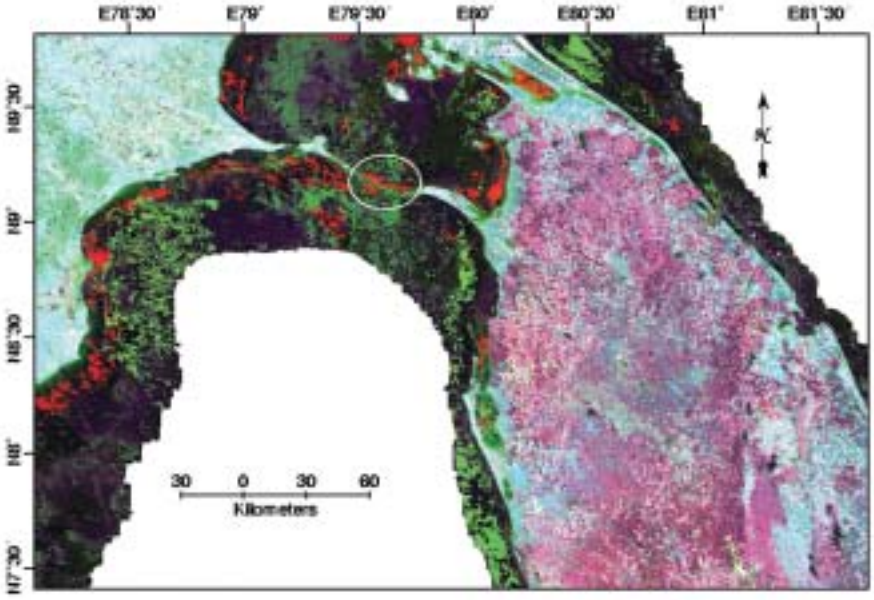

constituting the GIS datasets are derived and/or heavily dependent on some form of satellite sensor data.

Also the continuity of datasets is assured over the next decades through National Polar Operational Environmental Satellite System (NPOESS) series of missions, which will succeed the current polar operational capabilities of the NOAA series of satellites (Figure 5). NPOESS carries Visible and Infrared Imaging Radiometer Suite (VIIRS). Prior to NPOESS, the NPOESS Preparatory Project (NPP) will be launched, acting as a bridge between the two MODIS instruments and the longer term advanced operational capability (Townshend and Justice, 2002).

2.2 Specific Needs of CP Thematic Research for Use of Remote Sensing Tools

The CP work in the benchmark basins (BBs) consists of five major themes ((see CP full proposal): (1) Crop-water productivity improvements, (2) Multiple use of upper catchments, (3) Aquatic ecosystems and fisheries, (4) Integrated basin water management systems, and (5) Global and national food and water systems. The CP is a partnership between five CGIAR centers, six NRAES, four ARIs, and three International NGOs.

Each of these themes will have a wide range of issues for which remote sensing data will be fundamental. In general, the RS datasets will be analyzed to produce “products” for decision support (DS) in Integrated Management of basins. Historical time series images will be combined with near real time images for continuous analysis and modeling of biophysical quantities and landform transformations. The remote sensing data will also be the primary source of secondary GIS data of many types (e.g., Figure 6). What is of critical importance and of great value to CP BB research

Figure 5. The AVHRR-MODIS-VIIRS transition schedule ensuring guaranteed data for the near future. Use of these consistent data in the large river basin studies will be invaluable for a number of applications. The oblique lines between sensors arise from the estimated uncertainties in its life. The NPOESS satellites have expected lifetime of 5 years. (Nelson and Cunningham 2002; Townshend and Justice 2002)

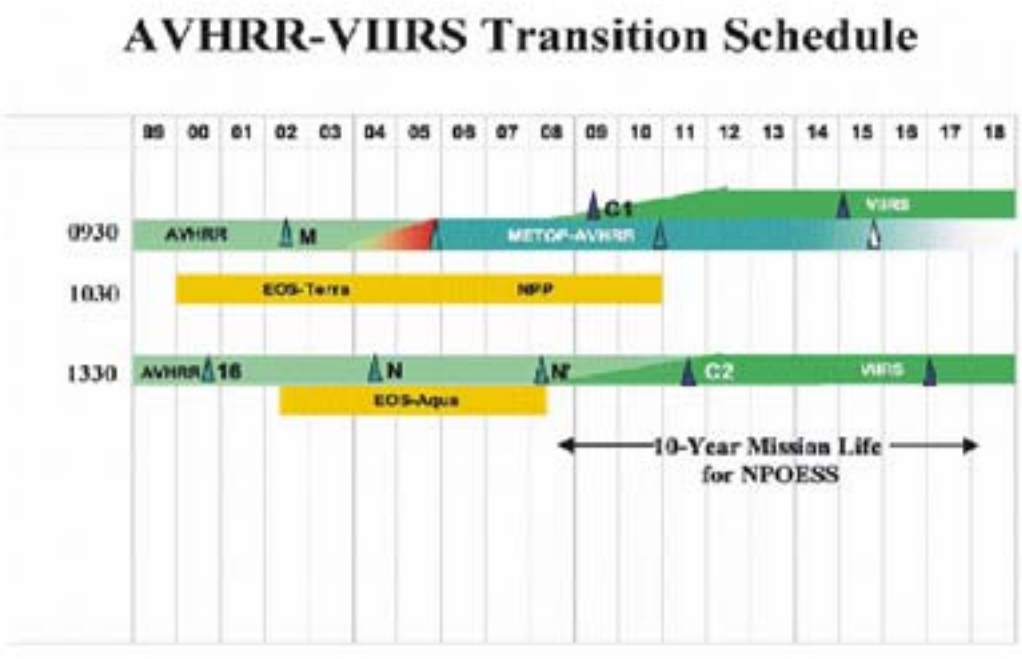

agendas will be in the feasibility of using satellite sensor data in many different scales or pixel resolutions over repeated time periods that were hitherto unimaginable. Many applications are anticipated. These applications will include: (1) Basin performance evaluations throughout the project duration in terms of factors such as change magnitude and its spatial distribution, change vector analysis, and land degradation, (2) Land use / land cover (LULC) change and dynamics within and between seasons that will provide input to hydrological models of the basins (3) Quantitative biophysical models of leaf area index (LAI), and biomass that are useful inputs to crop models, (4) Crop types and/or growth stages that help determine yield, productivity, and consumptive use (CU) of water, (5) Quantitative geomorphologic parameters (e.g., drainage density, drainage frequency, and watershed shape) that have implications in predicting floods, (6) Normalized difference vegetation index (NDVI) progression as a drought indicator within and between seasons, and (7) Rainfall pattern and spatial variability.

Figure 6. Secondary 1-km DEM data for basins. Illustration of a typical secondary DEM dataset for the basins. The secondary datasets are generated by various groups, by processing primary datasets. Secondary datasets are also used in conjunction with primary datasets, for example, for improved classification accuracies or spatial modeling.

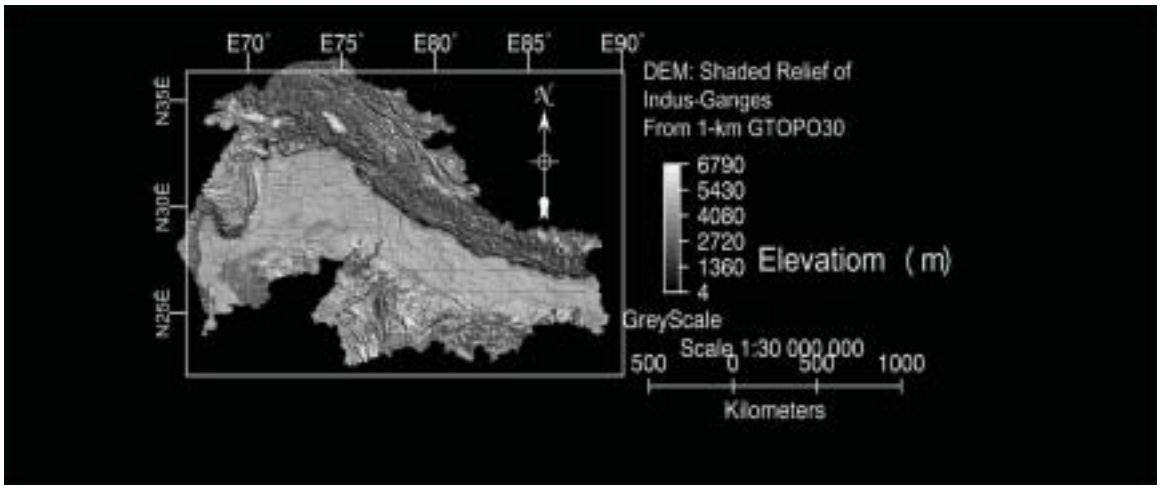

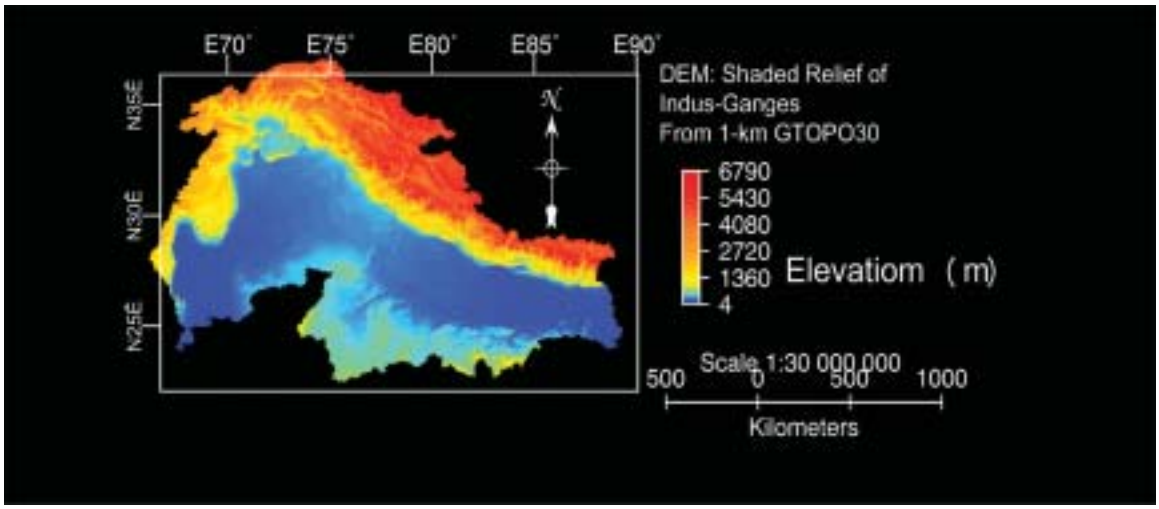

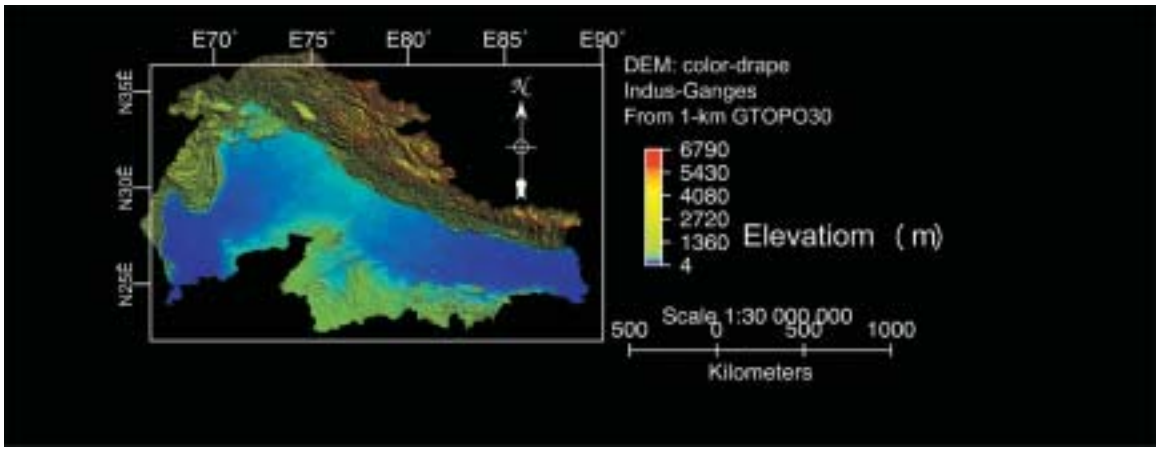

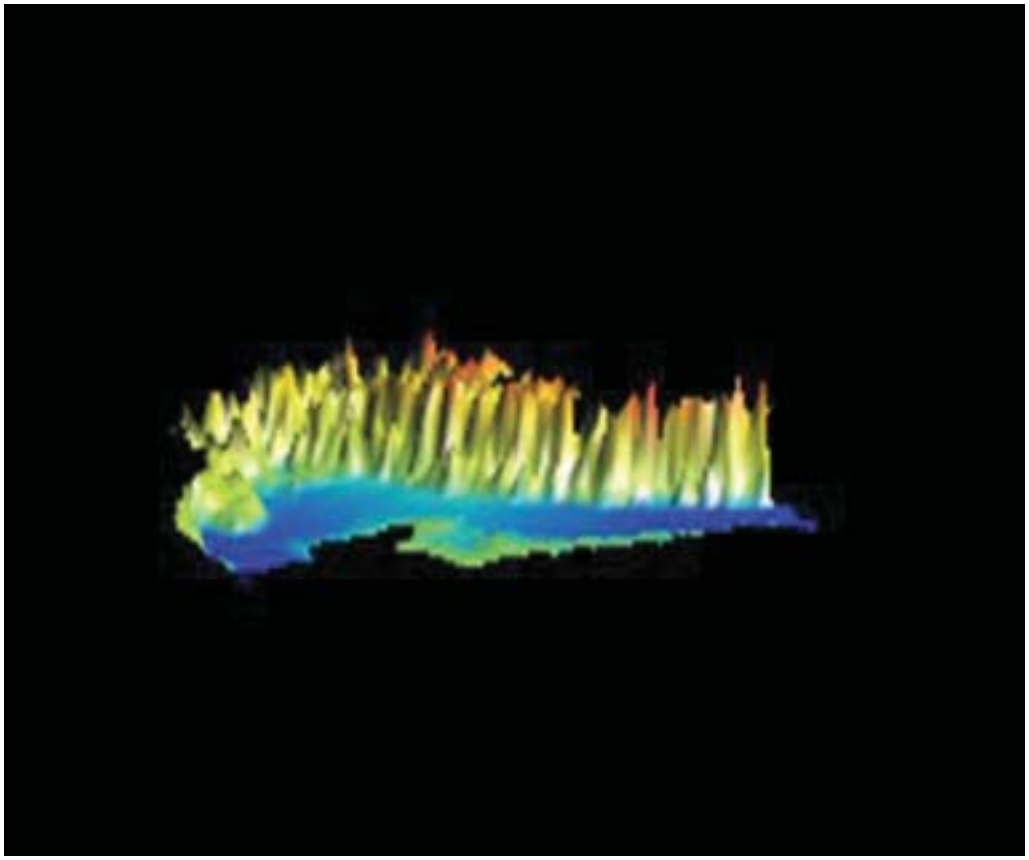

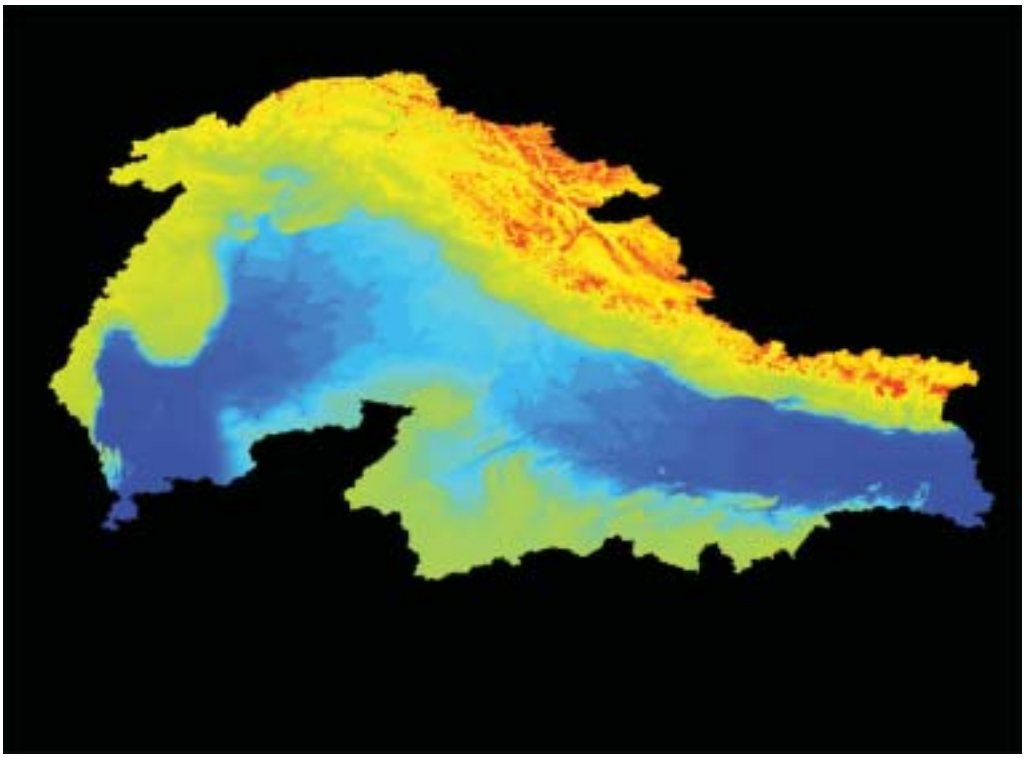

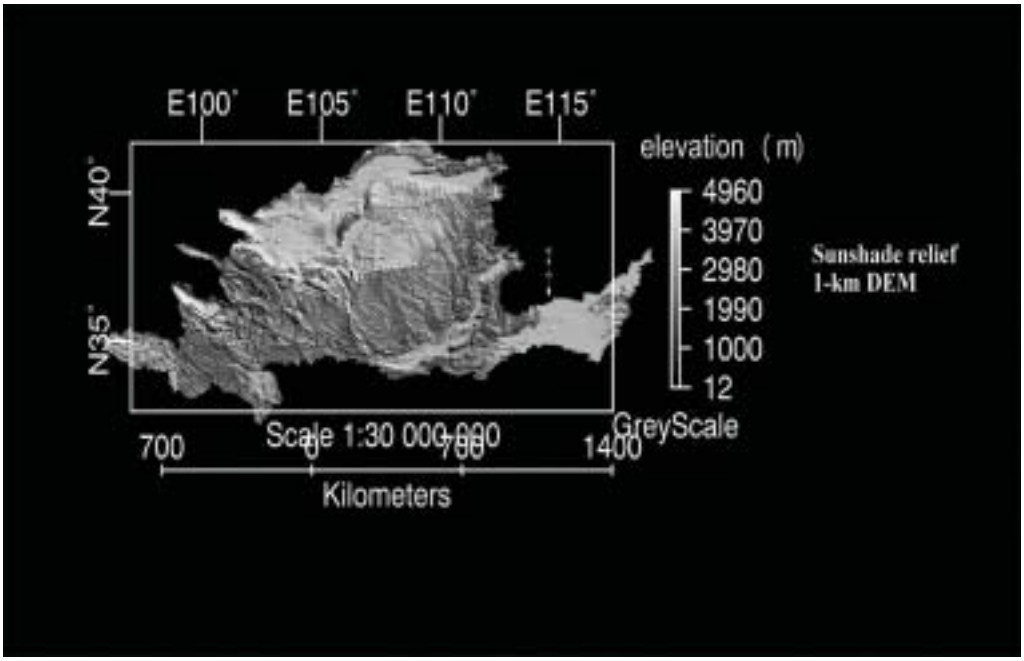
E100°
E105°
E110°
E115°
N40°
N35°
elevation (m)
4960
3970
2980
1990
1000
12
GreyScale
Sunshade relief
1-km DEM
Scale 1:30 000 000
700
0
700
1400
Kilometers

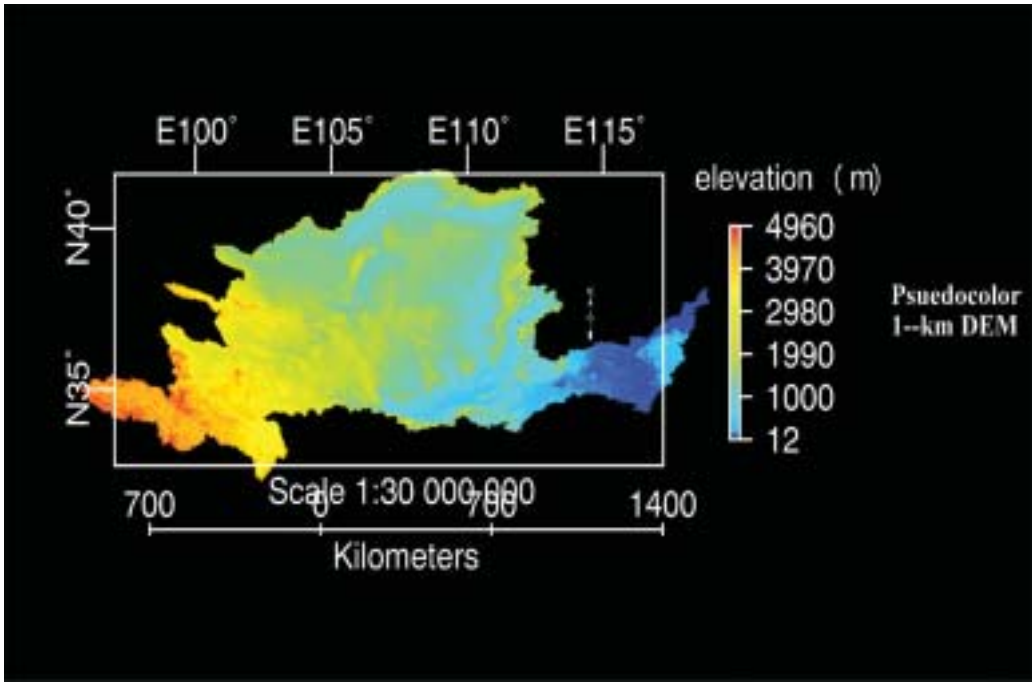
E100°
E105°
E110°
E115°
N40°
N35°
elevation (m)
4960
3970
2980
1990
1000
12
Psuedocolor
1--km DEM
Scale 1:30 000 000
700
0
700
1400
Kilometers

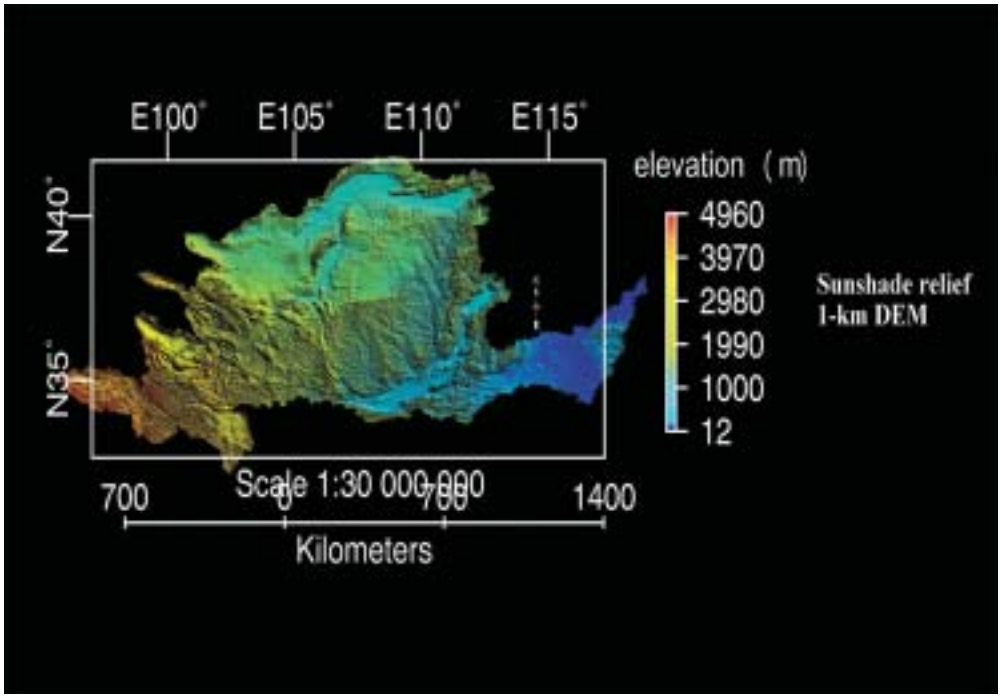

3.0 Remote Sensing Datasets from Different Eras Available for Benchmark Basin Characterization

Overall, the remote sensing data can be organized into four broad levels that have different values and implications in the study at basin, subbasin, and watershed level. The datasets currently available at IWMI for the four levels are mentioned in Appendix 1. Use of these high quality RS datasets across benchmark basins, will go a long way in providing high quality inputs to your hydrological, biophysical, and socioeconomic models and decision-making tools.

This is an era of advanced sensors that can provide data for basin research at a wide range of scales. Three distinct eras characterize satellite sensor data: (1) Earth Observing System (EOS) era, (2) New Millennium (NM) era, and (3) Historical time series era of observations of last three decades that have lead to the pathfinder datasets of AVHRR and Landsat. Most of these datasets are free of cost. The Moderate Resolution Imaging Spectroradiometer (MODIS) sensor, for example, is providing a series of products of unparalleled quality and sophistication (Figure 2 to 4) for the observation and biophysical monitoring of the terrestrial environment (Townsend and Justice, 2002) that is ideal for basin level work.

Each one of these datasets has a key role in study of terrestrial issues based on their unique spatial, spectral, radiometric, synoptic characteristics, and acquisition periods (Figure 7). A wall to wall coverage of the globe at 8-km and 4-km is available for every 10-day and monthly composites for the 1981-2001 period from the NOAA AVHRR system. These data provide a historical background for the MODIS 8-16 day time composites at 250-1000 meter and in 2 to 28 bands. A three-decade long archive also exists at a much finer spatial scale of 30 to 80 meters, from Landsat family of satellites (MSS, TM, and ETM+). These data do not have the same time series strength of the AVHRR-MODIS, but have greater regional value. However, wall to wall coverage of the globe from the two epochs (1990s and 2000s) have also the advantage of orthorectification resulting

Figure 7. Characteristics of three of the most advanced sensors at three distinct scales or pixel resolutions. Modern era sensors-coarse spatial resolution with high temporal frequency or high spatial resolution with low temporal frequency. Images are all displayed in false color composite (red = 850 nm, blue = 650 nm, blue = 555 nm) of MODIS, ETM+ and IKONOS imagery (Morisette et al. 2002).

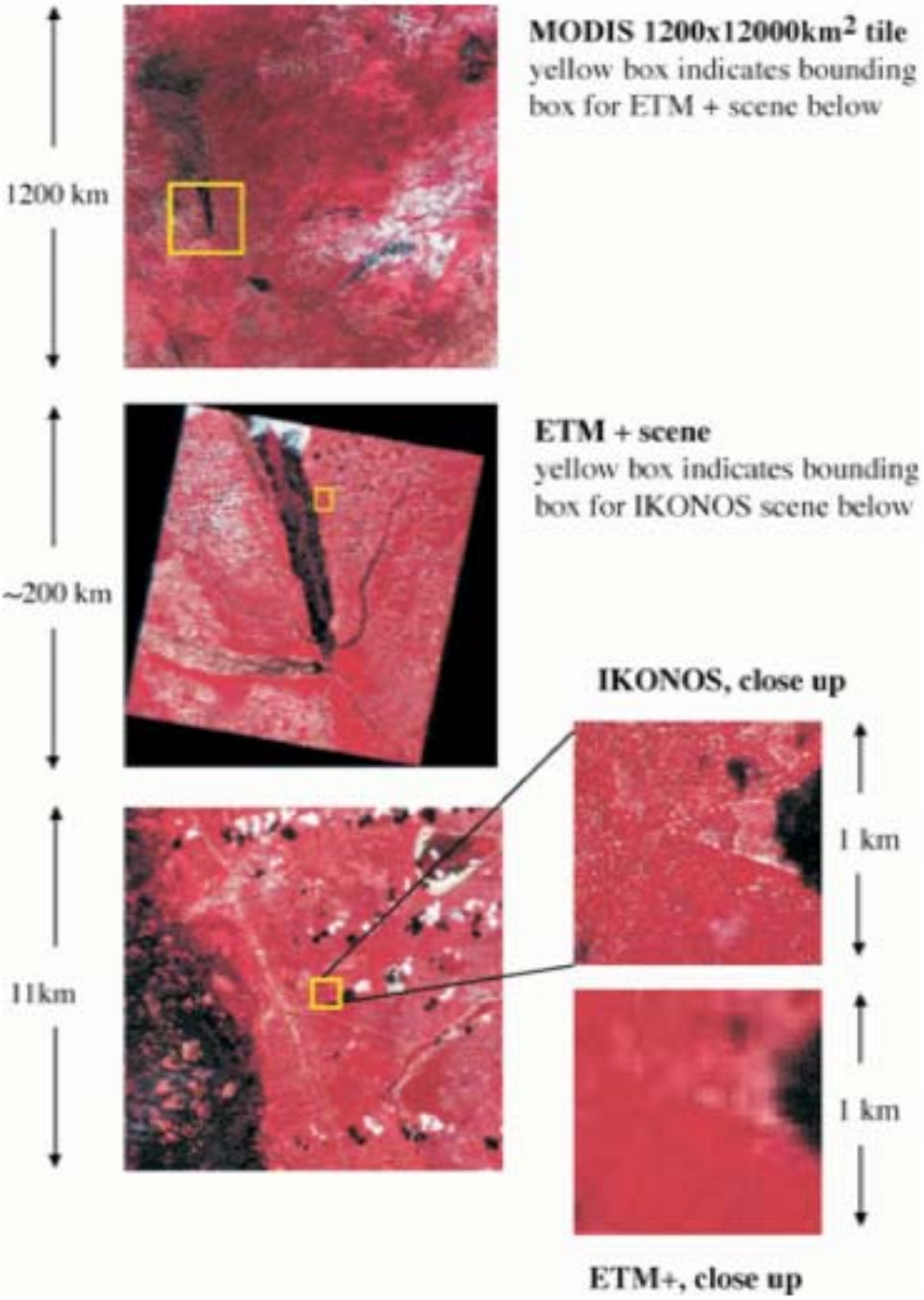

in wide use of these data as base maps with specific use of: (a) rectifying all other spatial datasets to these base images, and (b) ground truthing use.

The most recent advances are in high-spatial and high-spectral resolutions. The EO-1 is launched as a test of concept satellite, and carries two advanced sensors-hyperspectral Hyperion with 220 bands in 400 to 2500 nanometers and ALI with 10 bands, each at 16-bit considered the next generation Landsat system that is cheaper and better. The private industry has made rapid strides in the sub-meter to 4-meter panchromatic and multispectral sensors with launches of IKONOS and Quickbird-2 sensors.

3.1 Basin Level

The use of remote sensing data is anticipated in many CP research themes.
At basin level, a wall-to-wall rapid quantitative assessment of all CP BBs will be performed at 30 meter to 8 kilometer pixel scales (or resolutions) using advanced MODIS-terra/aqua data from the Earth Observing System (EOS) era of sensors from the recent years, long-term NOAA AVHRR time-series data over the last two-decades, and at more finer resolution using the pathfinder Landsat datasets such as the geocover products.

Almost all of these data are available at IWMI headquarters and can be shared (a mechanism needs to be worked out). What is required is to delineate these datasets for precise basin boundaries (Figure 8). A number of secondary data such as IGBP LULC, USGS LULC, MODIS LULC are also available in ERDAS Imagine formats for the entire globe at 1-km resolution (Figure 8). These data sets form the basis of a first level understanding of benchmark basins. A much higher resolution basin boundaries at 30-m are developed using Landsat Geocover products (Figure 9).

3.2 Subbasin Level

For more detailed characterization at regional and local scales, we will relay on high spatial resolution data such as ASTER, ETM+, and older TM, MSS, IRS. These have nominal costs (about 60 dollars for 3600 KM^2 of ASTER). Many of these data can also be freely shared (e.g., ETM+) between partners, but we need to set up mechanisms. At 30-meter or lower resolutions we can extract detailed features such as the basin drainage systems (Figure 10; Thenkabail and Nolte 1995).

3.3 Watershed Level

For detailed assessments and modeling of the landscape, there is a definitive need for use of Hyperspectral (e.g., Hyperion and Spectroradiometer), hyperspatial (e.g., Quickbird and IKONOS), advanced multi-spectral (e.g., ALI and ETM+), and historical images (e.g., AVHRR and Landsat TM) to quantify and model spectro-biophysical relationships at different scales or pixel resolutions, radiometry, bandwidths, and time of acquisitions. A suite of hyperspectral and multispectral indices will be evaluated to model crop growth, yield, biomass, LAI, and crop moisture. As a result wavebands and indices that are best in explaining spatial variability due to crop types, growing conditions, and management practices will be identified.

At local scales, Quickbird-2, IKONOS-2, IRS-1C/1D, and SPOT are available and one may consider a minimal use of these for highly detailed work (e.g., Figures 11-13). But these are generally very costly (about $10,000 for 100 KM^2 of IKONOS) and may have data copyrights that may restrict their use.

Figure 8. The seven key challenge program (CP) benchmark basins (BBs) at 1-km pixel resolution. he LULC classes are derived from the work using NOAA AVHRR data for April, 1992-March, 1993.

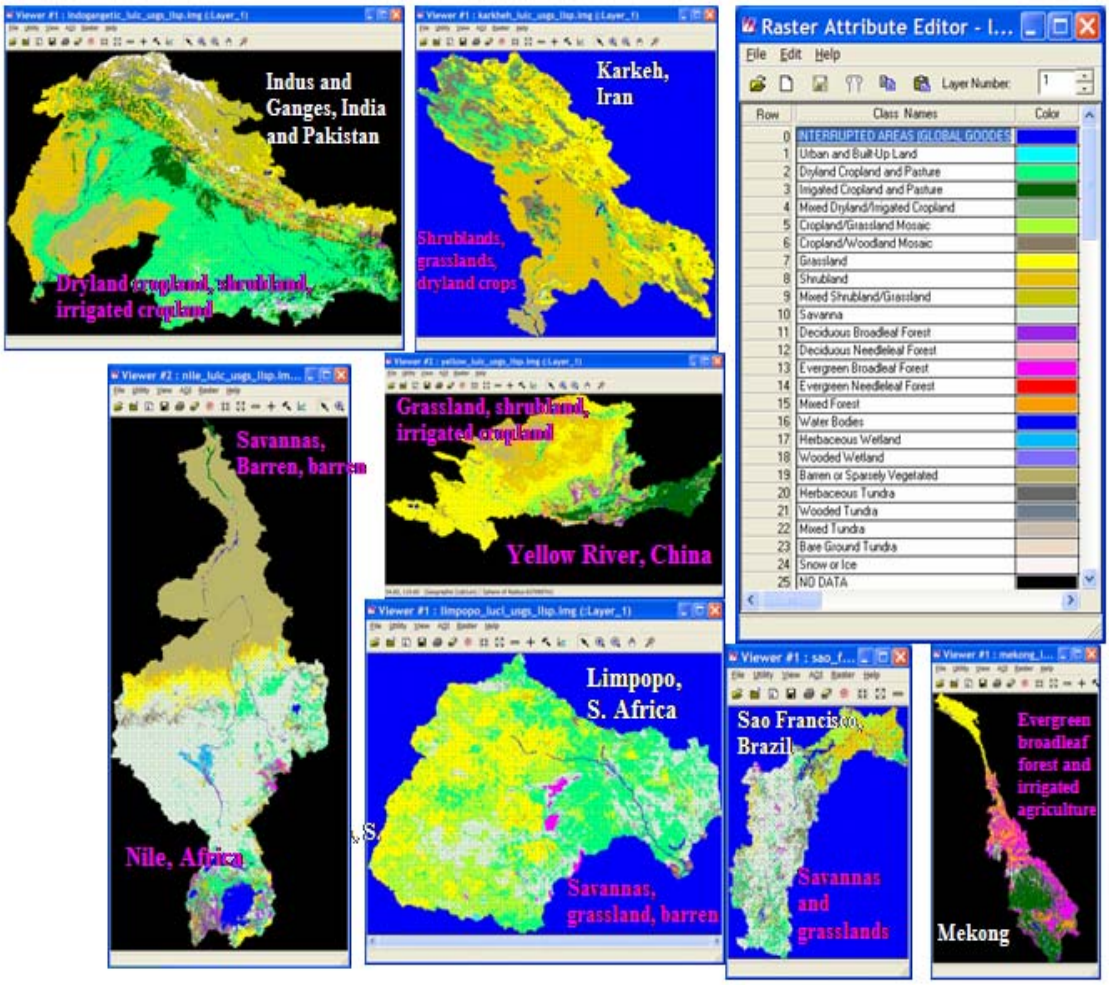

Figure 9. The Indus River basin delineated using 30-m Landsat TM mosaic. Color key: RGB (FCC): 7,4,2. The basin is derived off Landsat 3-band Geocover mosaic of the globe for 1990s. This is invaluable data as: (a) base map and (b) orthorectified image.

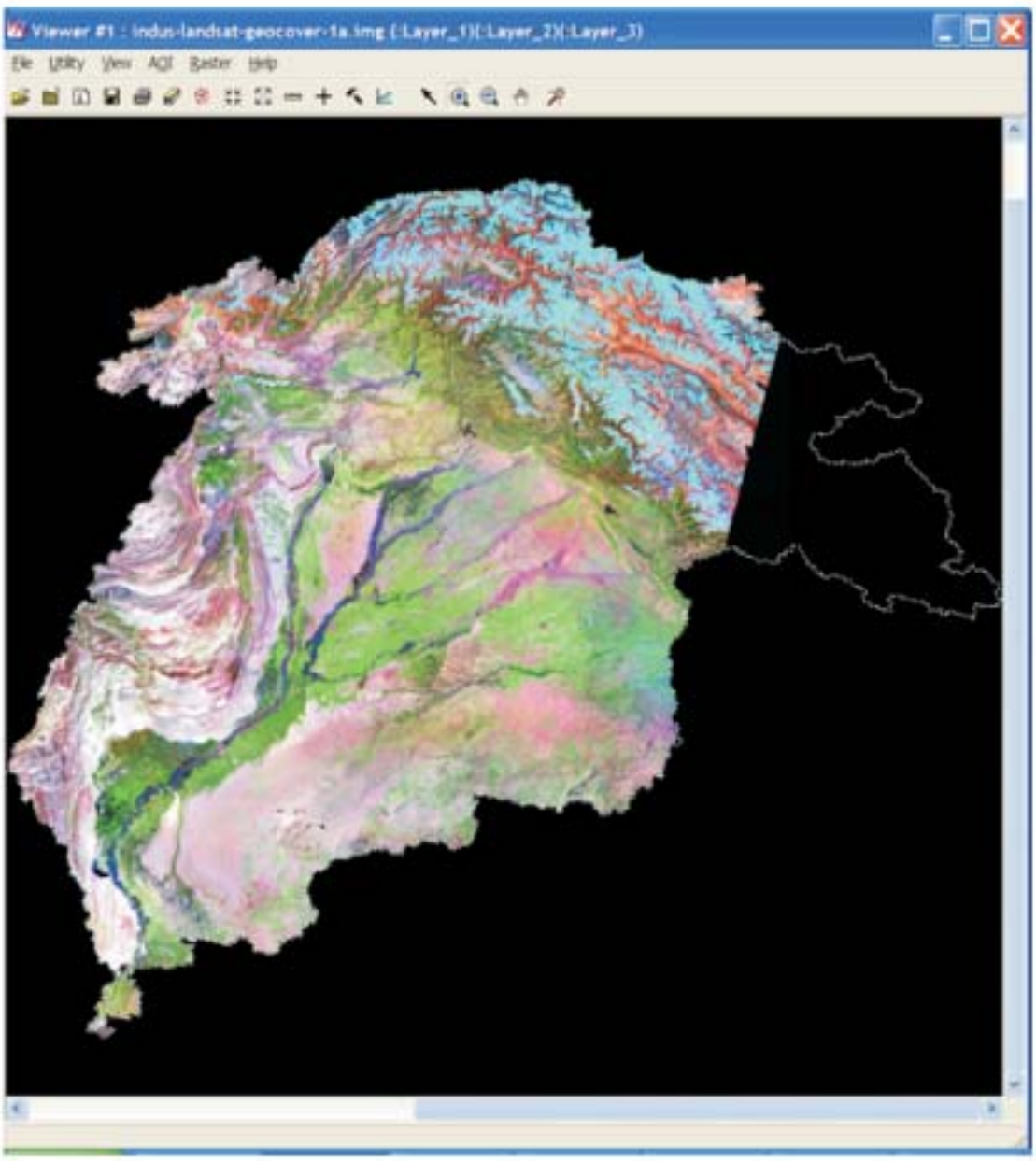

Figure 10. Subbasin level specific studies are conducted using medium resolution datasets such as SPOT ..HR 20-m data. The above image is a subbasin in Volta basin. SPOT HRV 30-m image was used to delineate stream network. Color key: RGB (3,2,1) of SPOT HRV.

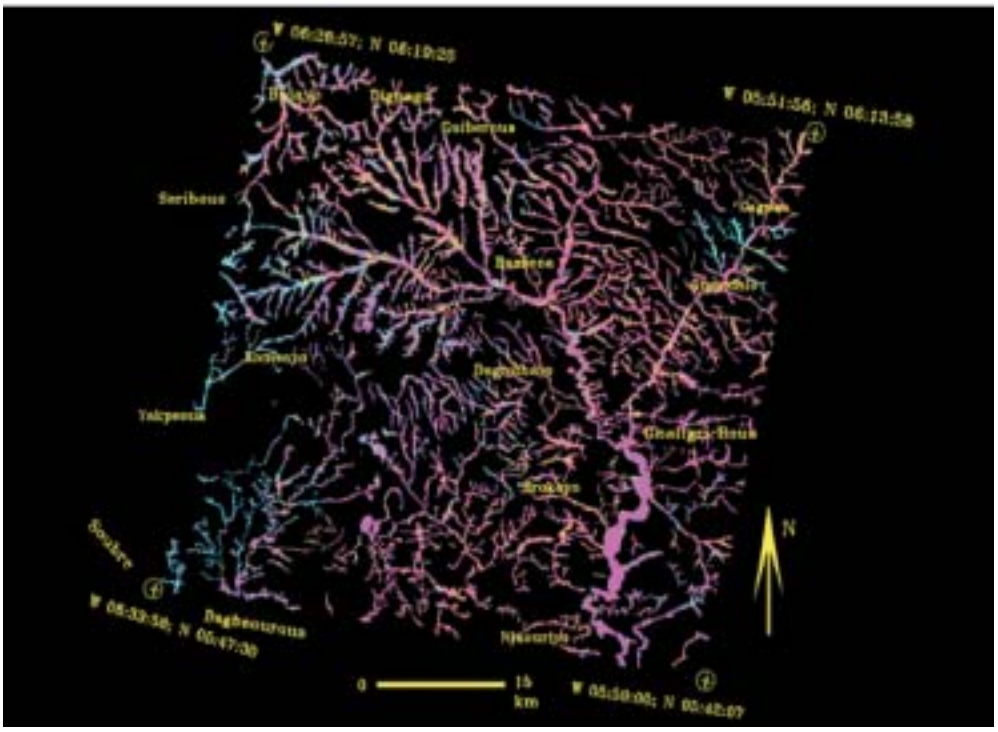

Figure 11. IKONOS 4-m data for watershed level studies. The image is in Karkeh River basin, Iran, covering the ancient historical city of Susa. Color key: RGB (FCC): 4,3,2. Data fusion technique involving the fusion of IKONOS multispectral 4-m and panchromatic 1-m.

Figure 12. Delineation of a settlement in Karkeh River basin using IKONOS 4-m data. NDVI threshold was used to delineate the settlements from the surroundings, which are intensely irrigated agricultural areas. Since most fields had crops, it became easier to delineate farmland from settlements.

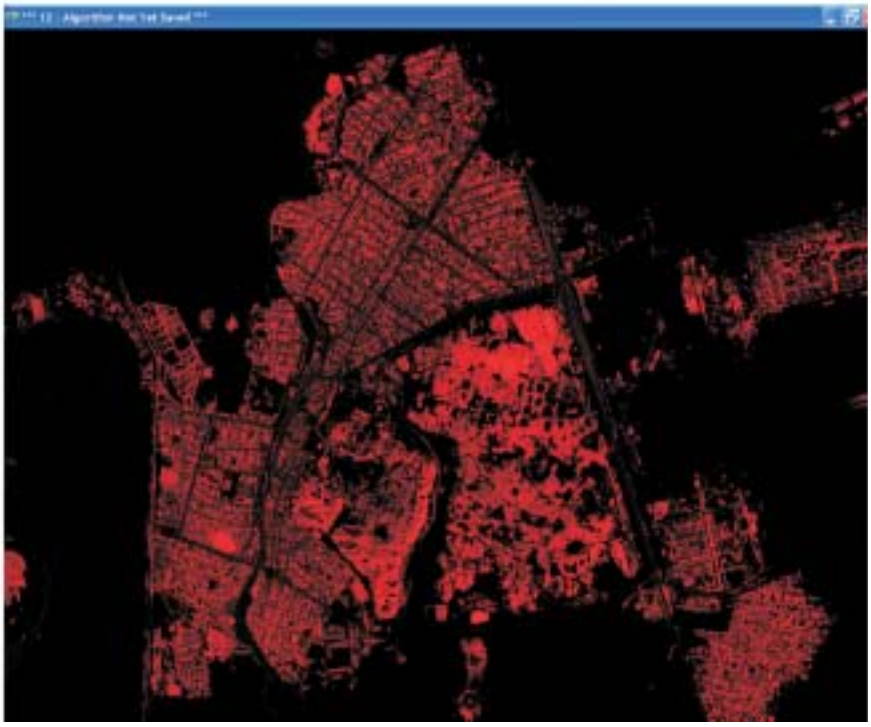

Figure 13. Delineation of farmlands from surrounding landscapes. Most farms had crops and were at vegetative growth stage. A threshold NDV> 0.4 is all irrigated farmlands and shown in red. The surrounding landscape is either barren or settlements, and is easily differentiated.

4.0 Data Access, Exchange, Handling, Metadata, and Data Analysis Strategy

The need for a centralized archive of RS/GIS at IWMI has been well established. The data exchange and sharing mechanisms between the CP BBs and the central facility at IWMI must be well established. A specialized workshop at the beginning phase of the thematic research will be required for a smooth and well understood flow of data and products both ways (from IWMI to BBs and vice versa).

- Cataloguing and archiving data products
- Data exchange formats and procedures

  Between IWMI, other CG centers, and CP basin partners at National level

  Flow both ways
- Data transfer modes
- Methods and procedures in analyzing data
- Data analysis techniques
- Producing the final products
- Validation
- Accuracy assessments

4.1 Standardizing Products and Publications

- Define and produce final products
- Set standards for the products
- Produce deliverables
- Distribute the deliverable digital products
- Create demonstration and visualization tools
- Publish a book and CDs compiling the work in the benchmark
- Peer-review articles

5.0 Remote Sensing and GIS Data and Information for the Challenge Program Benchmark Basins

The sources of data access have been organized for basin, subbasin, and watershed levels. This organization is indicative of the main use of data at levels and scales. However, many of the data useful at one level is also often useful at another level. Much will depend on how the user manipulates, analyzes, and utilizes the data. Different levels and types of processing will be required to obtain information at different levels and scales using the same data.

Under each category, primary and secondary data source links are identified separately. The primary data refers to satellite sensor data that have in physical units (e.g., radiance, reflectance, and digital numbers) that can be processed to obtain a wide range of information (e.g., land use and biophysical quantities). In contrast, the secondary data are processed data and are available as products that have little or no option for user modifications or interpretations.

5.1 Basin Level Data

The typical pixel resolution (or scales) of basin level data are between 250-1,000 meters. These are extremely useful to cover large areas, repeatedly. Also, such data have excellent time series archives that make these data attractive at basin level. Landsat type data are also suitable, but will require greater resources to handle and analyze.The sources listed and discussed are to provide a balance of using these multifaceted data.

5.1.1 Primary Data

The primary data at the basin level are from the advanced as well as historical time series satellite sensors. The web links to these data sources are provided in Figure 14.

5.1.1.1 *MODIS*

Taking into consideration the advanced nature of the datasets, wall-to-wall coverage of the basins, high frequency of availability every 8-16 days, high level of processing with time composited imagery, and availability of imagery free of cost have made the MODIS imagery the most attractive single dataset that is a must for all CP BBs. The MODIS data are acquired using two satellite systems (Terra and Aqua). Currently, the data are in level three (radiometrically, geometrically corrected and girded) and version four (V0004). The V004 is validated data, for which the product uncertainties are well defined over a range of representative conditions. The MODIS instrument collects data in 250-1,000 meter, 12-bit, and in 36 spectral bands over 0.4 μm to 14.4 μm wavelength. The custom tailored products include:

1 250 m 2-band reflectance data,

2 500-m 7-band reflectance data,

3 1,000 m, 29 band reflectance data, and

4 NDVI and EVI products.

Also available are NDVI and EVI products. All data products are available for the entire globe every 8-16 days and are downloadable as 1,000 km by 1,000 km Integerized Sinusoidal grids (Figure 15; http://modis-land.gsfc.nasa.gov/mod09/html/integerized_sinusoidal_grid.htm). MODIS data for basins are downloaded from EROS Land Processes Distributed Active Archive Center (LP DACC) site (see under MODIS in Figure 14) based on specific tiles (Figure 15) you are interested for your basin. Specific products and their descriptions can be obtained from MODIS Reflectance, NDVI, EVI product web sites, MODIS Land Discipline Web site, Boston University Climate and Vegetation Research Group, and MODIS Terra and Aqua home pages.

5.1.1.2 *AVHRR*

The 8-km and 0.1 degree AVHRR 10-day and monthly time series data are available for 1981-2001 periods for all basins, continents, as well as for the entire globe (Figure 16, Table A1). The data include: NDVI, Band 1 (red), Band 2 (NIR), Band 4 (TIR1), and Band 5 (TIR2). These data are downloadable via ftp sites (see Figure 14 for links) for relevant basin tiles (Figure 16). A nice feature is to reprove data to projection of interest before downloading.

The AVHRR data provides an excellent historical time-series link to advanced sensors of modern era such as MODIS-Terra/Aqua, and SPOT Vegetation.

Long time series, georegistered (Level 1b) single scene 1-km AVHRR data is not free and can be obtained for the basins according to user-specified parameters such as projection, resampling method, and pixel size from EROS LP DAAC. The process involves: (1) Conduct a search on Earth Explorer in order to preview scenes and obtain scene IDs, (2) Complete the AVHRR Georegistered Processing Form (Download Adobe Acrobat Reader), and (3) Fax or mail the form to USGS customer service. This data is worth pursuing only if long time series at this scale is a must and there are considerable resources for data management.

5.1.1.3 *Landsat Data and Mosaics of the Globe for 1990s and 2000s*

A “wall-to-wall” coverage of the orthorectified images of the basins are available from Landsat TM (circa 1990) at 28.5 m. Currently, Landsat ETM+ (circa 2000) at 30 m are also becoming available. These data for all Landsat TM or ETM+ bands can be downloaded from EROS LP DAAC (URL in Figure 14). The earlier era Landsat MSS data, composited for 1972-1979, are also available for the Globe. These data are produced under GeoCover program, sponsored under NASA’s Scientific Data Buy program, and has been designed to create a geodetically accurate digital database of images covering the entire earth’s land mass. The EarthSat Corporation was contracted to produce these data for NASA.

A useful by-product of this project was the creation of the image mosaics of the entire globe in false-color composites of 7, 4, and 2 for the Red, Green, and Blue layers. The images are created from 12 to 15 Landsat TM images using bands. The raster cell resolution is 28.5 meters and the horizontal positional accuracy is less than 50 meters. The scenes are segmented into tiles of approximately 250,000 square kilometers. Each tile covers 5 degrees of latitude and 6 degrees of longitude. The scenes are identified by Universal Transverse Mercator (UTM) zone and minimum latitude of the tile. The mosaic tiles are approximately 50 MB each and can be downloaded from the NASA website for MrSid image mosaics. The tiles are identified by the hemisphere, N (north) or S (south) and UTM zone (range from 01 to 60), and the minimum latitude of the 5 degree span of the tile. Much of the Indus River basin will be covered by N-42-25, N-42-30, and N-43-30 (see Figure 17).

Figure 14. Internet access to sources of basin level primary remote sensing data.

data	
s: 250-1000m; 2000-current	
ODIS Data Products (9, 12, 13): Reflectance, NDVI, EVI	http://edcdaac.usgs.gov/modis/dataprod.html
ODIS Land Discipline Web Site: Reflectance, Land cover	http://modis-land.gsfc.nasa.gov/
ODIS LAI and FPAR: Research at Boston University	http://cybele.bu.edu/modismisr/index.html
ODIS Terra Home Page	http://modis.gsfc.nasa.gov/
ODIS Aqua Home Page	http://eos-pm.gsfc.nasa.gov/
DAAC of EROS: ASTER, MODIS, Landsat	http://edcdaac.usgs.gov/main.html
r: 1-8 km and 0.1 degree; 1981-2001	
VHRR 8-km and 0.1 degree Data Access:GSFC	http://daac.gsfc.nasa.gov/data/dataset/AVHRR/
VHRR 8-km and 0.1 degree Gridded FTP Data Products	http://daac.gsfc.nasa.gov/data/dataset/AVHRR/01_Data_Products/04_FTP_Products/index.html
VHRR 1-km 10-day composite	http://edcwww.cr.usgs.gov/landdaac/1KM/comp10d.html
VHRR 1km.html	http://edcwww.cr.usgs.gov/landdaac/1KM/1kmhomepage.html
sat TM and ETM+ mosaics: 28.5 m-30 m; 1990s, 2000s	
SA web site for MrSid image mosaics: for 1990s	http://zulu.ssc.nasa.gov/mrsid/mrsid.pl
ndsat TM mosaics of globe: 1990s	http://www.geocover.com/
ndsat TM Geocover product from Earthsat: 1990s	http://www.geocover.com/Stock_Scenes.htm
ndsat ETM+: BSRSI Landsat ETM+ 2000s	http://www.bsrsi.msu.edu/
AAC, EOSDIS, Earth Explorer: Master storehouse of Imagery; 1960s-curr...	
nd DAAC: source of all land based remote sensing	http://edcwww.cr.usgs.gov/landdaac/
rthExplorer: aerial photos, satellite images including EO-1	http://edcsns17.cr.usgs.gov/EarthExplorer/
DAAC Products	http://edcdaac.usgs.gov/order.html
ROS home page	http://edcwww.cr.usgs.gov/eros-home.html
DSPSO Homepage	http://eospso.gsfc.nasa.gov/
: 90 m DEM for the Globe from space shuttle: release 2003-04	
tm: Shuttle Radar Topography Mission	http://www.jpl.nasa.gov/srtm/
he NASA/JPL Imaging Radar Home Page	http://southport.jpl.nasa.gov/
ifs global terrestial and sea data: 1000 m; 1998-current	
eaWiFS Project - Homepage	http://seawifs.gsfc.nasa.gov/SEAWIFS.html

Figure 15. Grid tile (path/row) reference map for MODIS 500-m or 250-m data. The circled area is for the Ganges and the Indus River basins.

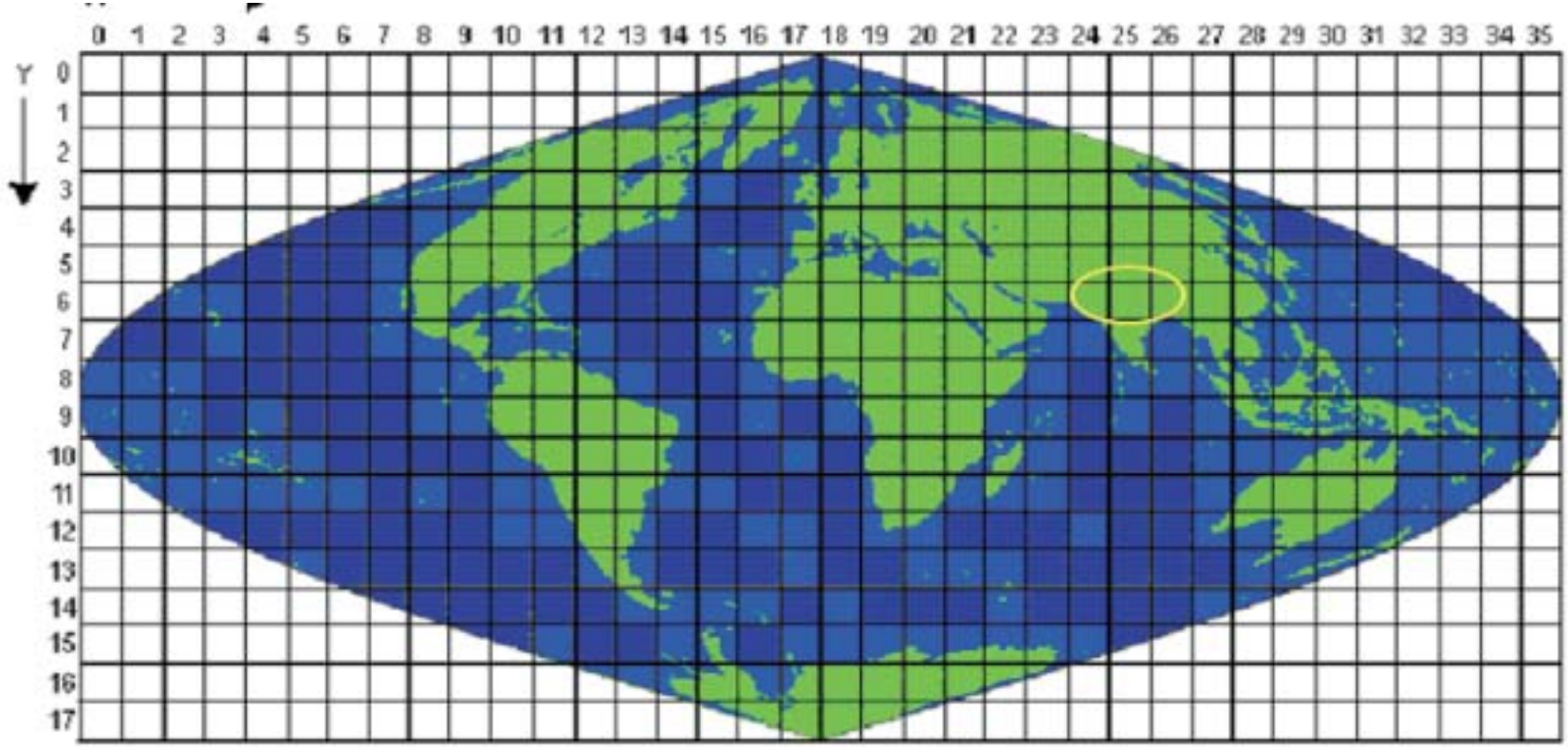

Figure 16. Grid tile (path/row) reference map for AVHRR 8-km and 0.1 degree data that is available free of cost for every 10-day or as monthly composites from 1981 to 2001. The uniformly processed global 1-km 10-day AVHRR data is available only for 1992 (April-December), 1993 (January-September), 1995 (February-September), and 3 months in 1996. Yet, this limited dataset is of considerable value due to far better spatial resolution relative to 8-km. The data is available for download free of cost from the AVHRR 1-km site (see Figure 14 for URL).

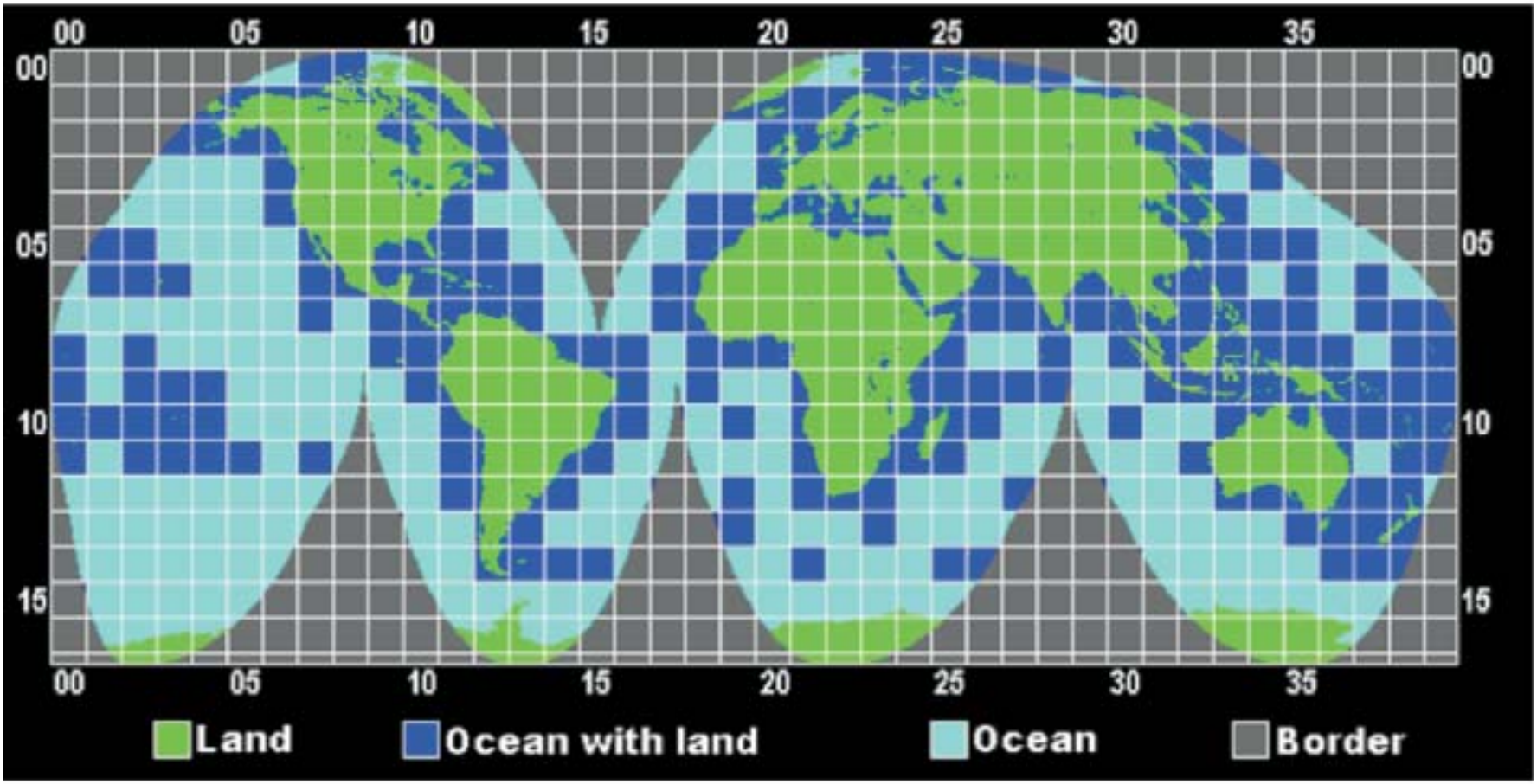

Figure 17. Grid tile (path/row) reference map for Landsat TM 3-band mosaic. The 1990 mosaic is available for the entire globe. The full 7 band data is also available. The data is free, orthorectified (geographically precise), and can play the role of a base map. These links and search tools form a key source of the best of the present day and historical satellite sensor imagery available for all CP BBs.

MrSid image mosaics of the basins will serve as useful tools for each CP BBs for the purposes of: (1) base maps, (2) ground-truthing reference maps, and (c) georectification tool for other images and maps of the basins.

5.1.1.4 *LP DAAC, EOSDIS, and Earthexplorer*

The Land Processes Distributed Active Archive Center (LP DAAC) was established as part of NASA's Earth Observing System (EOS) Data and Information System (EOSDIS) initiative (URL in Figure 14). LP DAAC is perceived a one-stop sto ETM+, higher processed ASTER, and MODIS-Terra/Aqua). Earthexplorer is a search and order tool (Figure 14) designed as an online shopping window for all sources of imagery. The type of imagery on Earth Explorer include Landsat 7 ETM+, Terra ASTER, Terra MODIS, Landsat Pathfinder NASA Science Data Purchase, AVHRR, Elevation, Global 30-Arc-Second Elevation Data SetLand Cover Global Land Cover Characterization, Airborne Imagery, and Radar SIR-C imagery. The LP DAAC, EOSDIS, and Earthexplorer constitute the center stage of all sensor-based imagery.

Earth Explorer: Data Set Selection

Aerial photos, satellite images including EO-1 search and order

5.1.1.5 *Shuttle Radar Topography Mission (SRTM)*

The C-band SRTM data is expected to soon produce a 90-meter DEM of all the land mass between +/- 60 degrees latitude and will be distributed through the USGS network (URL in Figure 14).

The SRTM 90-meter horizontal resolution DEM datasets will be the most consistent and highest resolution DEM data that will be available "wall-to-wall" for all CP BBs. This data is expected to

play a major role in numerous basin studies and will be used widely for visualization, 3-d displays, modeling, and to “fly-over” the basins.

5.1.1.6. *SeaWiFS Data for Basins*

SeaWiFS data well compliments and supplements AVHRR and MODIS imagery at 1,000 m resolution and is available globally for all basins starting 1998 to date. Originally, designed for Ocean applications, SeaWiFS has a useful role in terrestrial applications and can be used to on its own and/or as a substitute for missing data from MODIS or AVHRR.

5.1.2 Secondary Data

The secondary data are the products produced by various global, regional, and national laboratories, mostly from satellite sensor data of one kind or the other. These datasets are products of major endeavors at different time periods using the best available imagery for the period in consideration. Some of the key secondary datasets available for the entire CP BBs will be in land use / land cover (LULC), forests, droughts, population, and net primary productivity (NPP) (see Figure 18 for the URL).

5.1.2.1 *Land-use / Land-cover (LULC)*

A number of well-established LULC global datasets are currently available (most available through GLCC link—see URLs in Figure 18). These datasets should ideally form the base LULC data layers for CP BBs. All these datasets are currently archived in IWMI HQ image server and are accessible via Intranet. The appendix 2 provides specific details on the datasets, publications, sources, legend, and header information. The lead LULC datasets consists of:

1. USGS global LULC dataset with 24 classes (e.g., see Figure 18; Loveland et al. 2000) produced from the 1-km AVHRR global product for April, 1992-March, 1993.

2. IGBP global LULC dataset with 17 classes (Loveland et al. 2000) also produced from the 1-km AVHRR global product for April, 1992-March, 1993.

3. Seasonal USGS global LULC dataset with 253 classes (Loveland et al. 2000) also produced from the 1-km AVHRR global product for April, 1992-March, 1993. The seasonal land cover regions are then translated into the Global Ecosystem framework (see point 4, below). The availability of a large number of classes will help a user working in a specific region of the world to use specific classes of interest, either directly or through manipulations of the data to aggregate more than one class.

4. Olson ecoregions of the world with 94 ecosystem classes (Olson 1994) that are based on their land cover mosaic, floristic properties, climate, and physiognomy. The Global Ecosystem framework provides a mechanism for tailoring data to the unique landscape conditions of each continent, while still providing a means for summarizing the data at the global level.

Figure 18. Internet access to sources of basin level secondary remote sensing data.

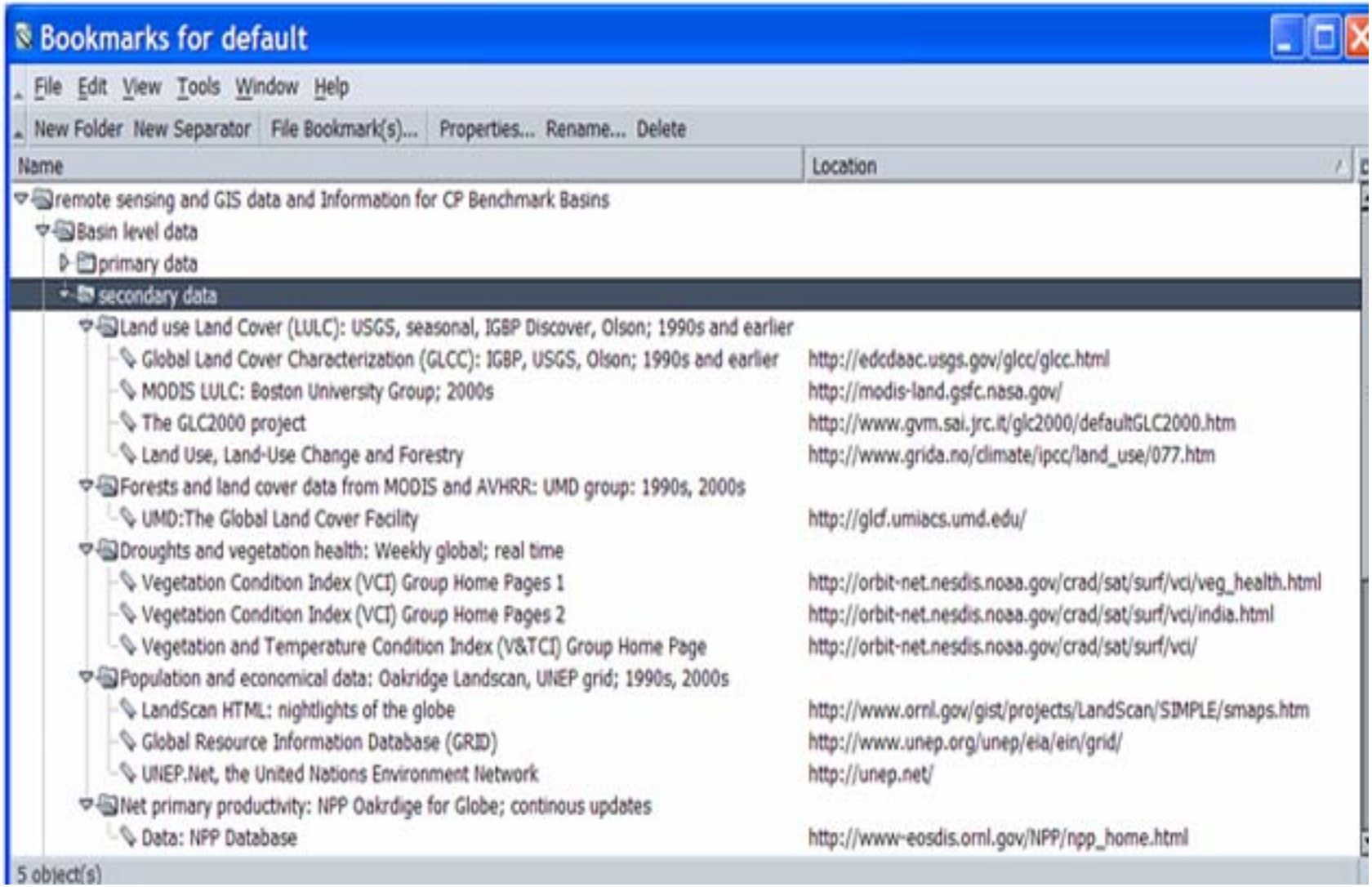

5. MODIS derived LULC classes with the same 17 classes as the IGBP system. With much of the other LULC classes for the earlier decades, MODIS provides continuity into the new millennium. The 2000289 product was made from MODIS data from the period 10/15/00 to 10/15/01. It is designated as "provisional," meaning that it contains useful science data but is subject to further improvement.

The appendix 2 also provides two other classification systems of interest: (1) Anderson (USGS) classification system (Anderson 1976) using remote sensing, and (b) global land use classification system for year 2000 (also see URL in Figure 18). The Anderson classification is a nice hierarchical system that follows different levels of classification detail and is highly recommended for a detailed classification at different levels of detail in the CP BBs. The **Global land cover 2000 Project** is a European effort to map global land cover using 14 months of data from the 1-km resolution SPOT 4 Vegetation sensor. The project involves collaboration with a network of partners around the world.

5.1.2.2 *Forest Cover and Density*

The University of Maryland (UMD) has produced two global datasets on forests. These are: (1) forest cover (5 classes), and (2) forest density (0 to 100 percent). The product is based on the 1995 AVHRR monthly composite images processed using a hybrid maximum-NDVI and minimum-red compositing technique. Modified mixture analysis, geographic stratification, and other classification techniques were used to estimate forest canopy density within 1 square kilometer pixels, which formed the basis for the first two classes: the closed forest (40% - 100% canopy cover), and open or fragmented forest (10% - 40% canopy cover). The remaining three classes were derived using the USGS global land cover characteristics database as a stratification tool. Appendix 3 provides an overview, legend, and header information for these datasets.

As a continuing effort, UMD is currently releasing similar forest cover and density products for New Millennium periods using MODIS 500-meter data.

5.1.2.3 *Drought and Vegetation Health*

At basin level, vegetation health or condition product is available every week. This product is produced using NOAA 1-km data by Dr. Kogan and group of the NOAA NESDIS. Downloadable is the Vegetation and Temperature Condition Index (VCI and TCI) server. This is a potentially very useful product at the basin level to observe drought conditions. Data and imagery provided on the VCI server and in the Historical Examples of VCI and NDVI pages are experimental and not supported operationally and, hence, may require substantial user efforts in data handling and management. Further, there is a warning that the Data services may be interrupted or discontinued at any time without notice.

Sample global and regional vegetation health data products are illustrated in Figure 19.

5.1.2.4 *Population Data*

At all levels of river basin study, population data will be of critical importance for much spatial analysis and to determine populations at risk from factors such as droughts and disasters. In this regard, the LandScan population data derived from DMSP-OLS nighttime at about 1-km resolution (30 Arc Second Grid) from the period of October 1994–March 1995 will be very useful. The product was produced by Dr. Christopher Elvidge and group of NOAA National Geophysical Data Center.

Figure 19. The USGS derived land use/land cover (LULC) Global dataset based on 1-km AVHRR data (see Loveland et al. 2000).

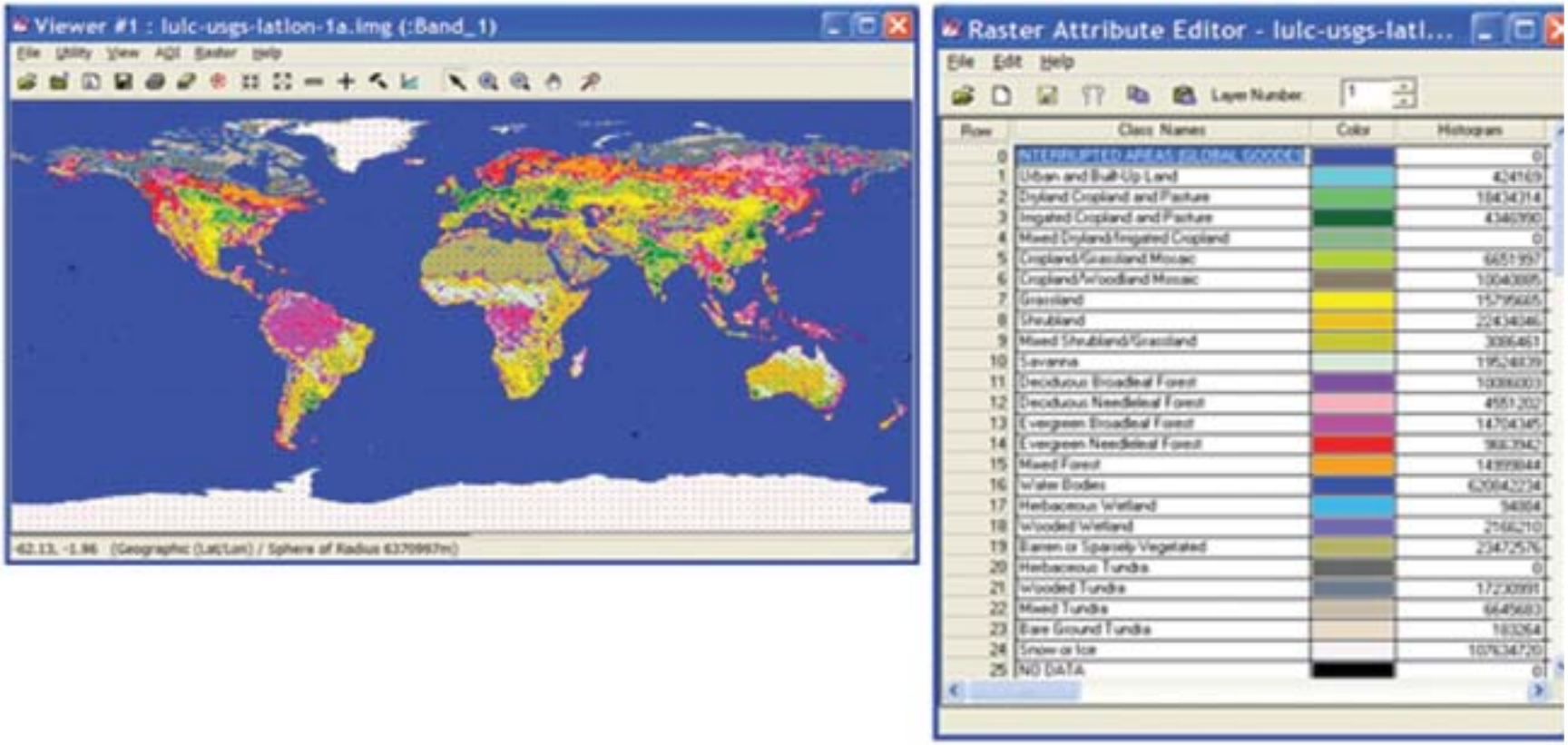

5.1.2.5 *Net Primary Productivity*

The Oak Ridge National Laboratory Distributed Active Archive Centers (ORNL DAACs) provide a reliable source of Net Primary Productivity (NPP) Database produced based on field measurements of biomass and estimated NPP. Data for selected NPP sites are available through the ORNL DAAC NPP search and order.

Figure 20. Landscan population data produced by Oakridge Laboratory using nighttime DMSP-OLS 1-km data. Other population data for the 1980s, 1990s, and 2000s is produced by UNEP GRID based on National census.

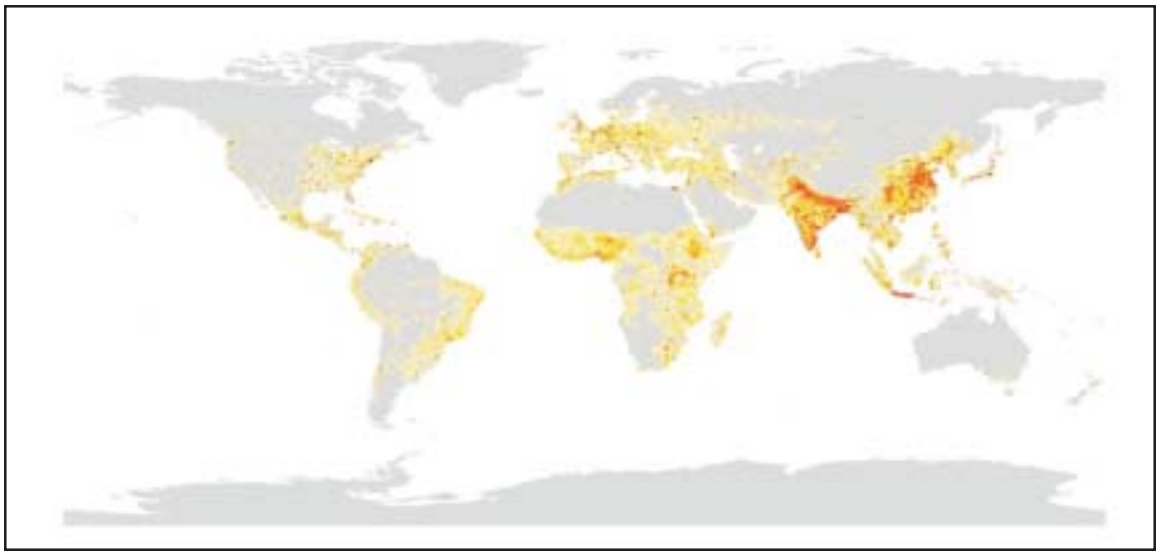

5.2 Subbasin Level Data

Much of the focus-detailed studies will be conducted within specific areas of the CP BBs—in the specific subbasins. The acquisition and analysis strategies for primary and the secondary datasets at subbasins will characteristically vary from that of the basins.

5.2.1 Primary Data at Subbasins

At the subbasin level the primary data is best acquired from specific satellite sensor systems (see Figure 21) in near-real-time, so that field investigations are carried out corresponding to satellite data acquisitions. Some of these data are free of cost (though mostly not in near-real-time) or have low cost. The nominal resolutions of most of these data are 30 meters, facilitating a very detailed investigation of the basins.

5.2.2 Secondary Data at Subbasins

The secondary data at the subbasin level is produced at pixel resolutions of 100 meters or better and requires substantial field's investigations. The detail mapping, characterization, and modeling

Figure 21. Internet access to sources of subbasin level primary remote sensing data.

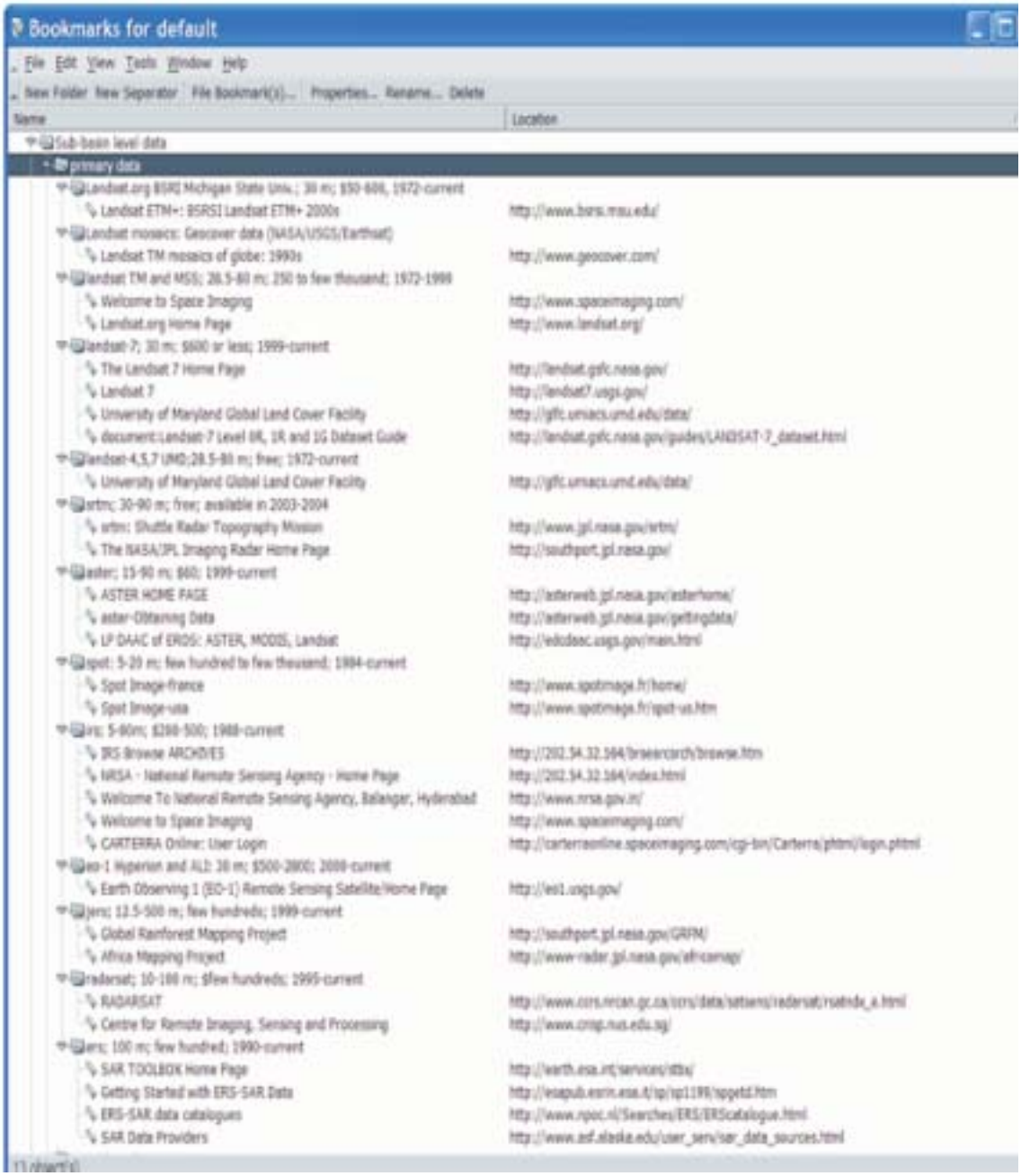

at subbasin level is thereby best conducted at national or regional level. The best URLs for these data for each CP BB will be determined during the workshop in May.

5.3 Watershed Level Data

Very detailed characterization, mapping, and spatial modeling work at pixel resolution of 30 meters or less will be taken up at watershed level in CP BBs.

5.3.1 Primary Data at Watershed Level

The most of the remote sensing primary data for this work will be 5 meters or less with exception of High-spectral resolution data such as Hyperion, which has a 30-meter spatial resolution but with 220 spectral bands in 400 to 2,500 nm range. The URLs for the primary imagery sources at watershed level work are provided in Figure 21. The cost of the commercial imagery is substantial, but is justified for detailed spatial modeling work.

5.3.2 Secondary Data at Watershed Level

There are hardly any secondary data products produced using high-spatial or high-spectral resolution datasets. Any work undertaken using these datasets will provide ample scope for innovative research and in producing state-of-the-art products.

5.4 *GIS Datasets for the Basins*

The secondary GIS data are invaluable in terms of building base data layers for CP BBs in terms of socioeconomics, soils, populations, administrative boundaries, and numerous other requirements. The quality and scale of these data vary widely. Most often than not, quality or accuracy assessments are done. The sources listed in Figure 23 provide some very reliable sources of secondary data, which publish only the data that have met certain quality standards. This list is by no means comprehensive and we welcome suggestions for inclusions here.

Figure 22. Internet access to sources of watershed level primary remote sensing data.

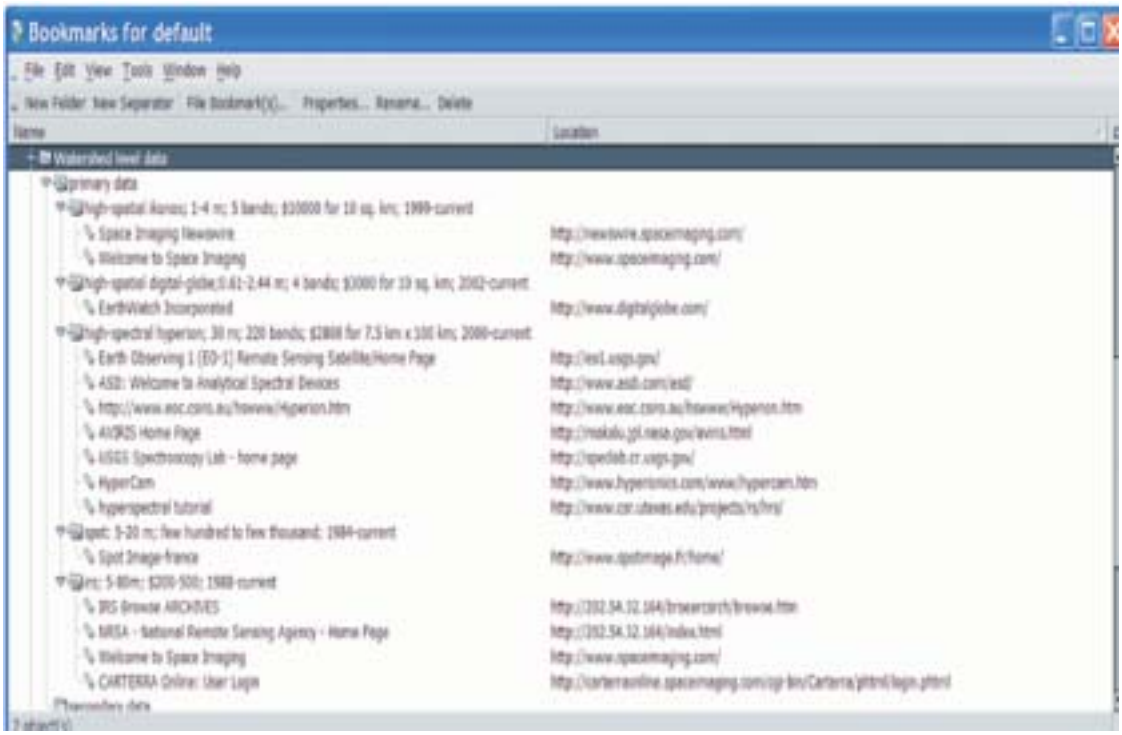

Figure 23. Internet access to sources of secondary GIS spatial databases for CP BBs.

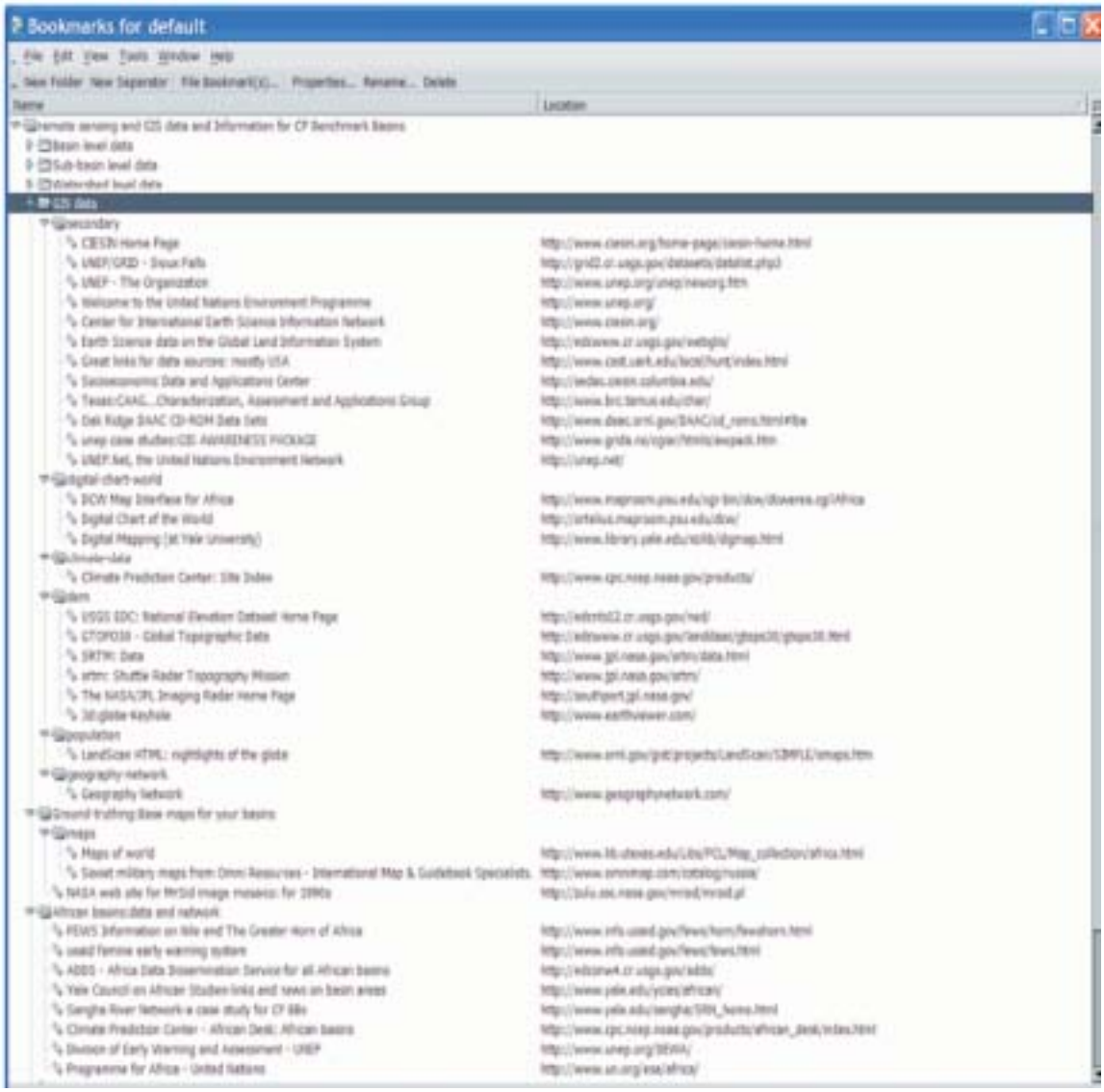

Figure 24. Capacity building for remote sensing–curriculum, societies, and software.

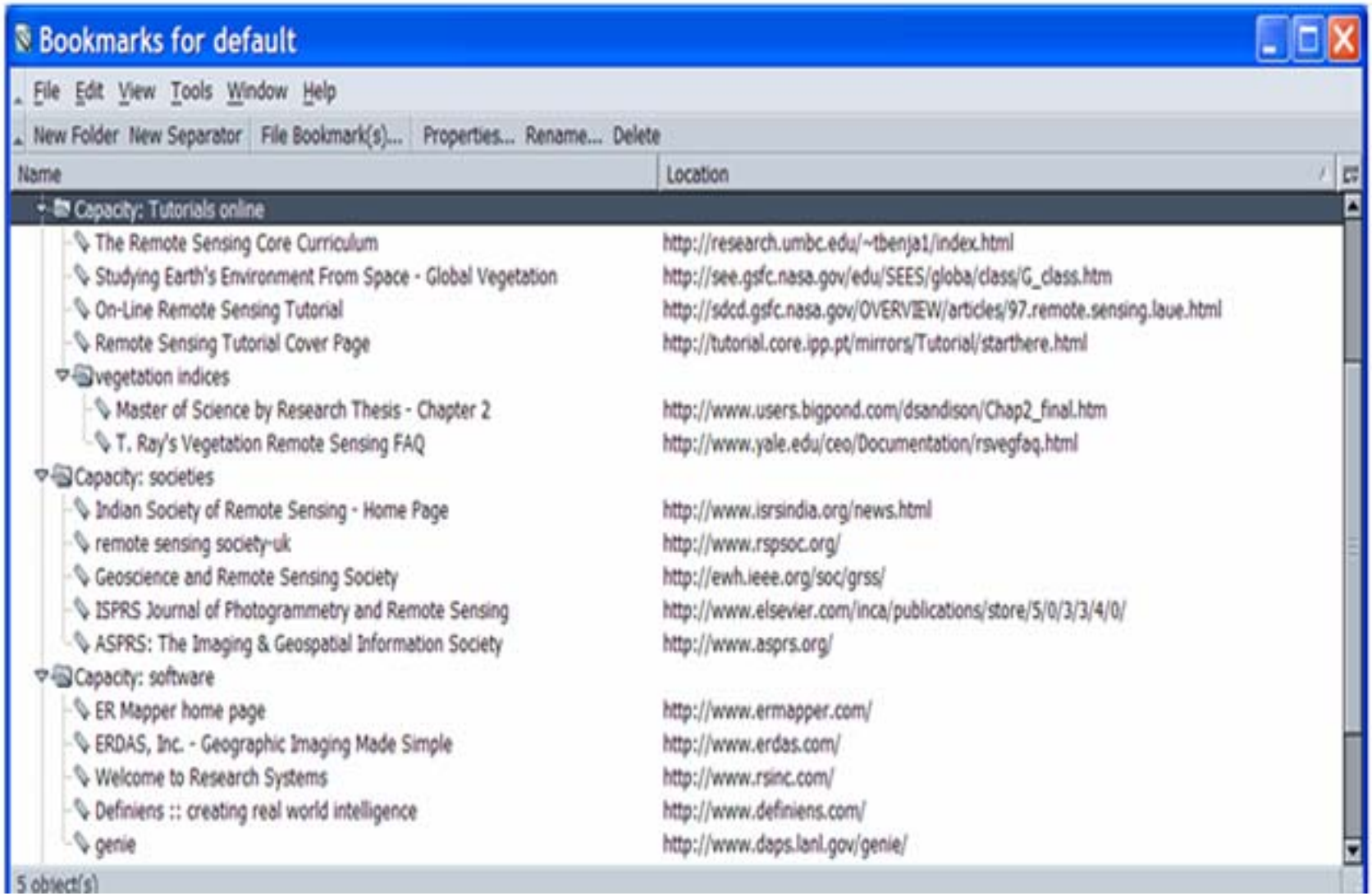

5.6 News and Knowledge about the Remote Sensing Applications for the Basins.

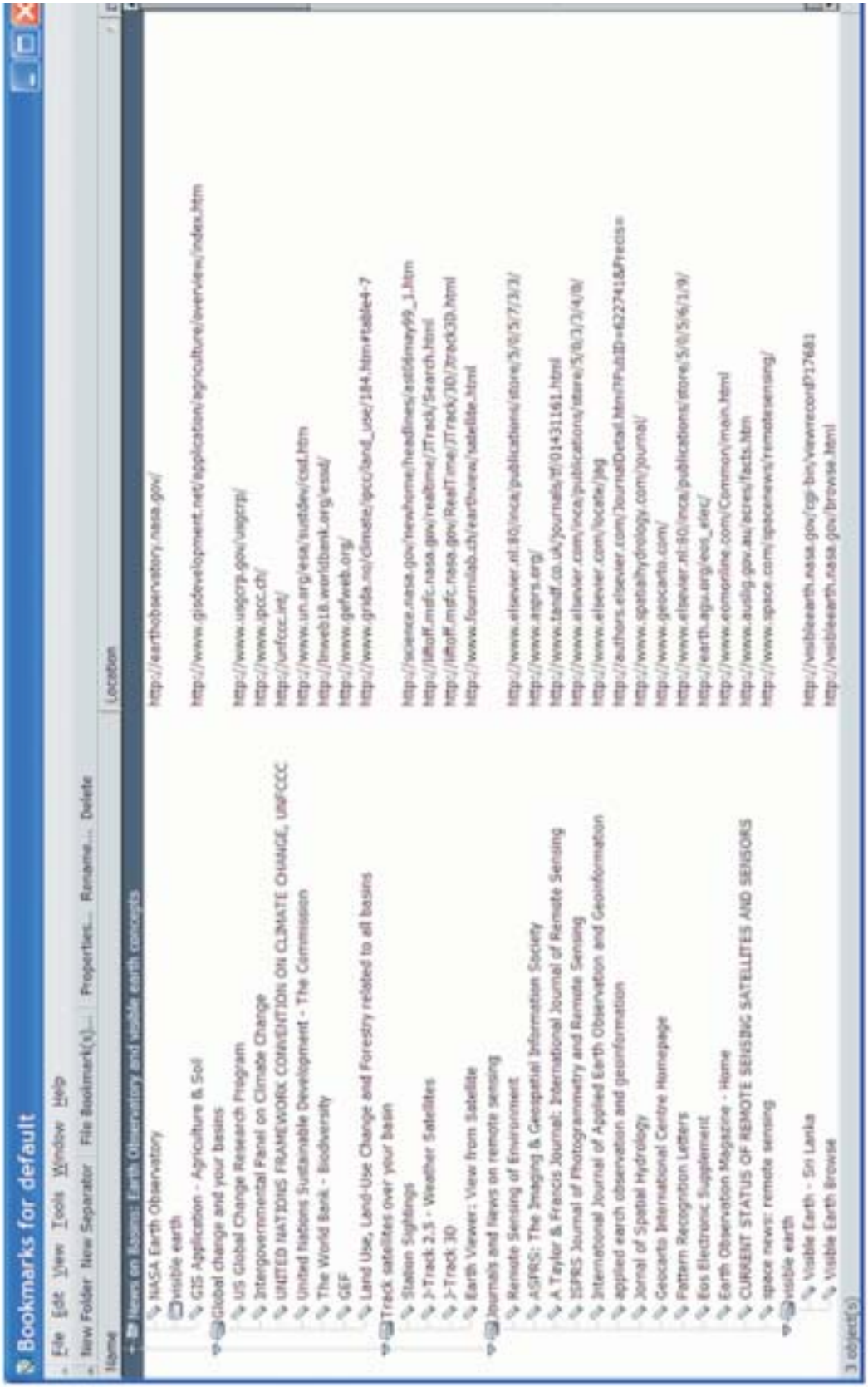

Figure 25. News, journals, satellites over basins, and global change news. Remote sensing publications and literature.

5.7 Network of Institutes Related to Spatial Data and the Information they have for Basins

Figure 26. Network of global institutes relevant to Challenge Program Benchmark Basins.

6.0 Products at Basin Level for all CP Basins

6.1 *Historical (for last 20 years)*

- Land use/land cover (LULC) at 8-Km based on last 20-year AVHRR data
- Land use/land cover (LULC) at 1-Km based on 1992, 1993, and 1995 AVHRR data

6.2 During the Project Period (monthly)

- Land use/land cover (LULC) at 250 m and/or 500 m using MODIS 7 band reflectance data (monthly)
- ` Maximum possible classes will be mapped based on the 2001-2003 MODIS data and the same classes mapped every month during the project period

6.2.1 Change Vector Analysis from LULC Product: Change from Month to Month

- Change magnitude
- Change type (e.g., deforestation and seasonal subtle)
- Change direction
- Change spatial distribution

6.3 Snow Cover of Basins at 250 m and/or 500 m using MODIS 7 Band Reflectance Data (monthly)

- Snow spatial distribution
- Snow depth
- Snow frequency

6.4 Vegetation Dynamics and Drought Assessment at 250 m and/or 500 m using MODIS 7 Band Reflectance Data (monthly)

Some of these are proxy for climatic variables. For example, NDVI/EVI is a good proxy for rainfall in rain-fed regions.

- Vegetation condition index (VCI) maps

- Temperature condition index (TCI) maps
- NDVI and EVI maps
- Analysis products/results
  - Month of beginning of green period
  - Duration of green period (amplitude)
  - End of green period
  - Number of peaks in a year
  - Number of troughs in a year
  - Absolute Maximum (e.g., Month of maximum NDVI/EVI)
  - Absolute Minimum (e.g., Month of minimum NDVI/EVI)
  - Twelve monthly NDVI/EVI means
  - Maximum monthly NDVI/EVI
  - Minimum monthly NDVI/EVI
  - Mean annual NDVI/EVI
  - NDVI/EVI range

6.5 Ecological/Biophysical Variables Product 250 m and/or 500 m using MODIS 7 Band Reflectance Data (monthly)

- LAI
- Biomass
- Yield (where possible)
- Crop type, growth stages, and stress
- ET/consumptive use
- Surface temperature

7.0 The need for a Centralized Archive: Role of IWMI Remote Sensing Group

A central archive of all remote sensing and GIS data for all basins cannot be over-emphasized. The main purpose will be to maintain a standard archive of all CP datasets for purposes of serving: (1) basin data needs, and (2) global public goods of data and products, generated from CP research. This also serves the purpose of cocoordinating a data sharing effort across basins and/or to researchers interested working in cross basins in a standardized format considering the data type, quality, projections, datums, and formats.

A centralized archive will involve acquiring, cataloguing, archiving, and analyzing RS datasets at various scales (or pixel resolutions), band-widths, radiometry, and time-periods stretching over three decades (see Tables 1 to 3).

Table 1. Satellite sensor data for Challenge Program Benchmark (CP) Basins. Data types, availability, pixels per hectare, number of images per basin, and costs per image.

		Data Frequency[1] (days/ months)	Available Period (years)	Cost per Image (US $)	Number of pixels per ha.	Challenge Program River Basins							
	CP River basin					Ganges-Indus	Karkeh	Mekong	Nile	Olifats	Sao Francisco	Volta	Yellow River
	Total area (Mha)[2]					196	12	69	252	36	53	34	95
1. Basin-level characterization													
	MODIS-Terra/Aqua (250-1000m) images per basin3	8-16 days	2000-current	0	0.16-0.001								
	number of images per basin[3]					5	1	3	6	1	3	1	4
	AVHRR (1000-8000 m; 0.1 degree)	10-day,monthly	1981-2001	0	0.001-00015625								
	number of images per basin[3]				0.0001 for 0.1 degree	1	1	1	1	1	1	1	1
	IRS-WiFS (188 m)	5 days	1995-		0.29	5	1	3	6	1	3	1	4
	number of images per basin[3]												
	SPOT Vegetation (1000 m)	weekly	1999-current	0	0.001								
	number of images per basin[3]					1	1	1	1	1	1	1	1
2. Basin and sub-basin level characterization	Landsat ETM+ (15-30 m)	16 days	1999-current	600	11.1-44.4								
	number of images per basin[3]					62	4	22	80	11	17	11	30
	ASTER (15-90 m)	16 days	2000-current	60	1.26-44.4								
	number of images per basin[3]					544	33	192	700	100	147	94	264
	ALI (10-30 m)	16 days	2000-current	500	11.1-100								
	number of images per basin[3]					252	15	89	324	46	68	44	122
	SPOT HRV (5-20 m)	3-8 days	1986-current	3000	25-400								
	number of images per basin[3]					544	33	192	700	100	147	94	264
	Landsat TM (30 m)	16 days	1982-current	250	11.1								
	number of images per basin[3]					62	4	22	80	11	17	11	30
	Landsat TM-global 1990	one time	1990s global	0	11.1								
	number of images per basin[3]					62	4	22	80	11	17	11	30
	Landsat TM-global 2000	one time	2000s-global	0	11.1								
	number of images per basin[3]					62	4	22	80	11	17	11	30
					400								
	IRS-series (1A to 1D and P) (5-80 m)	8-16 days	1988-current	400	2.26-400								
	number of images per basin[3]					544	33	192	700	100	147	94	264
	Landsat MSS (56 x 79 m)	16 days	1972-1995	200	2.26								

(Continued)

	number of images per basin[3]					62	4	22	80	11	17	11	30
3. Watershed-level characterization	Hyperion (30 m)	15 days	2000-current	2800	11.1								
	number of images per basin[3]					2613	160	920	3360	480	707	453	1267
	IKONOS (1-4 m)	5 days	2000-current	11000	625-10000								
	number of images per basin[3]					13611	833	4792	17500	2500	3681	2361	6597
	Quickbird-2 (0.61-2.44 m)	5 days	2002-current	3000	1680-26875								
	number of images per basin[3]					2178	133	767	2800	400	589	378	1056

Note: 1 = Many satellite systems have off-nadir viewing capability which will increase frequency of observations. What is presented here is most common acquisition frequency.
2 = Is nominal area of the benchmark watersheds that is dependant of the basin boundary delineated by 1 km DEM. The exact basin areas may vary by 5-10 percent.

3 = The number of images may vary slightly if you consider images on the edges of the basin boundaries.

Table 2. Characteristics of Remote Sensing datasets for Challenge Program Benchmark Basins.

Satellite/Sensor	Spatial resolution (meters)	Spectral bands (#)	Data points or pixels per hectare	Time-composites (intervals)	Period (from-to)
Global Scale coarse resolution modern era					
MODIS -Terra	250-1000 m	36	0.16, 0.01	8-16 days	2000-current
-Aqua	250-1000 m	36	0.16, 0.01	8-16 days	2000-current
Global Scale coarse resolution historical era					
AVHRR -1-km	1000 m	5	0.01	10 days	1992-1995
-8-km	8000 m	5	0.000156	10 Days/Monthly	1981-2001
Regional Scale Moderate resolution modern era					
ASTER	15 m, 30 m, 90 m (VNIR, SWIR, TIR)	4,6,5	44.4,11.1,1.26	16 days	2000-current
Landsat-7 ETM+	15 m (P), 30 m (M)	7	44.4, 11.1	16 days	2000-current
ALI	10 m (P), 30 m (M)	1, 9	100, 11.1	16 days	2000-current
Regional Scale Moderate resolution historical era					
Landsat-4, 5 TM	30 m (M)	7	11.1	16-days	1984-current
Landsat-1,2,3 MSS	56 x 79	4	2.26	16 days	1972-current
IRS-1C LISS	5 m (P), 23.5 m (M)	3	400, 18.1	16-days	1990-1995
IRS-1D LISS	5 m (P), 23.5 m (M)	3	400, 18.1	16 days	1992-current
SPOT-1,2,3,4 HRV	10 m (P), 20 m (P)	4	100,25	3-5 days	1983-present
Local scale Hyperspatial modern era					
IKONOS 2	1 m (P), 4 m (M)	4	10000, 625	5-days	2000-current
SpaceImaging					
QUICKBIRD	0.82 m (P), 4 m (M)	4	14872, 625	5-days	2002-current
EarthWatch					
EROS A	1.82 m (P)	1	3020	5-days	2001-current
Imagesat					
SPOT-5 HRV	5 m (P), 10 m (XP)	1,4	100,25	3-5 days	1983-present
Regional scale Hyperspectral modern era					
Hyperion	30	220 (400-2500 nm)	11.1	16 days	2000-current

Table 3. Cost of Comprehensive Image Acquisition per CP Benchmark Basin.

Benchmark basin	Area (Mha)	Image type	Time interval days	Number of scenes to aquire	Cost per scene (US$)	Total cost (US$)
Niile	450	MODIS (Terra and Aqua)	8/16 days	45-90 per year	0	0
		AVHRR 1-km	10-day	78 (1992-1995)	0	0
		AVHRR 8-km	10-day	2400 (1981-2001)	0	0
		AVHRR 8-km	monthly	240 (1981-2001)	0	0
		ASTER		30 of 1200	55	1650
		ETM+		10 of 450	600	6,000
		ALI		2 of 1200	500	1,000
		Quckbird-2		2 of 45000	3,000	6,000
		IKONOS		1 of 45000	10,000	10,000
		Hyperion		1	2,800	2800
				Total cost of images		27,450

- Data catalogue and browse
- Header information and documentation
- Populating datasets—primary and secondary
- Data formats and exchange
- The role of benchmark basin remote sensing group
- Image server for CP basin RS datasets
- Copyright issues and data sharing
- Network of institutions and experts working on remote sensing in benchmark basins
- Expertise and personnel in the CP BBs
- Workshops and training courses
- Advocacy in CP BB nations and regions

8.0 Remote Sensing Capacity in Benchmark Basins

The issues to note in remote sensing activities in the benchmark basins will be harmonize hardware, software, and data acquisitions. This will be critical for data exchange in compatible formats and will save considerable time and resources for all CP activities related to remote sensing.

8.1 Hardware

The following minimum hardware is recommended.

- PC-based systems
- Color laser printer
- USB drives
- CD read/write
- DVD burner
- Digitizer

8.2 Software

The recommended software is:

- ERMapper 6.3
- ERDAS Imagine 8.6
- Arcview 3.2
- ArcGIS
- Statistical Analysis System (SAS)

8.3 Primary Satellite Sensor Data

The primary data at three different levels will be required:

8.3.1 Basin Level

MODIS time series
AVHRR 8 km time series
AVHRR 1 km time series

8.3.2 Subbasin Level

ETM+
ASTER
TM Geocover
TM MrSid
IRS
SPOT

8.3.3 Watershed Level

IKONOS-2
Quickbird-2

8.4 *Secondary RS Datasets at Basin Level*

IGBP LULC
USGS LULC
MODIS LULC

8.5 Base Maps and other Secondary GIS Datasets

The minimum GIS datasets for the basins will include:

- Basin drainage network (Source: USGS)
- Soils (Source: FAO)
- Elevation/DEM (Sources: GTOPO 30-available; SRTM; ASTER DEM, if required)
- Population (Sources: UNEP GRIDand Landscan)
- Administrative boundaries (Sources: DCWand National systems)
- Other more detailed information from each basin (Source: National system)

9.0 Capacity Building

Is there a need for seeking base funds for building remote sensing and GIS capacity for the CP BB work or are there adequate capacity already—something we will know only through consultations with basin coordinators. It is expected that substantial funding for the CP BB RS/GIS work will come out of thematic research groups and their needs. Requirements may vary from basin to basin for hardware, software, data, and expertise. However, we need to have some standards that would facilitate compatible exchange of data. A brainstorming session during the workshop will help us all understand where we stand at present and the needs during the 5-year CP research period.

10.0 Standardization and Normalization of Satellite Sensor Data across CP Basins

10.1 Approach

First, the need for standardization arises from the fact that the studies conducted in different river basins under any of the five CP research themes should be made inter-comparable. This is possible through use of well-understood consistent sets of data. The standardization will require a set protocol (Appendix 1) on what data to use at basin, subbasin, and watershed level, and to some extent methods adopted to analyze the data.

10.2 Radiometric and Atmospheric Corrections and Normalization

Multiple date images will be used in all CP basin work. The images acquired on multiple dates are subjected to variations in radiometry such as satellite sensor characteristics (e.g., sensor degradation and look angle) and illumination conditions (e.g., sun elevation), or atmospheric conditions (e.g., haze and aerosol). Thereby, the multiple date images are only comparable when effective radiometric and atmospheric correction models are applied. Since sensors such as MODIS acquire data in many different viewing directions compared to nadir-view from sensors such as ETM+, normalization for these effects is a must.

The process will involve one or more of the following steps depending on the type of data obtained:

1. Digital numbers (DNs; unitless) to radiance (W/m^2 Sr mm);

2. Radiance (W/m^2 Sr μm), to apparent or at-satellite reflectance (percent); and

3. Apparent reflectance (percent) to surface reflectance (percent).

The MODIS 7-band reflectance and AVHRR time series composite products come as scaled apparent reflectance. These are scaled 8 or 16-bit integer values that require dividing by a scaling factor to obtain values in percent apparent reflectance. Most of the other satellite sensor data come in the form of digital numbers or DNs (unitless) or radiance (W/m^2 Sr mm). The three-step process outlined above and described in detail in appendix 5 provides a framework for radiometric and atmospheric normalization of multi-date images from a wide range of satellite sensor systems.

Atmospheric normalization model for time series MODIS and AVHRR data involve using time invariant desert sites and developing calibration coefficients. The hypothesis here is that deep in the desert (e.g., specific locations in Libya and Saudi Arabia) there are areas that never change with time (time invariant). Theoretically, reflectance from these locations must remain the same throughout, except due to atmospheric influences. So the coefficient to be applied for each image is calculated by:

$$C_{i(1-n)} = \frac{NDVI_{mean}}{NDVI_{mi(1-n)}}$$

Ci = Calibration coefficient for layer i (1-n)
NDVImean = Mean NDVI value at the reference site calculated from all layers i1-n (81 – 00)
NDVImi (1-n) = Measured NDVI value at the reference site in layer i (1-n)

The products from sensors such as MODIS are corrected for molecular scattering, ozone absorption, and aerosols, and adjusted to nadir with the use of a BRDF model, as input to the VI equations (Huete et al. 2002).

Figure 27. Atmospheric correction of time series NOAA AVHRR data. Calibration coefficient computation for every 10-day period of 1981-2001. The time-invariant ("never changing") site was selected in the Saudi Arabian desert.

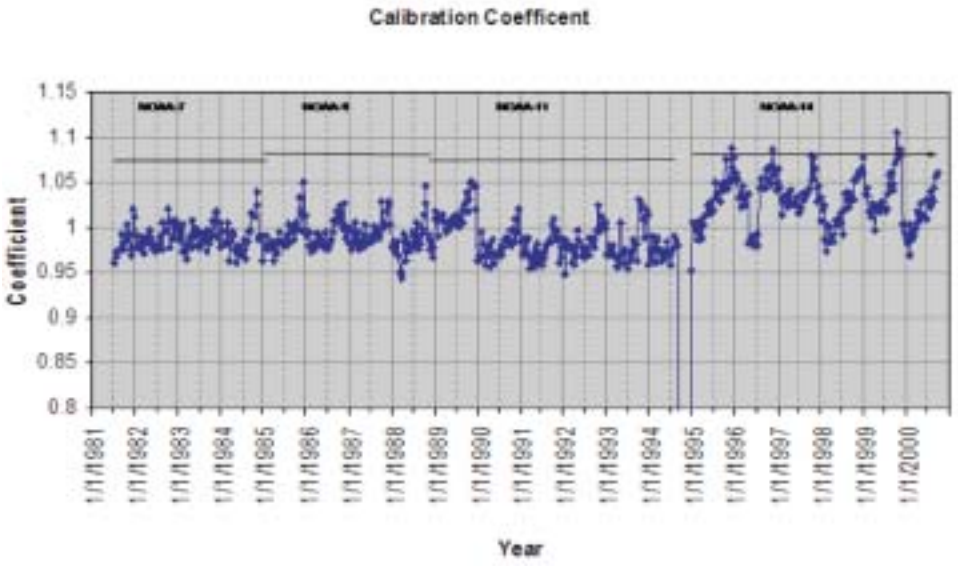

Figure 28. MODIS reflectance data for one of its 36 bands. MODIS products are provided as scaled at-satellite exo atmospheric (apparent) reflectance. A scaling factor of 100 is used to divide the data and arrive at apparent reflectance.

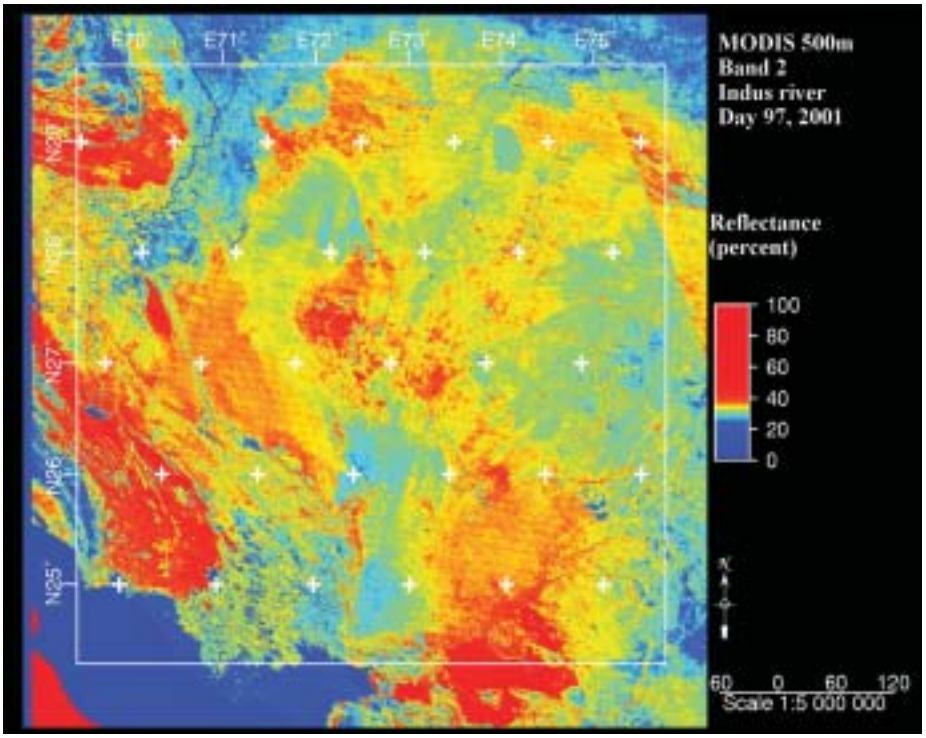

Figure 29. AVHRR surface reflectance data computed using the split window technique based on AVHRR thermal bands 4 and 5. This global data is available every 10-day and monthly for the 1981-2001 period. Data continuity is through MODIS thermal bands.

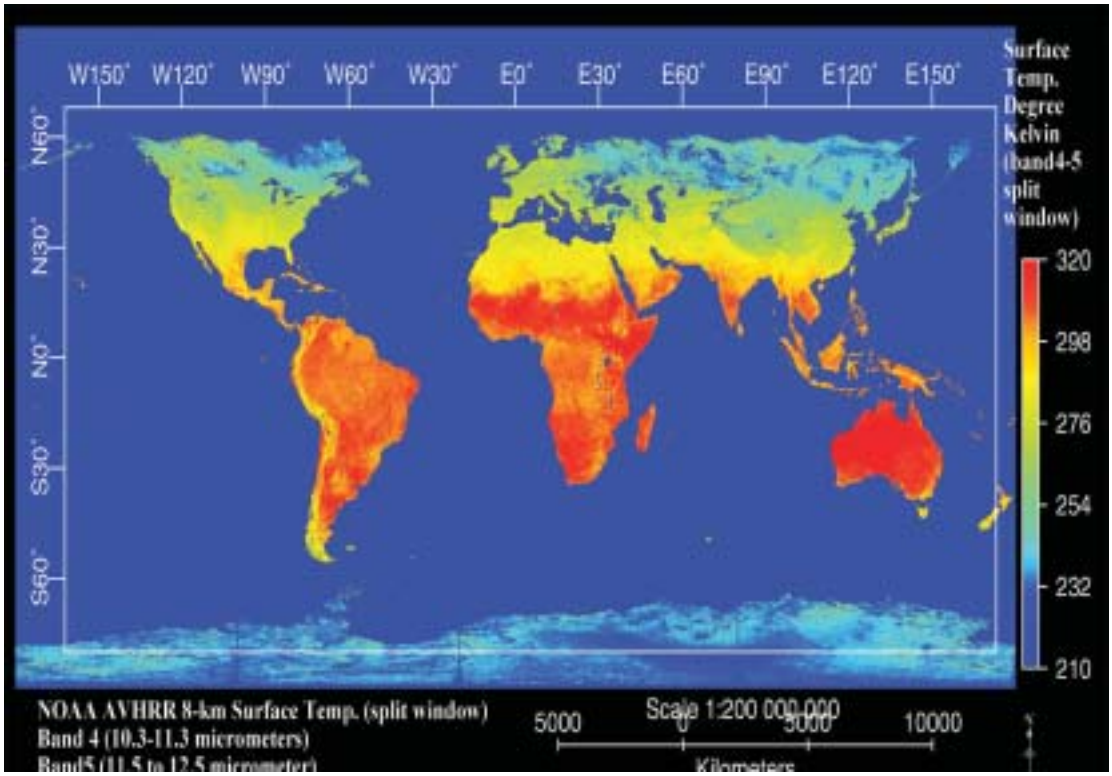

10.3 Inter-Sensor Relationships

When data from different satellite sensor systems are used within and between basins, we should be in a position to compare these results. This is feasible by developing inter-sensor relationships as illustrated in Appendix 4 between IKONOS and ETM+. Indeed, developing inter-sensor relationships will lead to rapid advancement in the effective use of remotely sensed data from multiple sensors and help harmonize and synthesize studies conducted using many different sensor systems. Over the years sensor systems and their characteristics have changed rapidly. For example, Landsat multispectral scanner (MSS) operated from 1972 to 1992 and is phased out. Landsat TM has operated from 1982, and Landsat ETM+ from 1999. It is likely these systems too will be phased out with the advent of sensors such as Advanced Land Imager (ALI). Thereby, in order to make the long-term analysis, spanning decades, inter sensor comparison studies are required. Recent studies have shown that the image products from Landsats 5 and 7 data indicate a high degree of similarity, which implies that monitoring activities initiated using Landsat 5 data, can be continued with a minimal amount of caution using Landsat 7 data (Vogelmann et al. 2001). Relationships between ecological variables and spectral derived indices using Landsat TM and ETM+ data were reported by Nouvellon et al. (2001). These relationships will differ when different sensors such as IKONOS or ASTER are used and related to ETM+ or TM as a result of the inherent differences in the characteristics of sensors.

Proliferation of data from a wide variety of sensors of very distinct characteristics such as from the Earth Observing Systems (EOS), New Millennium Systems (NMS), and older Landsat or Landsat-type systems have made it imperative to develop inter-sensor relationships that would in turn facilitate use of data from multiple sensors for the same application. Inter-sensor relationships between various sensors will help to understand and interpret the relationships between ecological variables and spectral indices developed for one sensor by using data from other sensors.

11.0 Science Goals of Benchmark Basins using Remote Sensing

The key science goals of CP research will need substantial use of satellite-based remote sensing data. This will be met through:

1. Use of data as envisaged within various full proposals: arising from the CP concept notes in the five thematic areas of research; and

2. Use of standard products: produced at basin level that will then be used in various research agendas to achieve specific science goals (e.g., input into models and testing model performance based on inputs). The products will be evaluated for accuracies and errors at various resolutions. The key will be to determine how errors propagate across pixel resolutions.

Basin performance indicators will be identified and extracted using advanced sensor systems of the New Millennium (NM) and Earth Observing System (EOS) era, as well as advanced multispectral sensors (e.g., ETM+, SPOT, and IRS), and historical datasets of the last three decades. At all levels of CP BB work, the essential spatial datasets will include Remote Sensing (RS), secondary datasets from Geographic Information Systems (GIS), various Global Positioning Systems (GPS) data, base map data, and field-plot data.

11.1 *Basin Parameterization or Basin Performance Indicators using Satellite Sensor Data*

11.2 *Land Use and Land Cover (LULC) in the Basins*

The land cover is likely to be the single most important factor of change in all the basins. It is well established that LULC change has significant effects on many processes in basin that include soil erosion (Douglas 1999), global warming (Penner1994), impact on biodiversity (Chapin et al. 2000), and is expected to cause greater impact on human habitability than climate change (Skole 1994).

Although there are some assessments of land cover for the basins, they are highly inadequate for the simple reason that the products are produced by groups who had little interest in the basins. The number of classes and relevance of these classes for basin research is limited, if not irrelevant. Primary goal in LULC analysis for the basins will be to: (1) understand history (inferences/ knowledge), (2) determine present state (truth as we see), and (3) model future trends.

Till recently, almost all LULC efforts at global and regional levels were derived from AVHRR time series NDVI (see Loveland et al. 2000). Currently, well-calibrated historical sensor data and advanced sensor data from modern generation of sensors are available to characterize basin land cover changes and degradation levels. This will enable us to characterize inter annual variability in land cover, and potentially to identify anthropogenic land cover change. Also, time series

Figure 30. Study of Ganges River basin using MODIS 500-m 7 band reflectance data. Many applications like snow cover, forests, and land use and land cover are possible.

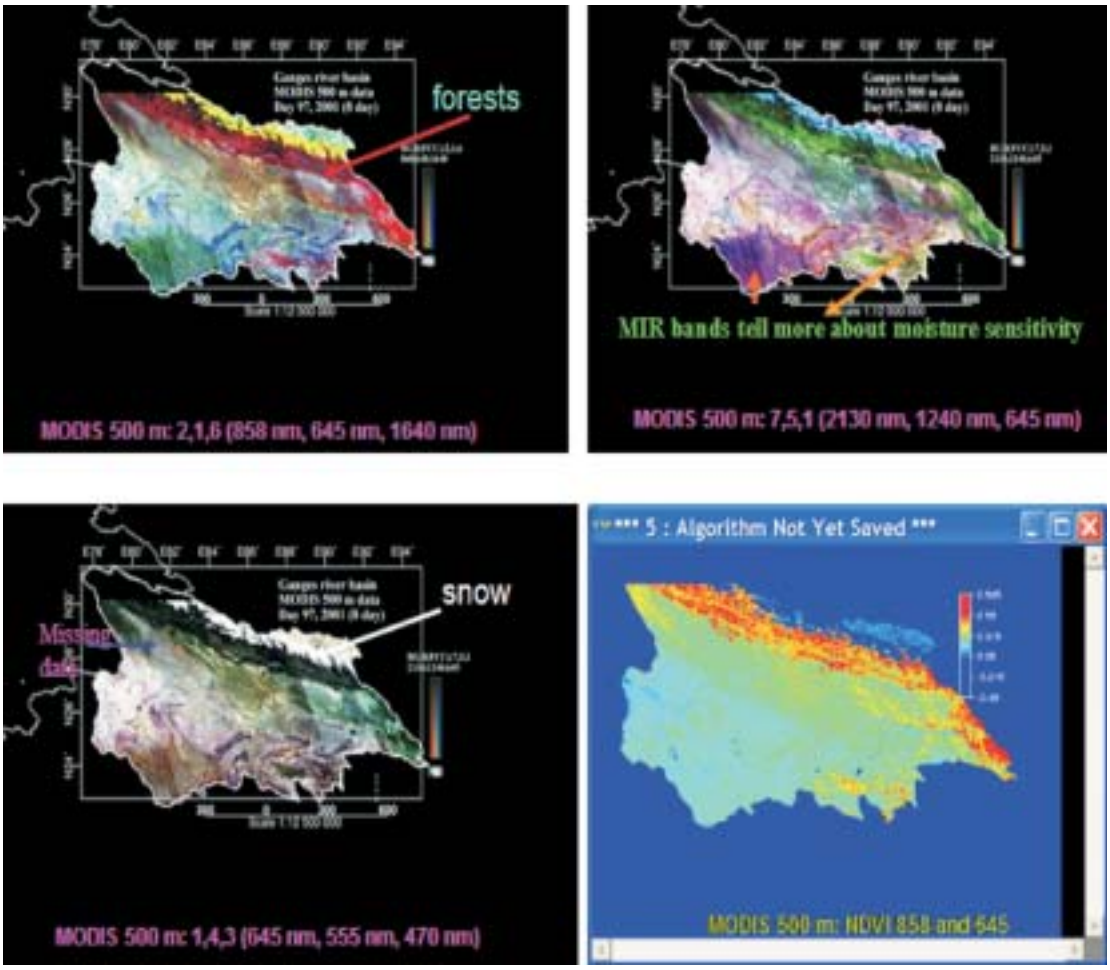

Images are powerful to determine land cover types based on their phenology, or seasonal signals (DeFries et al. 1995). A more powerful approach is to use a time series of the ratio of surface temperature to NDVI that isolates interannual climatological variability (Lambin and Ehrlich 1996). Availability of MODIS 500-m data with 7 spectral bands for terrestrial applications has opened new opportunities for making rapid advances in LULC characterization.

Rather than relay on secondary datasets produced by anonymous groups, the focus will be to define needs and target to map LULC at different scales (or pixel resolution) and for various time periods. The specific outputs expected are to map LULC:

1. classes of interest
2. change dynamics
3. change magnitude
4. change spatial spread, and
5. change vector analysis

11.3 Basin Level Studies Using Historical Time Series

The AVHRR 1-8 km data offers the best source for al long-time series analysis of LULC for the basins (e.g., Figure 10 and the CP basins shown in Figure 8). Most of these products produced based on maximum likelihood algorithm are known to provide low classification accuracies that ranges between 16–54 percentages when point based reference points are used for accuracy evaluations (Strahler et al. 1999; Friedl et al. 1999). Further, the decision tree and the nearest neighbor algorithms produce accuracies that are only marginally better than those produced by the maximum likelihood algorithm, and the highest accuracy from four different algorithms was only 51.4 percent. The poor spectral information of the AVHRR NDVI based classification and possible cloud contaminations are the likely reasons for poor LULC classifications from AVHRR data. In addition, the lack of studies at regional and local levels using these time composited data have resulted in lowering classification accuracies as the classes may not be relevant locally. Furthermore, classifications were conducted and classes labeled without significant visits to the field.

However, the best approach to map greater number of classes and with increasing accuracies will be to use data from additional wavebands other than just NDVI or NIR and red bands that are used to compute NDVI. For example, the inclusion of the thermal band increases the classification accuracies of LULC by about 5.5 percent (Maxwell et al. 2002). Similarly, it is established that the ration of T_s/NDVI increases LULC accuracies (Wen and Tateishi 2001).

11.4 Advanced Modern Sensors for Basin and Subbasin LULC Studies

In contrast to AVHRR, which has several limitations, the present era of modern sensors such as MODIS that provides numerous spectral, temporal, spatial, and radiometric advances (e.g., Figure 33) makes it possible to study LULC to provide greater details and increased accuracy at basin and subbasin levels. The spatial resolution is likely to be inadequate at watershed level. In addition, the presence of rigorous cloud/haze cleaning algorithms and time compositing make the inherent quality of data richer.

However, the MODIS LULC classifications produced by the global research groups are surprisingly limiting the classifications to 17 IGBP classes similar to Figure 19. This meets one key objective of providing data continuity with historical datasets. However, in basin and subbasin level LULC studies, there is a need to utilize the rich spatial, spectral, radiometric, temporal, and rigorous cloud/haze cleaning algorithms to increase the number of classes mapped to maximum spectrally as possible. This may not be possible at global or continental scales due to lack of resources for detailed field investigations. But at basin or subbasin level MODIS offers a perfect data source for multitude of studies, including a detailed study of LULC and its dynamics.

Advanced methods and techniques involving multi-temporal, multi-band, multi-sensor layer stacking, classifying, analyzing, and modeling techniques will be adopted that lead to detailed classes (e.g., Figure 33) that are well separated spectrally (Figure 34 through Figure 36). Typically, for each basin this will result in a layer stack of 100s or 1,000s of spatial-layers. Rigorous data mining techniques such as change vector analysis, principal components (Thenkabail et al. 2003), hyperspectral indices (Thenkabail et al. 2002), decision trees (Landgrebe 1991; Friedl and Brodley 1997; and DeFries et al. 1998) and rule-based spatial modeling will be adopted in order to analyze, understand, and model LULC and LULCC.

Figure 31. The International Geospere-Biospere program (IGBP) secondary LULC product produced using 10-day 1-km AVHRR composites from April 1982-March 1993 (Loveland et al. 2000).

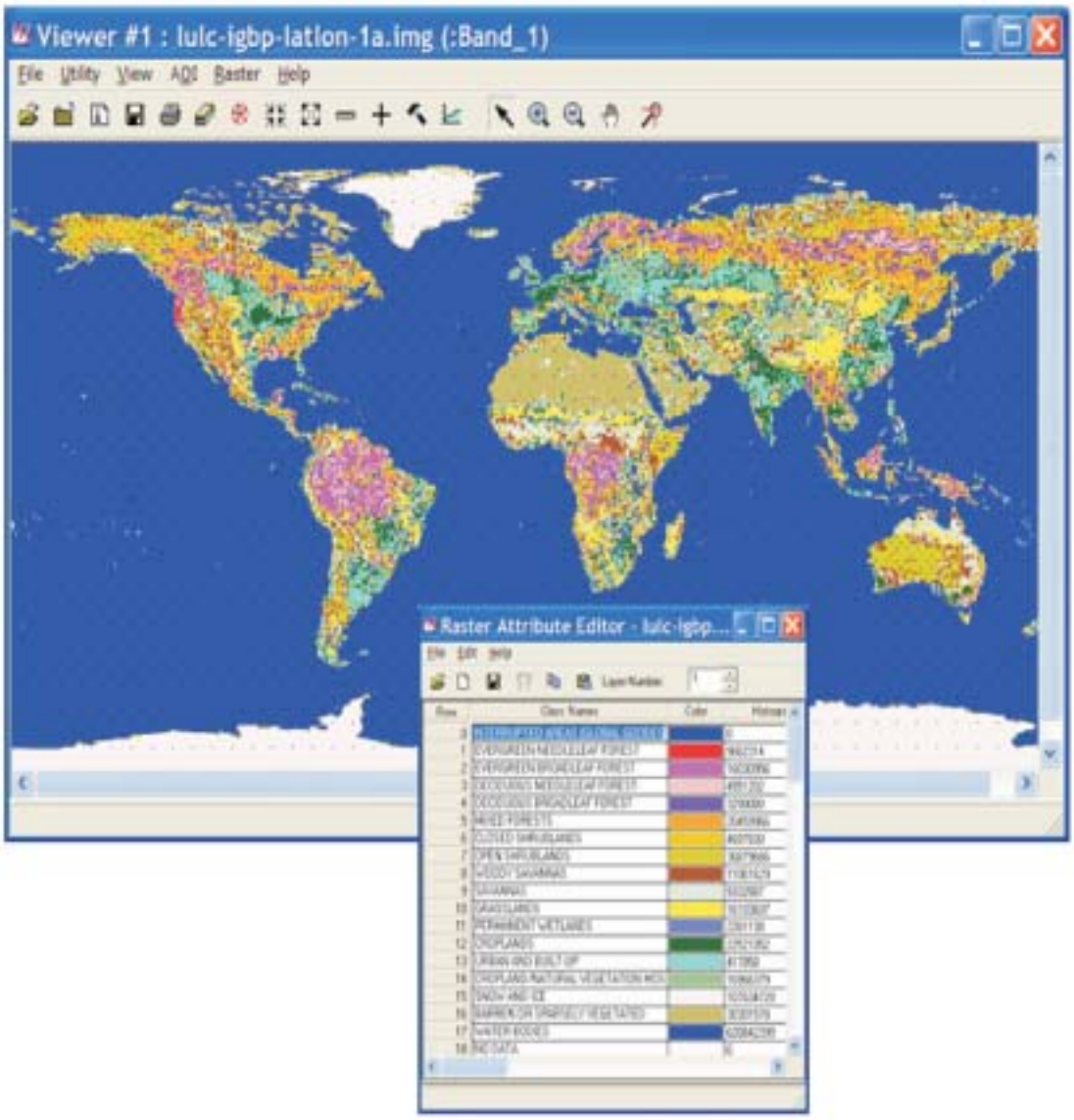

Figure 32. Temporal images of MODIS 500-m data for part of the Indus River basin. Earth Observing System (EOS) era data from MODIS-Terra and Aqua satellites are available globally every 8-days. Planned acquisition from the family of sensors will stretch into decades ahead.

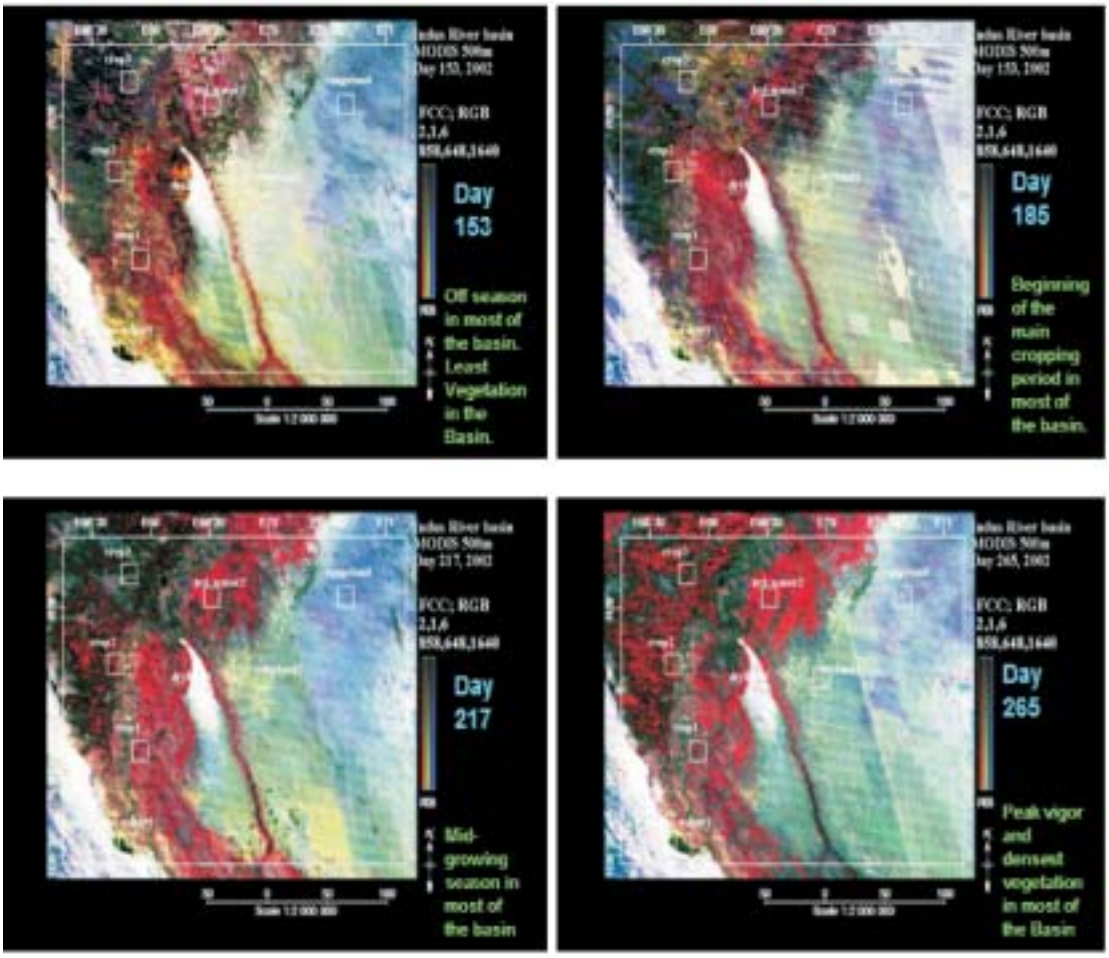

Figure 33. Classes from Multi-temporal and multi-band detailed layerstack for Indus River basin subarea. Land use/land cover (LULC) classifications in the Indus River basin using classifications performed on 12 images (one for each month) and 84 bands (7 bands per image) for the year 2002. The left image is labeled for most likely classes. In the right image, there are 20 classes, unlabeled. Indeed, the data can provide more than 20 distinct classes. The challenge is to identify and label these classes.

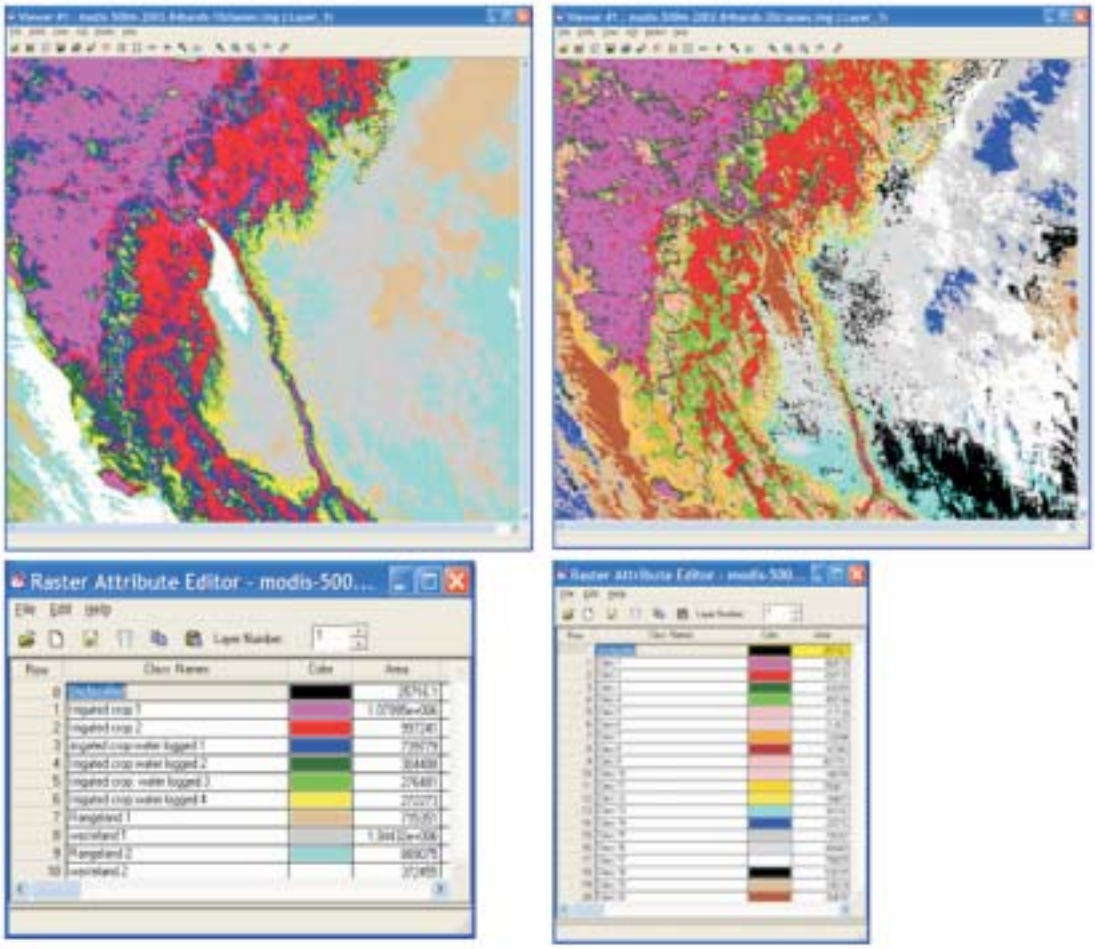

Figure 34. Temporal MODIS NDVI profile of the 10 unsupervised classes obtained from multi-temporal, multi-band layer stack classification for Indus River basin subarea shown in Figure 33. Peak khariff crops around day 265. Peak rabi crops around day 57. Between day 124 and 185 most of Indus command area is without any crops (fallow farms).

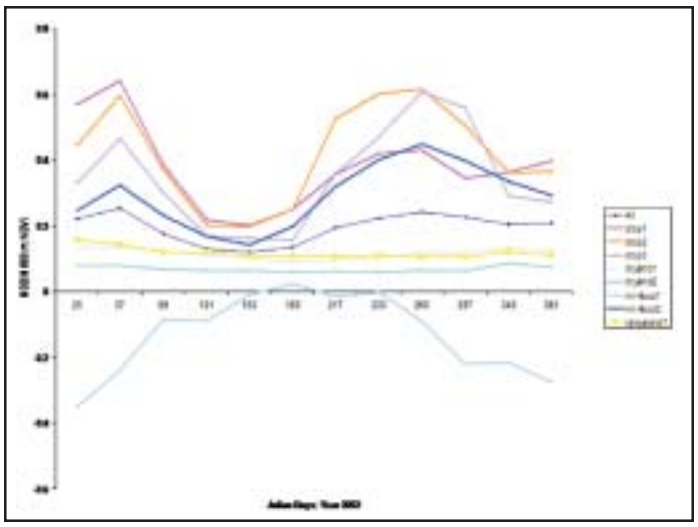

Figure 35. Changes in landscape over time captured in four plots for the Indus River. The same 10 LULC types shown in Figure 33 are plotted for four different times in four plots. In the first plot we see most LULC across the spectrum follow soil reflectivity indicating dry and/or fallow conditions. In the last plot, some LULC types have very high absorption in red (see between 600-700 nm), which is indicative of high biomass levels and crops or other vegetation vigorous and in healthy conditions.

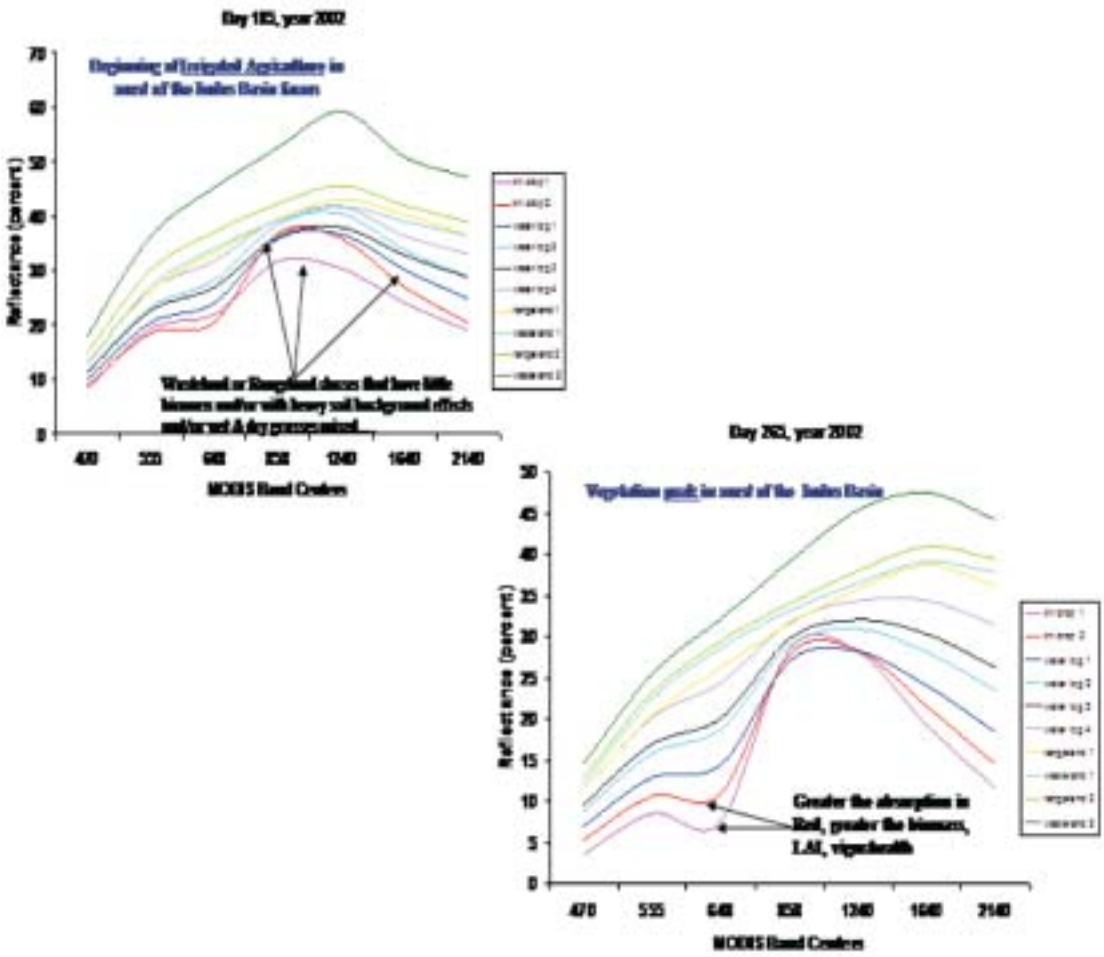

11.5 Land Degradation and Subtle Changes in Basins: Change Detection, Change Vector Analysis, and Tassel Cap Transformations

Land degradation and subtle changes in basins occur as a result of both natural and anthropogenic perturbation over time and space in any basin landscape. Although land cover conversions are important, they are only one component of land cover change (Foody 2002). Subtle transformations,

Figure 36. Indus River reflectance data over 365 days in one band after the other for the 7 MODIS 500-m reflectance bands shown for the 10 LULC classes during the year 2002. Look into the unique differences in reflectivity between the mid-infrared bands (band 6 and 7) and others (band 1-5).

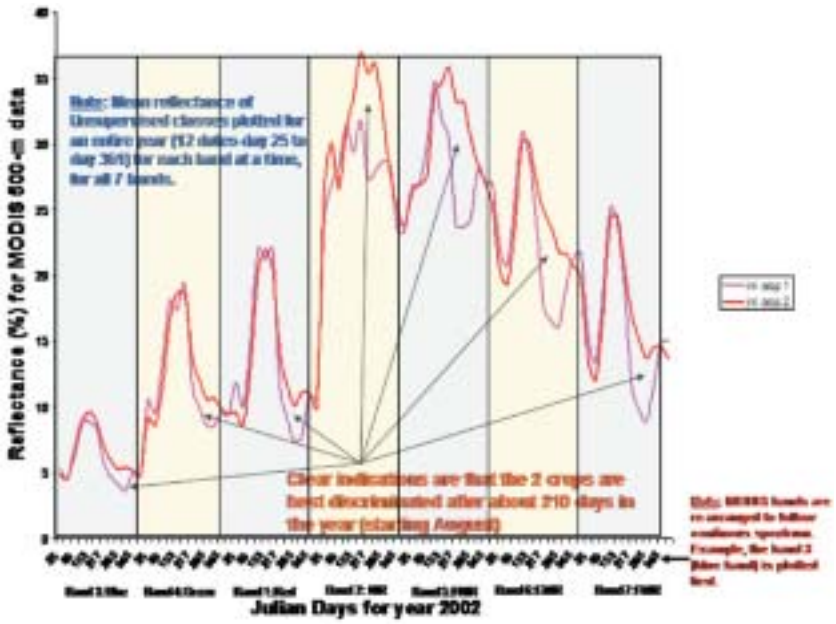

land cover modifications, in which the land cover type may have been altered but not changed (e.g., grassland degraded and a forest thinned), need to be monitored within and between seasons to understand events such as drought and degradation. Such change detection will help us inform environmental policy and decision making that underpins sustainable resource use.

Abrupt or permanent changes in the basins as a result of factors such as deforestation or natural disasters (Tucker et al.1984; Malingreau et al. 1989) will be determined through a simple change detection technique.

$$D\,X^{k}_{IJ} = D\,X^{K}_{IJ}(t_2) - D\,X^{K}_{IJ}(t_1)$$

where X^{K}_{IJ} is the pixel value for band k, and i and j are line and pixel numbers in the image; t_1 is the first date and t_2 is the second date (Singh 1989).

Most degradation occurs around road network and settlements. So an analysis of long time series data for the buffer lands within 2–5 km (walking distance) of settlements or a distance of 2.5 km, along either side of the roads must provide a fairly good indication of degradation over time.

Elsewhere, in the forest zones, degradation can be measured by fragmentation and its spread. The entire protected lands can be a unit to measure degradation, if any.

11.5.1 Change Vector Analysis

More subtle changes in basins involving land degradation and seasonal vegetation dynamics will be monitored using change vector analysis (Lambin and Strahler 1994) that provides:

1. Direction of change in time and space

2. Magnitude of change in time and space

The above phenomenon is best represented by NIR-red change vector procedure. This procedure is based on the magnitude (e.g., Figure 37) and angle of vector defined by pixel at time 1 to that of time 2. The change angle (è) and change magnitude (M) are computed using equations.

$\theta = \arctan (\Delta\lambda_{red} / \Delta\lambda_{NIR})$

$M = \text{Sqrt} [(\Delta\lambda_{red})^2 + (\Delta\lambda_{NIR})^2]$

Where, θ = change direction or angle; and M = change magnitude

$\Delta\lambda_{red}$ = red reflectance at time 2 – red reflectance at time 1

$\Delta\lambda_{NIR}$ = NIR reflectance at time 2 – NIR reflectance at time 1

For example, the change between every 8-day MODIS composites are computed using the above equations as illustrated in Figure 37.

11.5.2 Phenological Changes and Land Cover Transformations Captured in Tassel Cap

Phenological changes and land cover transformations (subtle or dramatic) in the basins are best captured in a tassel cap. The tassel cap is perhaps the best graphical representation of change direction (angle) and magnitude occurring at any point and at any scale. In most classical representation of tassel cap, LULC classes are plotted in a two-dimensional feature space of NIR versus red for time period 1 (e.g., Figure 38), time period 2 (e.g., Figure 39) and so on. In these plots we see how classes move around in feature space, in what directions they move, and what the magnitude of these movements are.

Land transformations are also efficiently captured by various principal components (PCs). The Principal Components Analysis (PCA) is especially important to reduce data volume in the present day data flood, yet capture the variability explained in a multitude of wavebands and temporal images. However, PCA is difficult to interpret, since each principal component (PC) is derived from the factor loadings (Eigen vectors) of all the bands of data. Hence, physically it is hard to explain what the particular PC represents even though factor loadings are indicative when 100s or even 10s of bands are involved, it is hard to describe what one single PC captures.

11.6 Landsat and Family of Satellites for Basin and Subbasin Studies

A new refreshing perspective is required in studies related to LULC at basin and subbasin level using high-resolution imagery. The present state-of-the-art make a whole range of advanced high resolution (aprox. 30 m) datasets very affordable or even free or nearly free (e.g., US$60 for an area of 3600 km^2 for ASTER). A critical point to note here is the advances made in terms of data quality and products produced using well-developed algorithms (unlike the primitives of the past), frequency of temporal acquisitions, radiometry, optics, and advances in processing and computer

Figure 37. Magnitude and spatial distribution of change over time depicted for 2 dates for a subarea in the Indus River basin. The red areas in the image below shows areas of 10 percent increase in magnitude during day 264 (image on top right) relative to day 153 (image on top left).

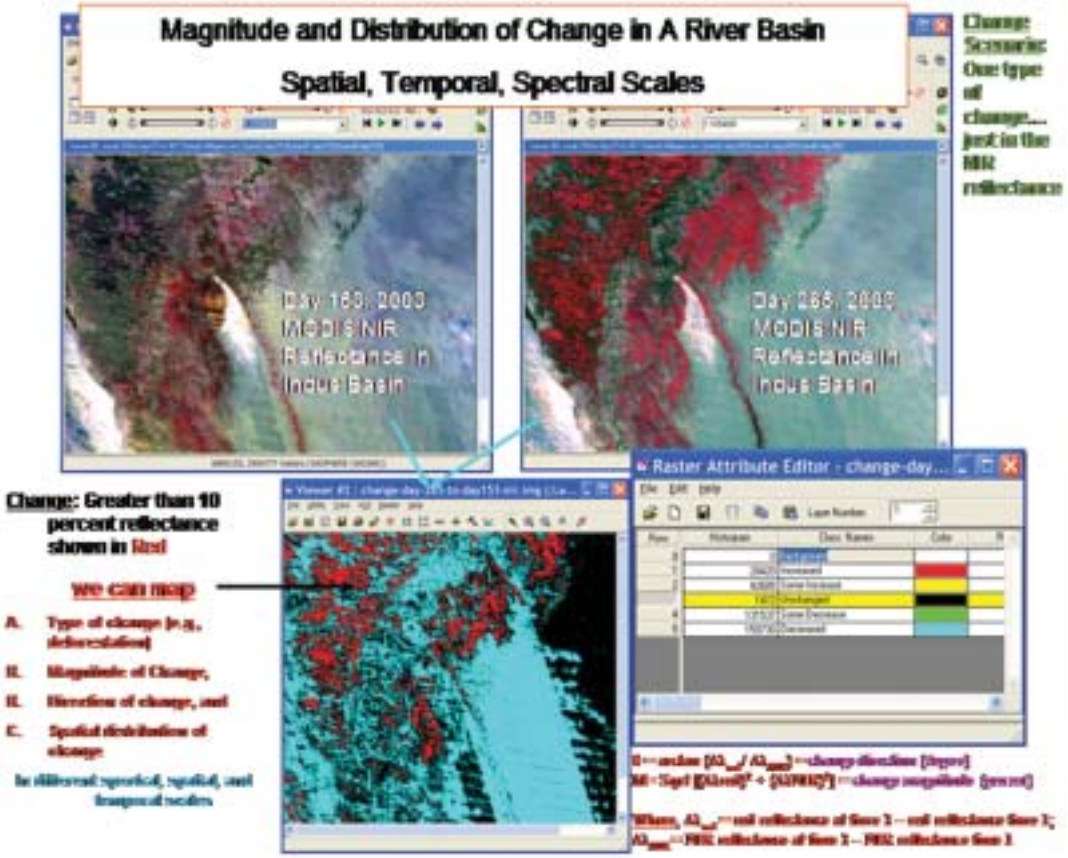

Figure 38. Tassel cap transformations on day 265, year 2002 in the Indus River basin. Each of the 10 classes moves around in the greenness, brightness and wetness spaces depending on vegetation dynamics in the landscape. Class 1 and 2 are in greenness space indicating high biomass and vigor. Again the subtle changes with time can be observed and monitored. Class 10 is in the brightness space (and is the brightest class) indicating high reflectivity from bare soil or settlements.

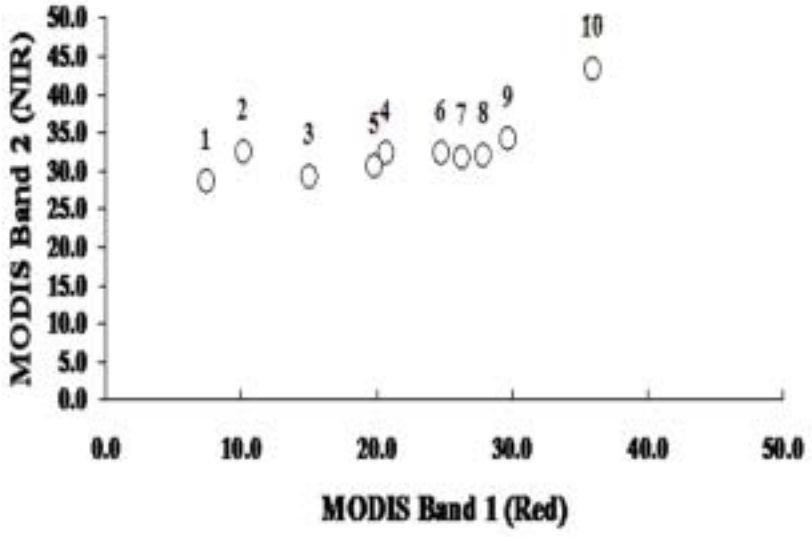

Figure 39. Tassel cap transformations on day 153, year 2002 in the Indus River basin. Each of the 10 classes moves around in the greenness, brightness and wetness spaces depending on vegetation dynamics in the landscape. All 10 classes are, more or less, along the soil line indicating that the entire landscape at this time of the year is mostly fallow or dry.

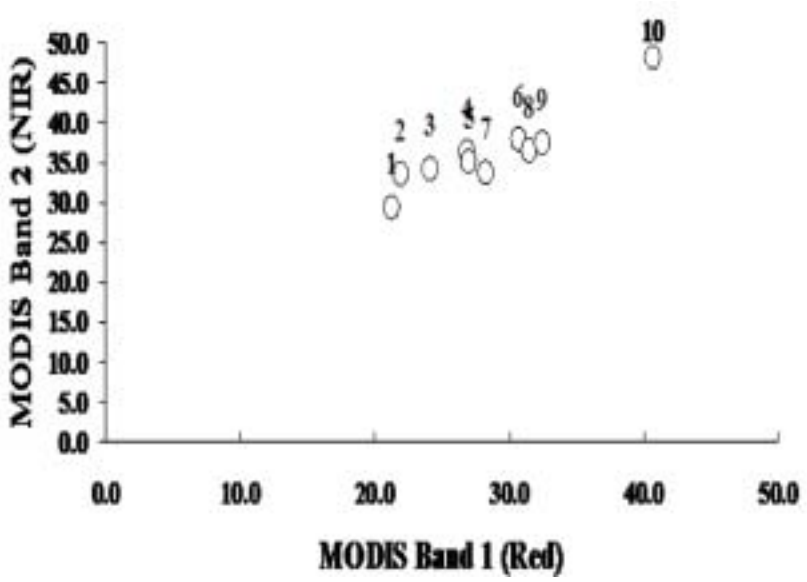

power that has made it possible for the first time to layer stack data from multiple sensors and for multiple dates. Combinations of these factors have taken any studies conducted using high spatial resolution data to new levels that are yet to be explored. Indeed, the scope of these investigations is yet to be fully comprehended.

What is really required today to handle and conduct scientific investigations using this high-resolution imagery is to focus on capacity in terms of expertise and people power, software, hardware, and data management and analysis. Time and resources here are critical.

A great advance in LULC studies at high resolution at basin and subbasin levels is feasible. Indeed, the perspective of the LULC studies will dramatically change when all the recent advances are taken into considerations and set a framework for generating the next generation of products.

Indeed, at basin and subbasin levels LULC studies should evolve into: (1) LULC continuous streams (e.g., monthly and quarterly), (2) great details (e.g., crop types and growth stages), (3) quantitative (e.g., LAI and biomass), and (4) information rich (e.g., crop moisture levels and crop stress levels). A matrix of possibilities exists.

11.7 Vegetation Dynamics and Phenology in Basins: Quantitative Parameters for Hydrological, Biophysical, and Socioeconomic Models

Within and between season vegetation dynamics need to be assessed all through the 5-year CP project period for every CP BB. A consistent study of all the basins is only possible through studies conducted using same datasets and same methods. At basin and subbasin levels, the MODIS 7-band reflectance data is ideal. Some characteristics that can be studied include:

Figure 40. The first principal component (PC1) image of the Indus basin area obtained from the principal component analysis (PCA) of 84 MODIS 500-m bands. Red is the brightest (least vegetation). Green has the highest vegetation and vigor, and blue intermediately. The light yellow is also a bright (low vegetation) area.

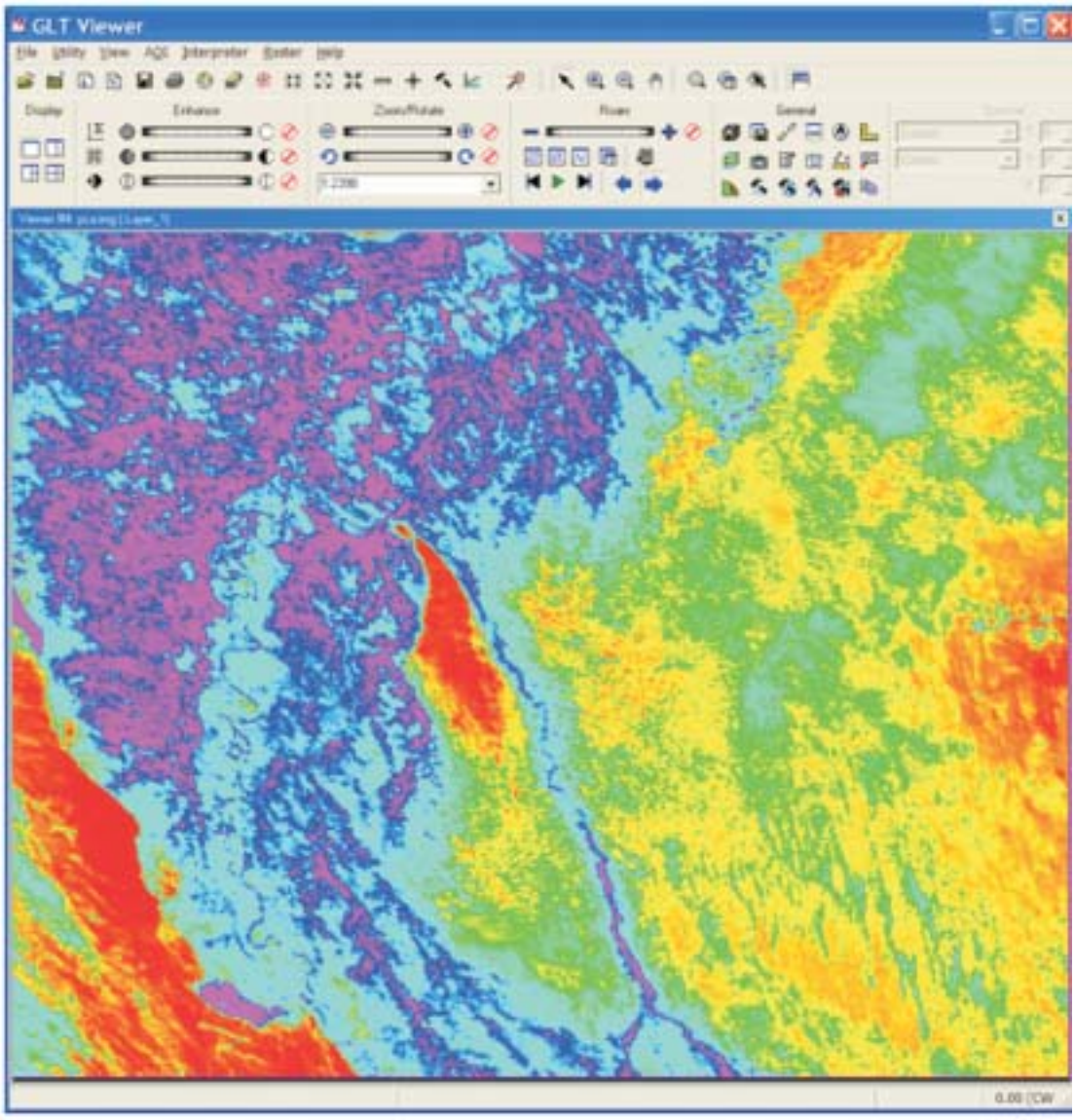

1. Beginning of green up stages or early growth phases: period of onset of photosynthetic activity;

2. Peak green period or critical growth phases: period of peak photosynthetic activity;

3. Senescence or beginning of "browning:" period of rapid fall in photosynthetic activity; and

4. Dormancy: end of photosynthetic activity.

This cycle is specifically dramatic and well defined in areas of rain-fed vegetation. It is more complex when irrigation is involved. Also in regions of bi-modal rainfall the vegetation dynamics is likely to have more than one cycle of green up to dormancy.

The study serves many purposes that include:

1. biomass productivity within and across seasons;

2. net primary productivity within and between seasons; and

3 onset of drought conditions, their magnitude and spread within and between seasons.

A typical, example of study of vegetation dynamics in a year is illustrated for Mekong basin in Figure 41.

Figure 41. Monthly mean vegetation dynamics in the Mekong River basin during year 2000 using the NOAA AVHRR 8-km data (coarsest available).

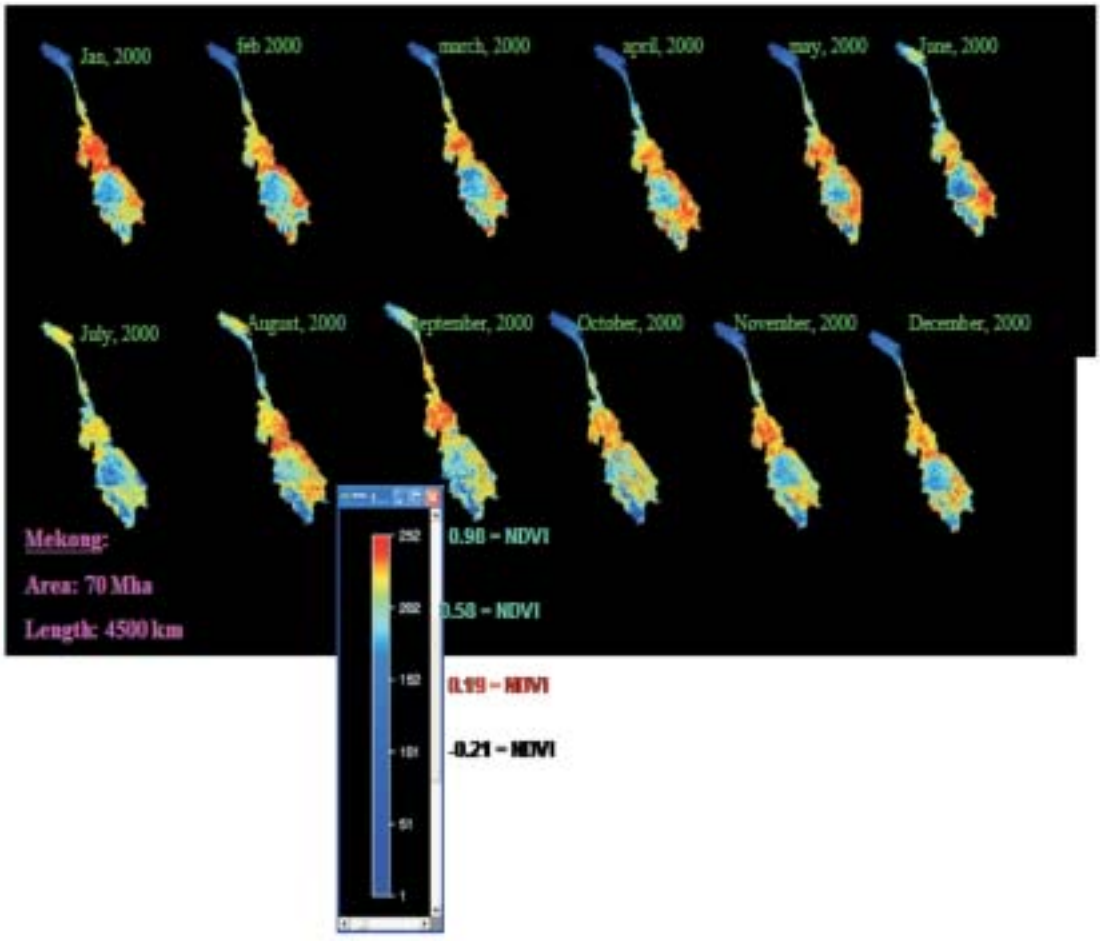

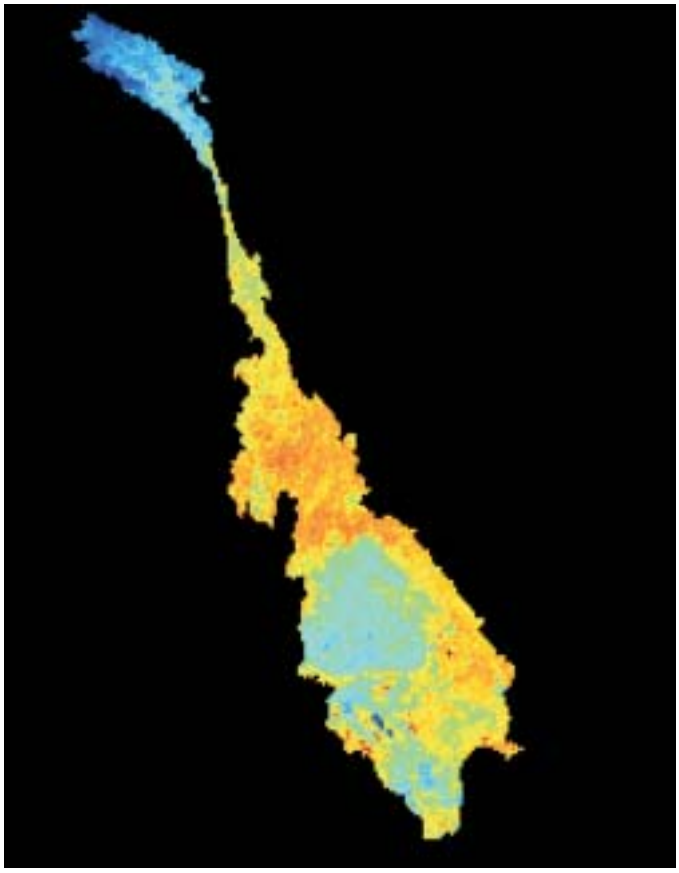

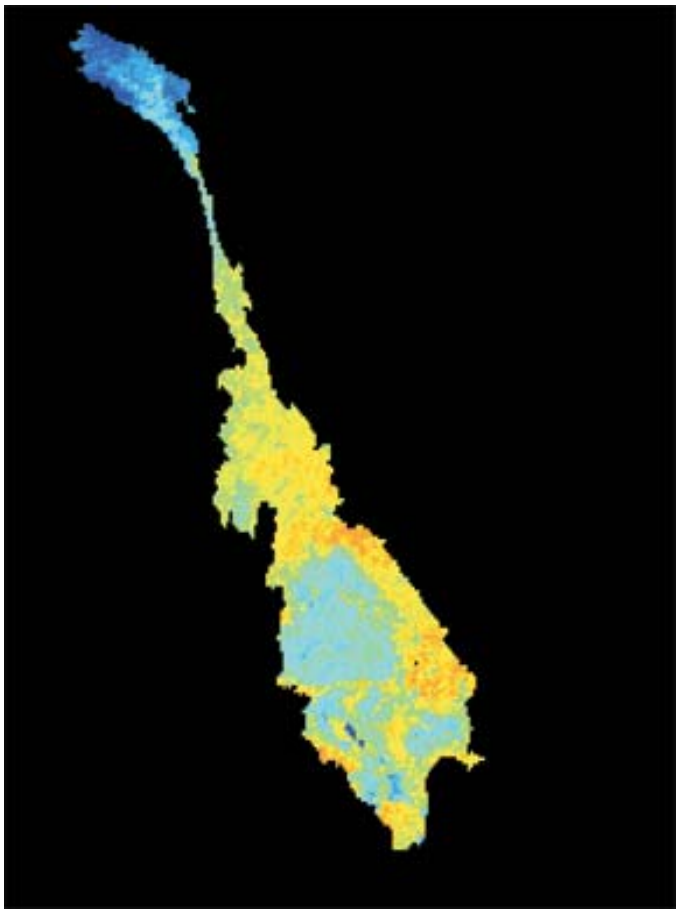

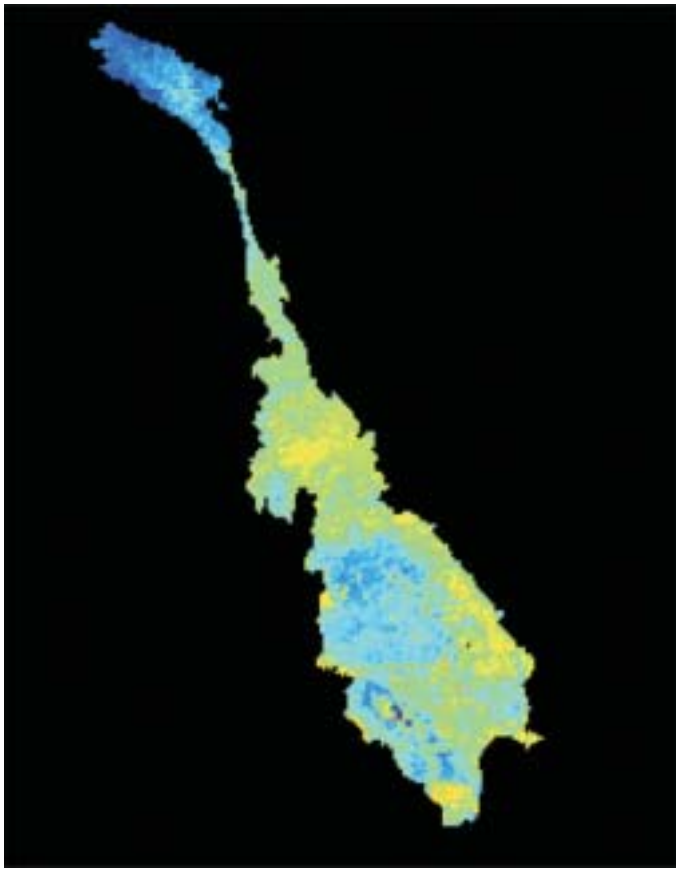

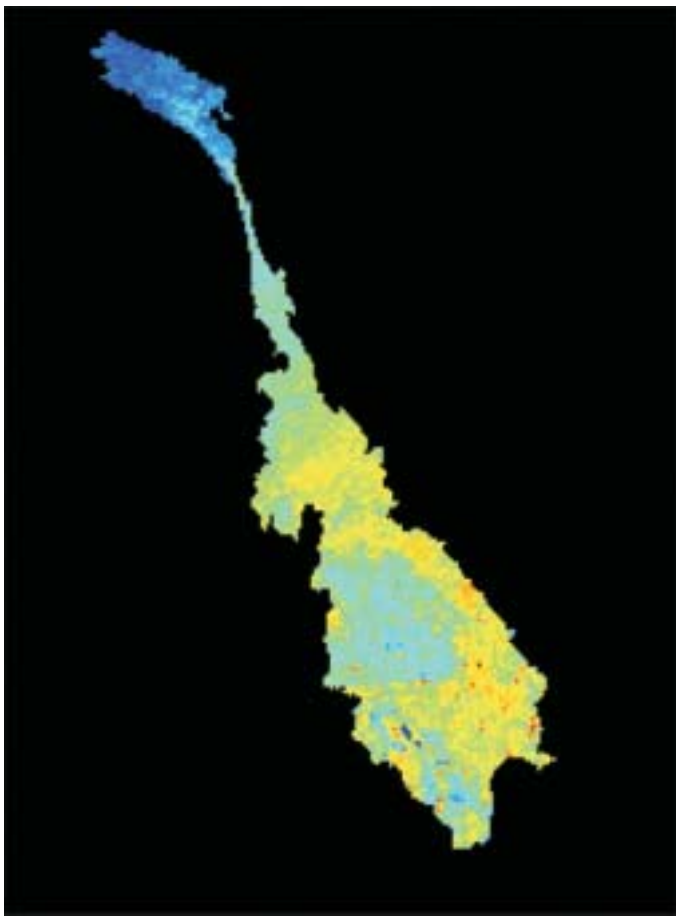

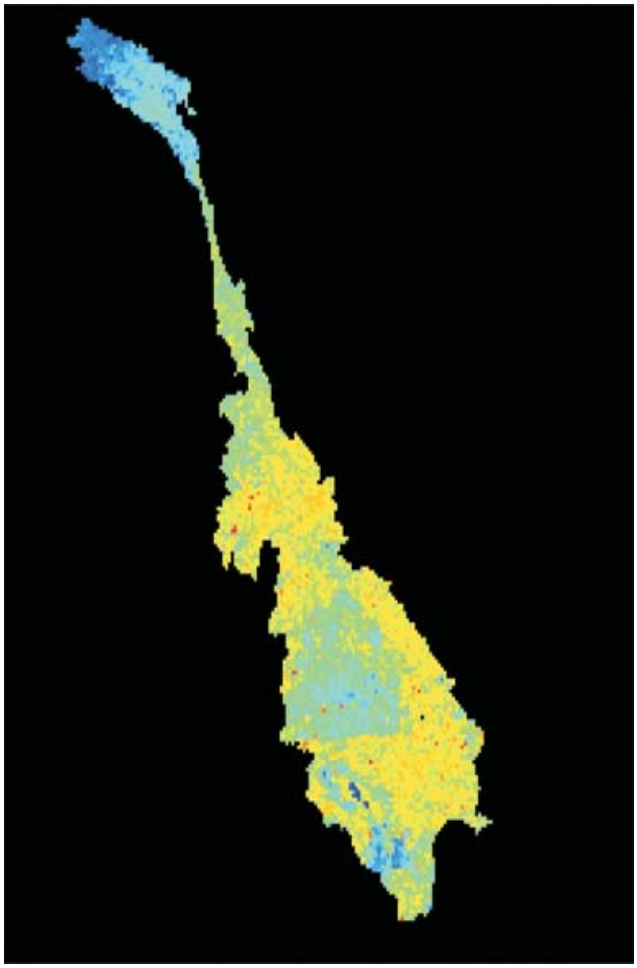

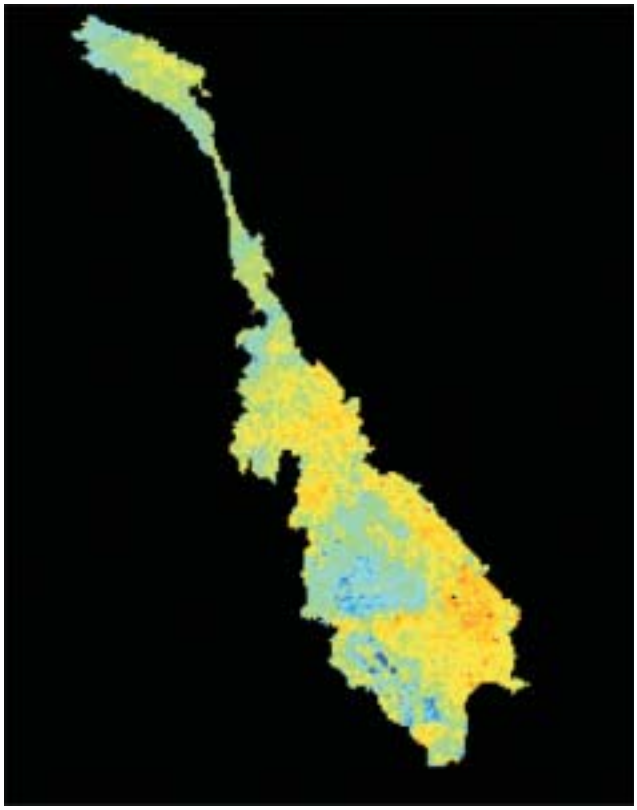

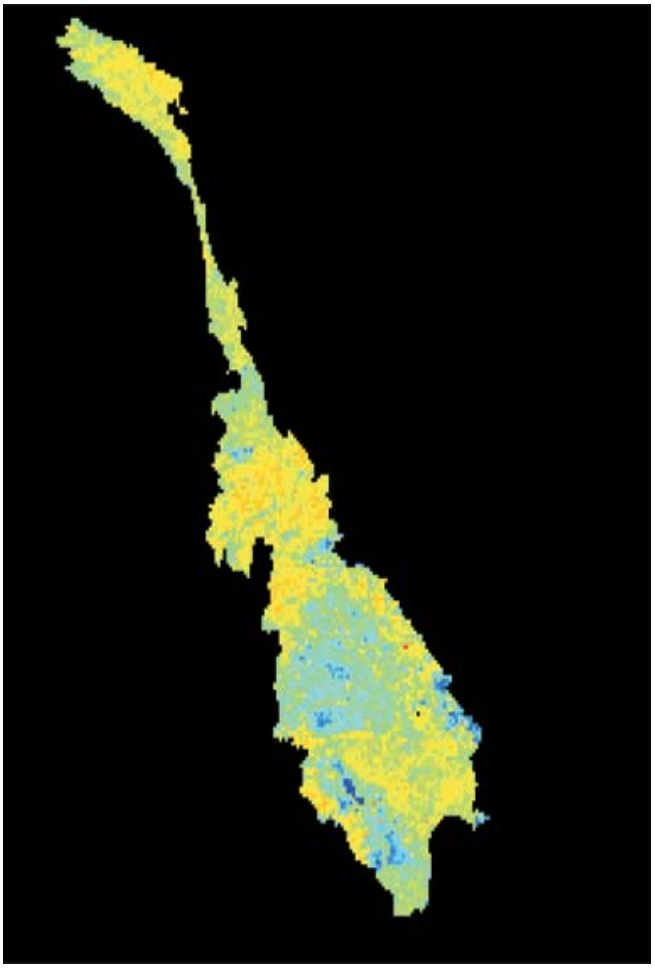

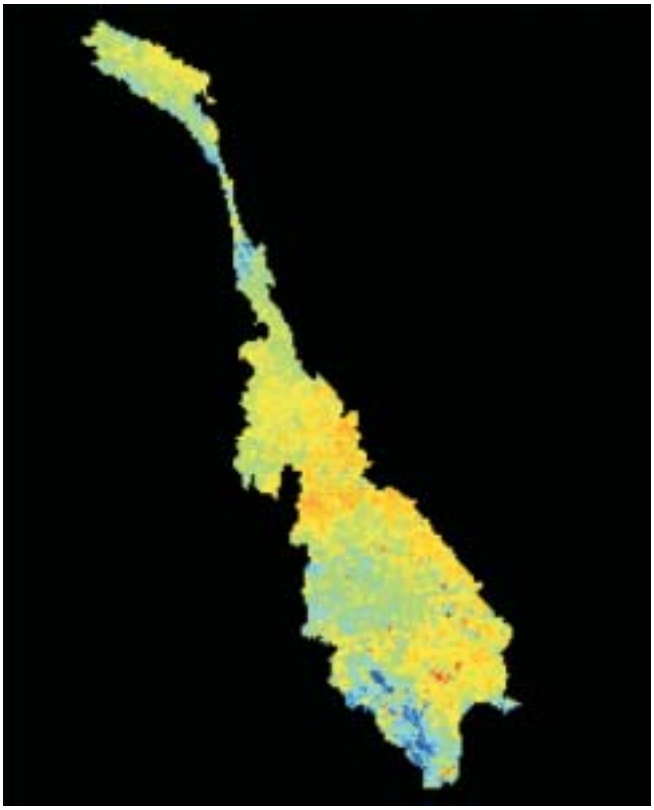

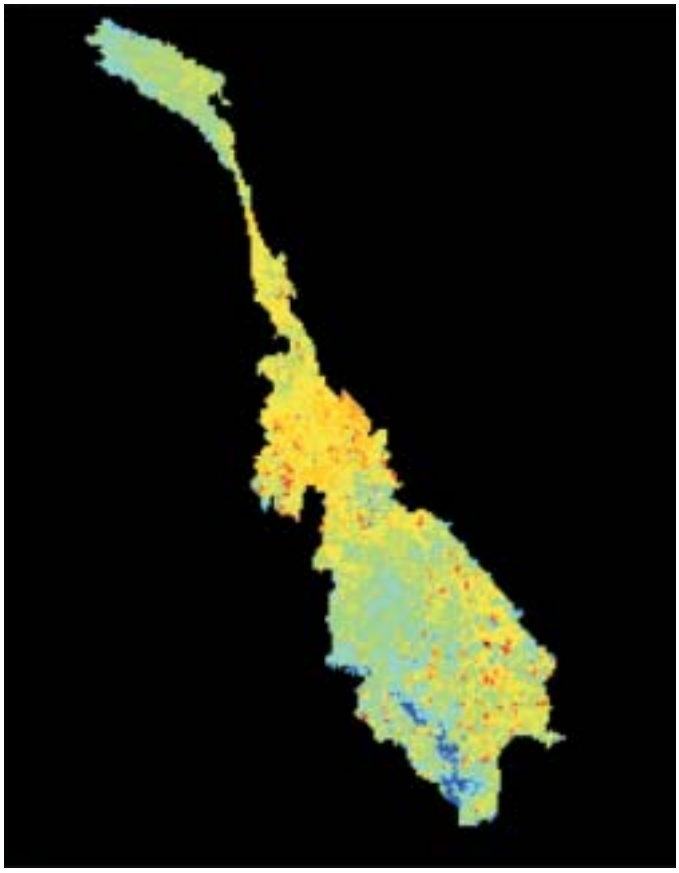

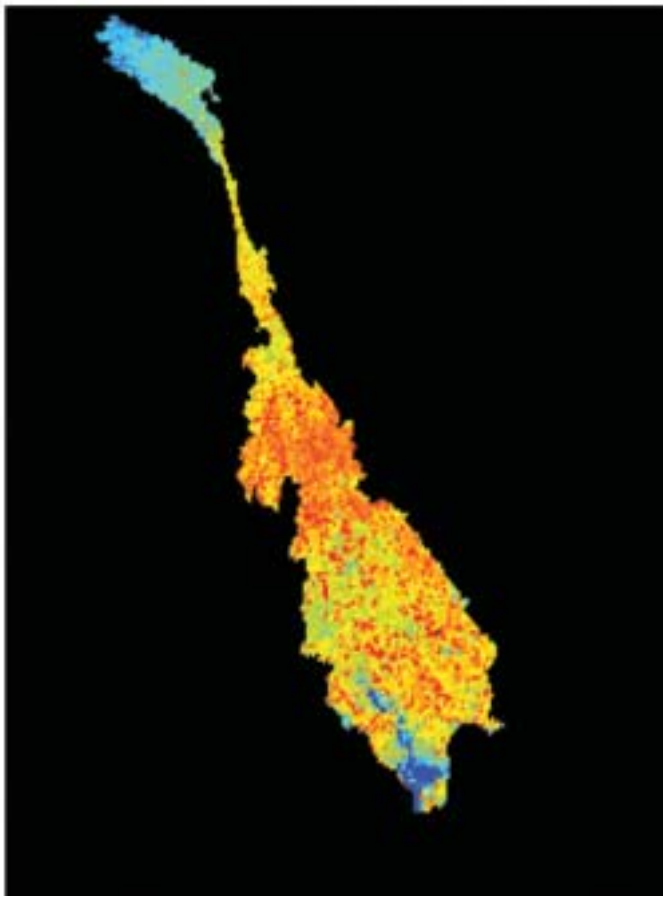

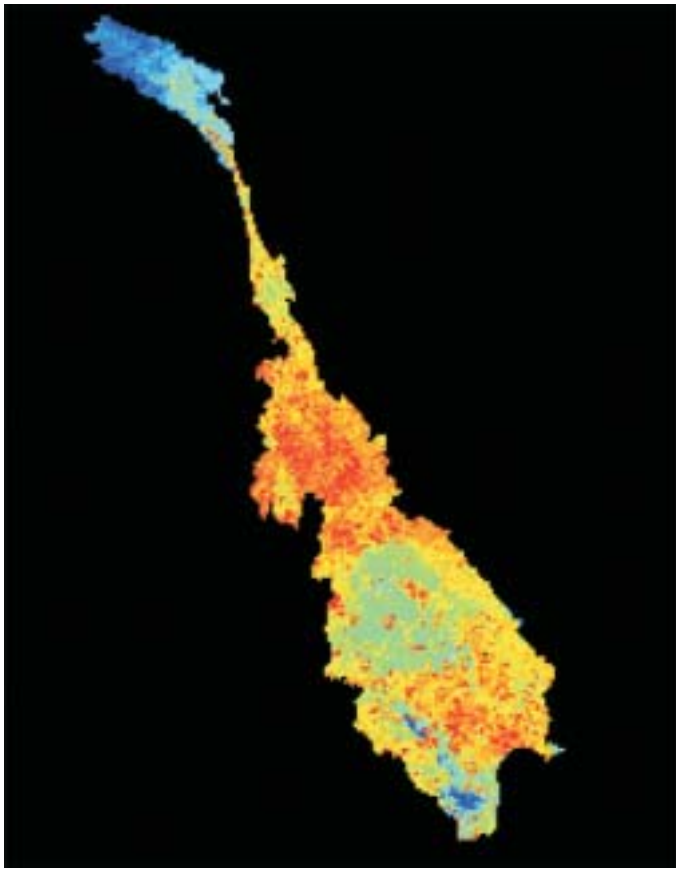

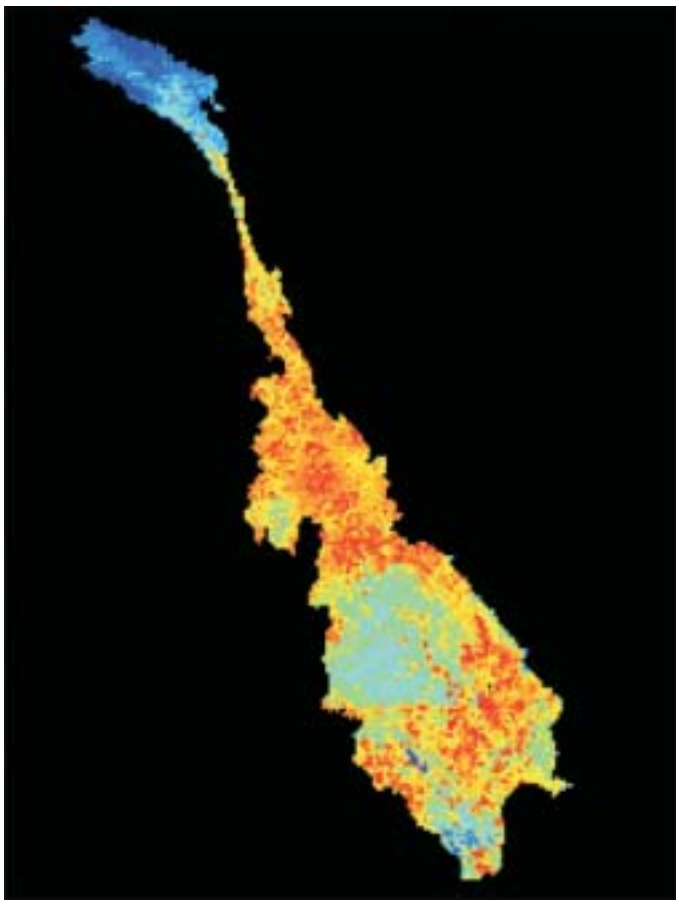

11.8 Snow Cover; Snow Depth; and Snowmelt Runoff of Large River Basins

The Ganges, the Indus, and the Yellow River have significant snowmelt runoff. The aerial extent, fluctuations in aerial extent within and between seasons, depth of snow extent, and snowmelt associated with rise in temperature can all be quantified and used in snowmelt runoff models.

The runoff resulting from snowmelt can be assessed for the three CP BBs using MODIS and historical AVHRR time series. The key snow products are:

1. aerial extent of snow cover and its spatial distribution every 8 days;

2. depth of snow and its water bearing potential;

3. frequency of occurrences of snow in different spots of the basins; and

4. variability of snow distribution and depth within and between seasons.

MODIS MOD10 is a snow product produced globally every 8-day at 500 m resolution. Hall et al. (2002) defined the MODIS snow index as:

$$\text{Normalized snow index (NSNI) for MODIS} = \frac{\text{Band 4} - \text{Band 6}}{\text{Band 4} + \text{Band 6}}$$

Where, bands 4 (0.545–0.565 µm) and band 6 (1.628–1.652 µm). However, such a snow index has many problems (see, Hall et.al. 1995 and 2002) and in the CP basin work, it will be more appropriate to all 7 MODIS Land bands reflectance data. Snow extent and distribution mapped at 500-m is shown in Figure 42. The 30-m data (Figure 43) can provide more detailed estimates, but will not have the same time frequency. The differences in snow cover mapping using different scales of data (Figure 44) are likely to be in snow depth, rather than in the snow spread area.

Earlier studies (e.g., Figure 45) have indicated that the visible and NIR bands have in particular been useful in snow mapping. However, the modern day sensors such as MODIS offer numerous wavebands and narrow bandwidths. These factors along with frequency of coverage of images will make the use of multiple waveband classification approaches very attractive in snow cover mapping of large aerial extents of large CP river basins.

11.9 Droughts

At basin and subbasin levels drought can be monitored at every 8-day period using MODIS 250-500 m data. Drought conditions are also reported globally by National Oceanic and Atmospheric Agency (NOAA) through weekly Vegetation Condition Index (VCI), Temperature Condition Index (TCI), and VCI/TCI ratio products (Kogan 1995). However, in CP basins we can produce more detailed assessment of drought conditions using MODIS data.

$$\text{Vegetation condition index} = VCI_j = \frac{(NDVI_j - NDVI_{min}) * 100}{(NDVI_{max} - NDVI_{min})}$$

Figure 42. Snow covers (white snow areas at the top of the basin) in the Ganges River basin using MODIS 500-m data. MODIS has MOD10 a snow cover product. But it is more powerful to generate snow cover, snow frequency, snow depth, and snow water potential data from MODIS primary products such as MODIS 7-band reflectance.

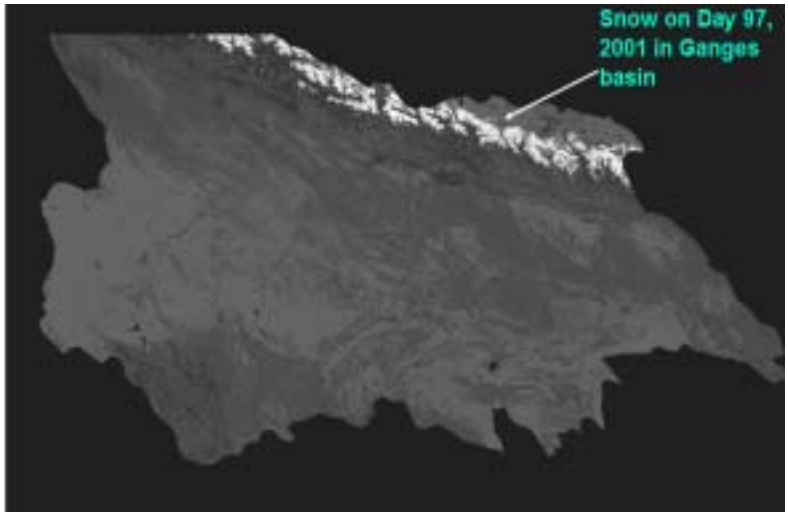

Figure 43. Snow cover area in the Indus River basin using Landsat TM 3 band Geocover product at 30-m depicted in simple RDB (FCC): 7, 4, 2. The geocover 3-band and 7-band data for the 1990s is available free of cost for the entire world. The data serves as orthorectified image (high geographical precision of ± 50 m) and as base maps useful for fieldwork.

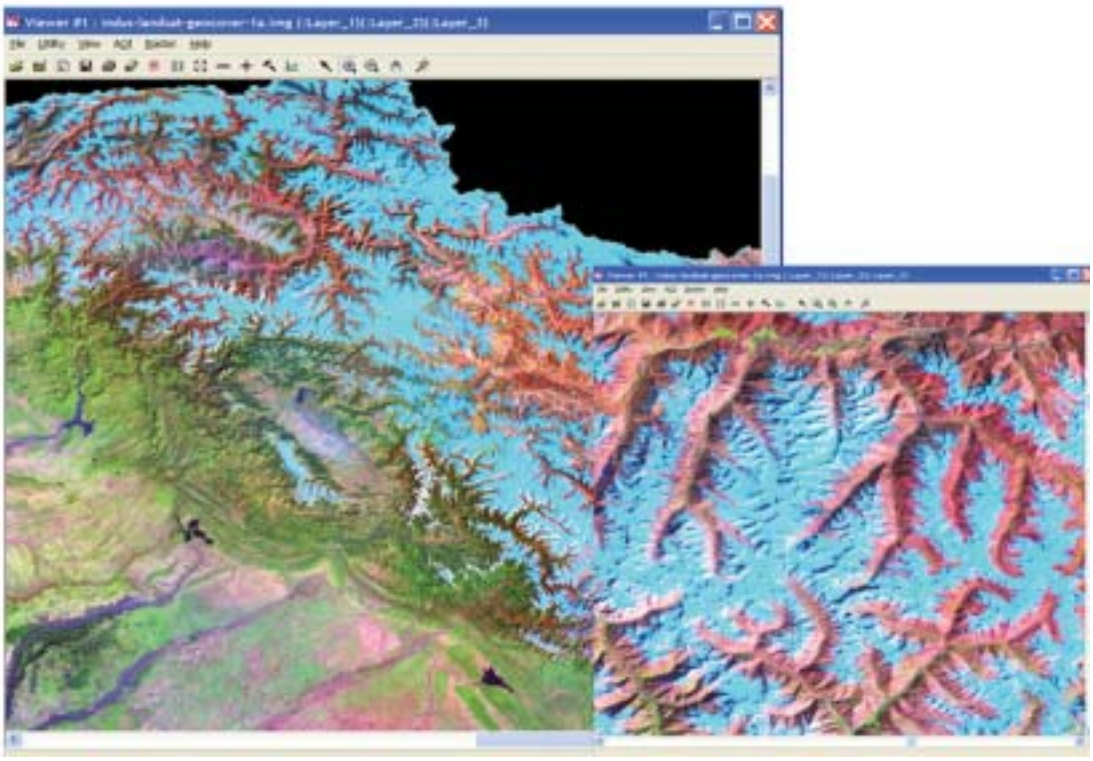

Figure 44. NOAA-AVHRR (a) and MODIS (b) derived snow cover for the Noguera Ribagorzana Basin (572.9 km2) in the Central Pyrenees of Spain on 7 April 2000. The different gray levels correspond to different percentages of snow cover in each NOAA-AVHRR and MODIS pixel (Schmugge et al. 2002).

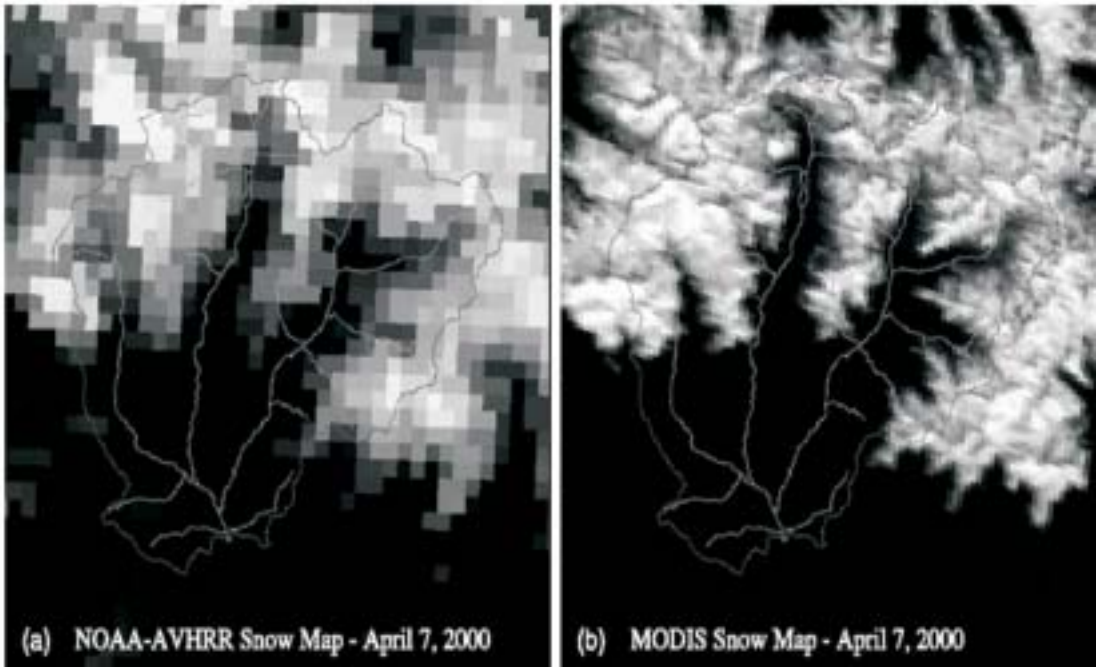

Figure 45. Snow frequency in the Euphratus and Tigris basins. The highest frequency of snow occurs along the Fertile Crescent.

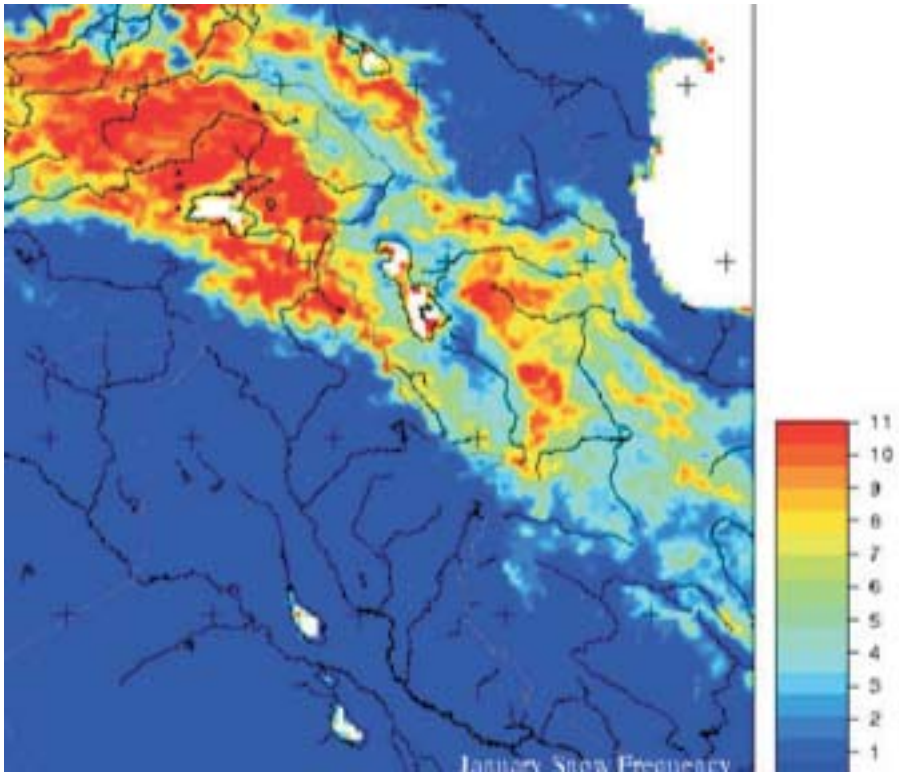

where $NDVI_j$ is the smoothed weekly NDVI, NDVImax, and NDVImin are absolute maximum and minimum NDVI, respectively, calculated for each pixel and week from multiyear smoothed NDVI data, *i* defines year. Low values of VCI indicate bad vegetation conditions and possible unfavorable weather impacts, while high values describe the opposite situation. VCI is known to capture rainfall patterns better than NDVI.

The temperature condition index (TCI) is similar to VCI, but expresses conditions contrary to VCI. When images are cloud contaminated the values of VCI or NDVI gets smoothed resulting in a false impression of stress or drought. As a result Kogan (1995) introduced TCI.

$$\text{Temperature condition index} = TCI_j = \frac{(BT_{max} - BT_i) * 100}{(BT_{max} - BT_{min})}$$

Figure 46. The weekly Vegetation Condition Index (VCI) during this year compared to the same week in the previous year using NOAA AVHRR 1-km data for the world. VCI is vegetation health, vigor, and drought condition indicator.

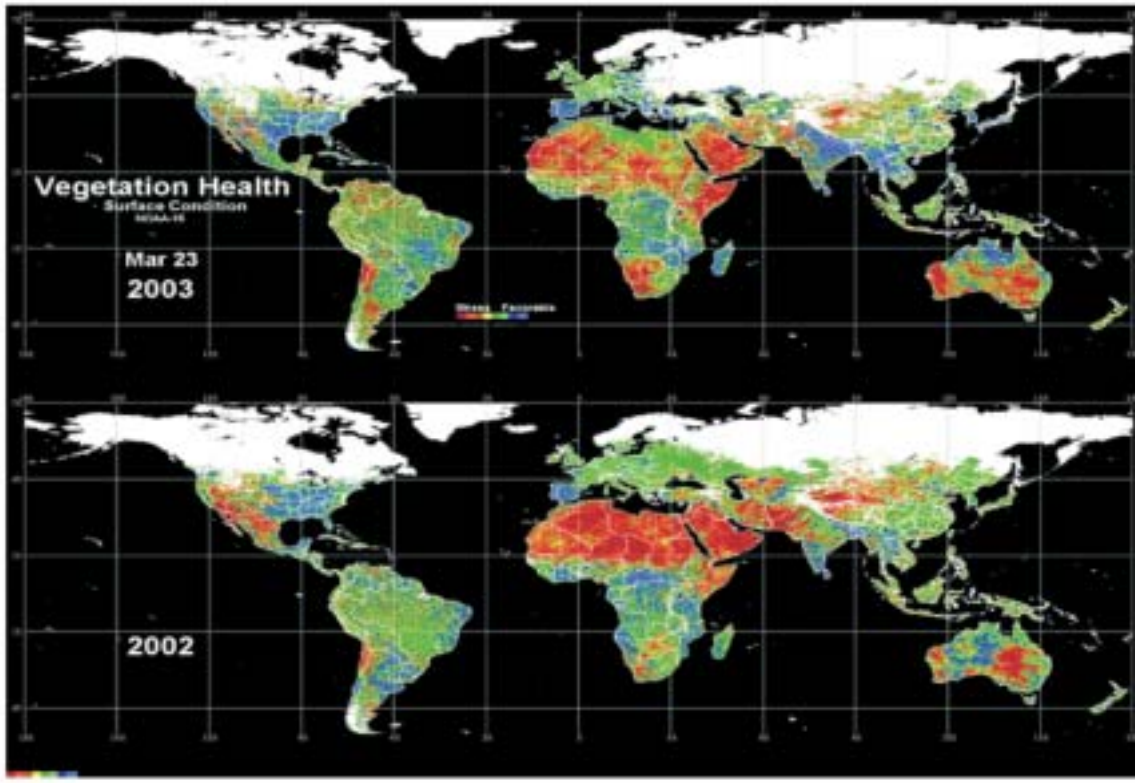

Figure 47. The weekly Vegetation Condition Index (VCI) during this year compared to the same week in the previous year using NOAA AVHRR 1-km data for Asia. VCI is vegetation health, vigor, and drought condition indicator.

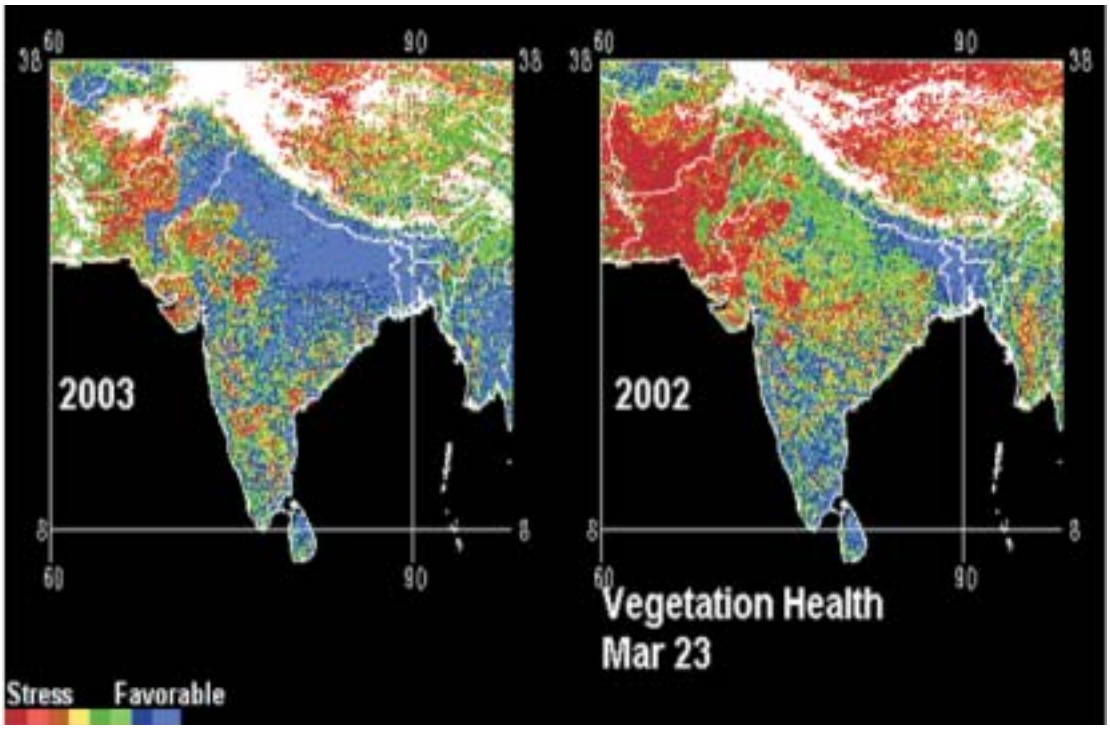

where BT, BTmax, and BTmin are smoothed brightness temperature, its maximum and minimum, respectively, calculated for each pixel and week from multiyear data; *i* is year. The BT is calculated from AVHRR Ch4 (10.3–10.3 *l*m).

11.10 Climatic Information Through Proxy from Satellite Sensor Data

The coarse resolution multi-temporal datasets will play a key role as proxy datasets for many climatic variables at basin and subbasin level studies. The climate data we would like to proxy include:

- Rainfall (e.g., MODIS and AVHRR NDVI)
- Temperature (e.g., AVHRR band 4 and 5 temperature)
- Growing degree days (e.g., MODIS and AVHRR NDVI)

11.10.1 Basin Precipitation

Direct estimates of precipitation using remote sensing data are not very reliable. The existing approaches include:

1. Global precipitation index (GPI) from the U.S. GOES geostatationary satellite;

2. Cold cloud duration (CCD) approach from the European METEOSAT;

3. A combination of GPI or CCD with rain gauge station data; and

4. Tropical rainfall measuring mission (TRMM) approach.

More accurate estimates of rainfall are feasible by gridding and classifying conventional rain gauge rainfall data as illustrated for the 1 degree (approx. 100 km) grid rainfall for the globe in Figure 48. The global resample NDVI from AVHRR and MODIS to 100 km grid and correlating with grided rainfall from conventional sources would provide interesting comparisons that needs to be taken up to develop definitive relationships between satellite sensor derived indices and rainfall amounts in space and time.

Figure 48. The 1 by 1 degree (100 km by 100 km) global rainfall grid for over 15 years (source: GPCC). We need to correlate this with the satellite derived rainfall estimates from METESAT cold cloud duration (CCD), GOES Global precipitation index (GPI), and Tropical Rainfall Measuring Mission (TRMM).

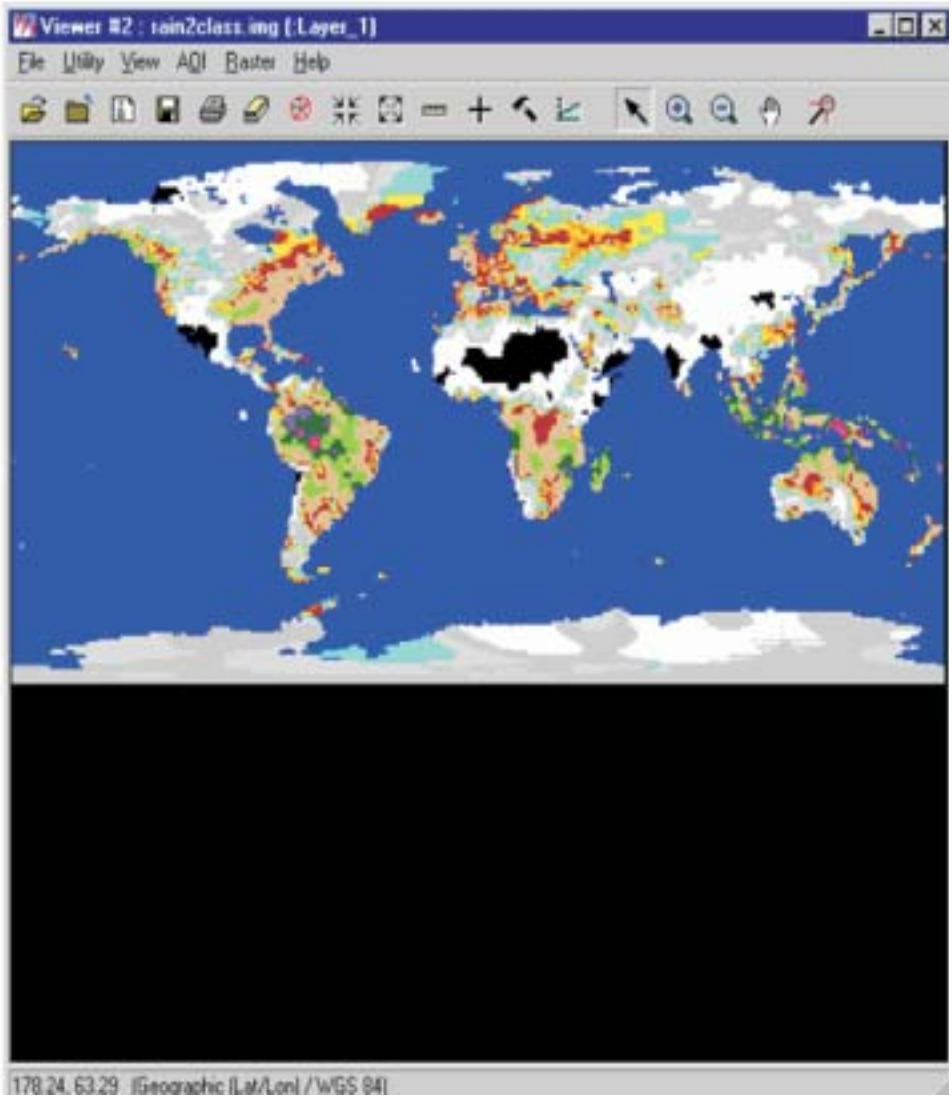

11.10.2 Basin Temperature

Basin temperature is reliably obtained from the thermal channels of MODIS band 29 (8.4-8.7 μm) and AVHRR band 4 (10.3-10.9 μm) and 5 (10.95-10.95 μm) and other thermal data (see for example, Figure 49). These data are also used to estimate evapotranspiration (ET).

11.10.3 Growing Degree Days

Significant correlations, for example, are known to exist between AVHRR NDVI and the ecoclimatic parameters GDD (Ichi et al 2002). The growing degree days (GDD) are calculated:

$$GDD = [(T_{max} + T_{min})/2] - T_{base} \quad (1)$$

where T_{max} is the daily maximum air temperature, T_{min} is the daily minimum air temperature, and T_{base} is the base temperature below which the process of interest does not progress.

Figure 49.

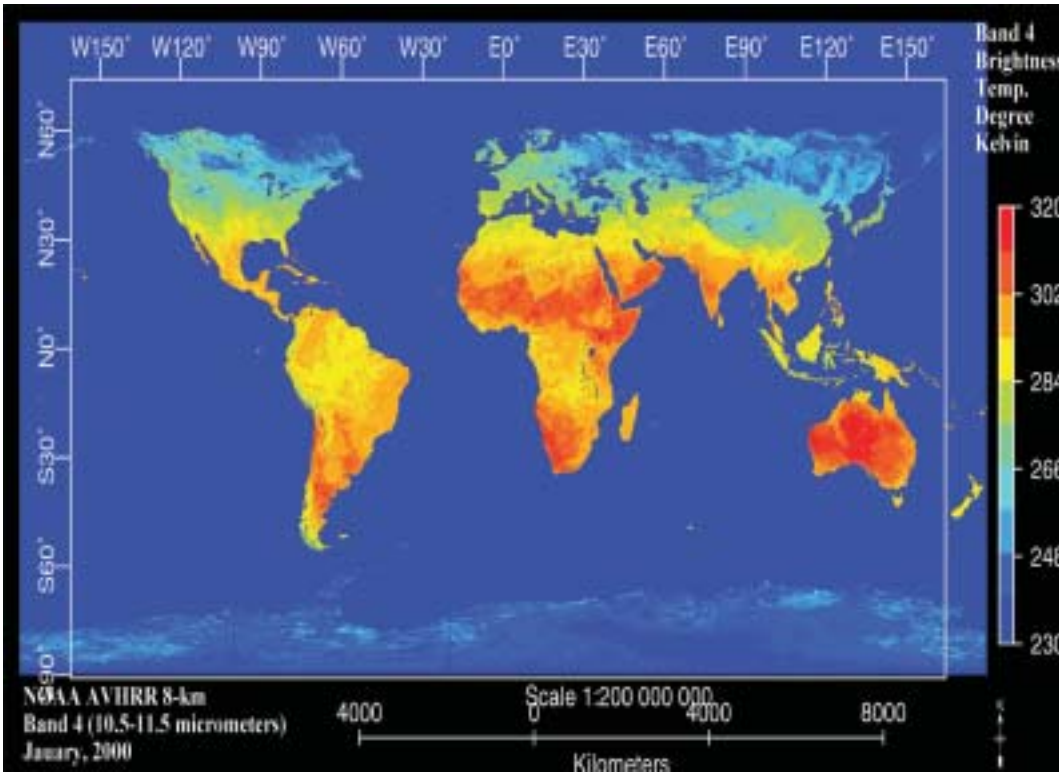

11.11 Agricultural Land Use; Fallow Dynamics; and Sustainable Development of Basins

Agriculture, by far, is the single largest consumer of water and, hence, a comprehensive study of agricultural crops in each basin in a must. With ballooning populations and increasing food

consumptions, a strategy needs to be adopted for sustainable development of river basins where yield per unit area increases but requirement of water decreases. Thereby, a comprehensive assessment of agricultural land use dynamics, fallow periods, crop water requirements, water harvesting techniques to supply moisture for crop in right amounts and at right times, crop biophysical characteristics, cultivation types (rain-fed versus irrigated), farming practices (e.g., till versus. no-till), cropping pattern (e.g., monocrop or multiple crops), and management practices is important for sustainable development of river basins and their preservation.

Remote sensing is a powerful tool in the study of many of these parameters. These are discussed below briefly:

11.11.1 Yield

Yield is the most sought after crop variable and perhaps most difficult to estimate using remote sensing, since there is not always a clear relationship between crop growth or conditions (which remote sensing can measure with reliability) and crop yield (which remote sensing has limitations to measure directly). However, with advances made using hyperspectral, hyperspatial, and advanced multispectral sensors the yield estimates are becoming increasingly more reliable (e.g., Figure 50). Models are typically used to predict end of the season harvest at various progressive time intervals of the growing season. The accuracies of such predictions are established in terms of probabilities or likelihood of being correct. It may also be appropriate to adopt a fuzzy accuracy framework.

Figure 50. Crop yield estimates using IKONOS on a field by field basis (Enclona et al. 2002). The same concept can be used to map spatial variability of yield across basins.

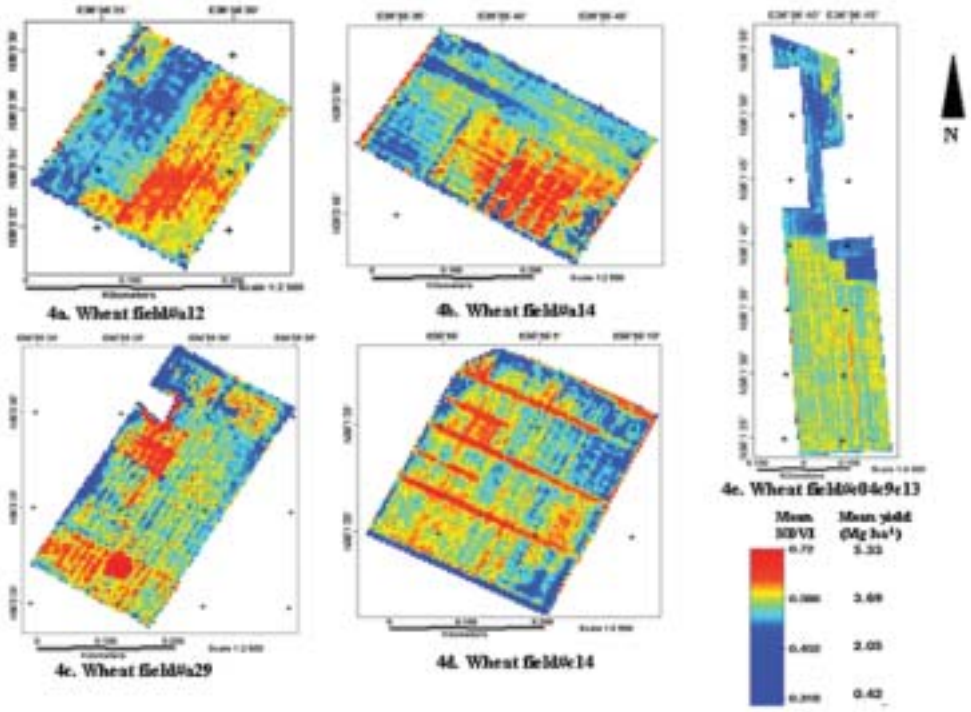

11.11.2 Biophysical Variables and Modeling and Their Relevance in Basin Studies

Crop biophysical variables such as LAI, fPAR, and biomass are key variables in characterizing crop growth, health, potential for yield, and are key remote sensing inputs in crop process models and hydrological models. Considerable improvements of the discharge simulations are possible by using remotely sensed LAI (Anderson et al. 2002).

Goal should be to have a seasonal assessment of crop development and yield by the thematic research groups highlighting stress indicators and plant water use over a range of spatial scales, from field, farm, watershed, subbasin, and basin. This will require establishing spectro-biophysical models. The methods of spectro-biophysical or yield modeling will involve:

1. Conventional Vegetation indices (CVIs): NIR and red based, soil adjusted, atmospherically corrected, and mid-infrared based indices as outlined in Table 4;

2. Two band vegetation indices (TBVIs): hyperspectral vegetation indices involving all possible two band combinations leading to models as illustrated in Figure 51 (see Thenkabail et al. 2003);

3. Optimum multiple waveband vegetation indices (OMBVIs): This approach permits the analyst to discover different relationships between the dependent variable and each waveband, including different polynomials, coefficients and transformations (Lawrence and Ripple 1998; Thenkabail 2002).

Relationships developed in above models will help us map the spatial distribution of the biophysical quantities on landscape for crop types (e.g., shown in 3-d display) or vegetation communities.

11.11.3 Crop Type and Growth Identification

The goal should be to map major crops at basin and subbasin levels that are mapped through:

1. Harmonic or Fourier analysis of time-series MODIS NDVI/EVI and/or AVHRR NDVI data by producing amplitude and phase images and incorporating the information in stepwise discriminant analysis to identify crop types. The harmonic analysis, or Fourier analysis, decomposes a time-dependent periodic phenomenon into a series of constituent sinusoidal functions, or terms, each defined by a unique amplitude and phase value (Jakubauskas et al. 2002).

2. Multi-band, multi-date classifications and tassel cap change vector analysis of various images.

11.11.4 Surface Temperature, Consumptive Use, and ET

The sensor data that will be used at basin and subbasin levels will have thermal bands that facilitate computation of temperature. For example, surface temperature is calculated by split window technique using NOAA AVHRR data. MODIS band 29 (8.4-8.7 μm) with 1,000 m spatial resolution like AVHRR provides surface temperature. There is a need to develop relationships between actual ET from different crops, specific vegetation categories (e.g., tea plantations), and a combination of all vegetation categories versus MODIS and AVHRR measured surface temperature. Such a

Table 4. Spectral vegetation indices and wavebands used in this study.

Vegetation Index Group	Vegetation Index name	Abbreviation	Definition[A, B]	Reference
1. NIR and RED waveband based vegetation indices	Normalized difference vegetation index	NDVI	$\frac{(NIR-RED)}{(NIR+RED)}$	
	Ratio vegetation index	RVI	$\frac{NIR}{RED}$	
2. Perpendicular vegetation indicesces	Perpendicular vegetation index	PVI	$\frac{(NIR-a*RED-b)}{\sqrt{(1+a^2)}}$	
3. Tassel cap based indices and non-linear indices	Greenness vegetation index[C]	GVI	$A_{2,1}X_1+ A_{2,2}X_2+\ldots.+ A_{2,n}X_n$ where, coefficient $A_{2,1}= \frac{g_i}{G}$ normalization factor is: $G=(\sum_{i=1}^{n} g^2_i)^{1/2}$ Choose a data point that represents green vegetation and forming the differences between that point and any point on the soil line $(x_g-x_s)_i$ $g_i=(x_g-x_s)_i - D_{2,1} A_{1I}$ GVI=0.056710*TM1+0.008573*TM2-0.423309*TM3+0.904168*TM4 (for spectrometer data) GVI=0.3088*TM1+0.2761*TM2-0.0642*TM3+0.8898*TM4+0.03618 *TM5-0.1764*TM7 (for actual Landsat TM data)	
	Global Environmental Monitoring Index	GEMI	$\eta(1-0.25\eta) - \frac{RED-0.125}{1-RED}$ $\eta = \frac{2*(NIR^2 - RED^2) + 1.5 * NIR + 0.5 * RED}{NIR+RED+0.5}$	
4. Soil adjusted vegetation indices	Soil adjusted vegetation index	SAVI	$\frac{(NIR-RED)}{(NIR+RED+L)}$ (1+L)	
	Transformed soil adjusted vegetation index	TSAVI	$\frac{(a*NIR-a*RED-b)}{(RED+a*NIR-a*b)}$ (1991)	
	Modified soil adjusted vegetation index	MSAVI	$\frac{NIR-RED}{NIR+RED+L}*(1+L)$ Where, L=1-2*a of soil line*NDVI*WDVI WDVI= NIR-g*RED g=a of the soil line	
	Optimized soil adjusted vegetation index	OSAVI	$\frac{(NIR-RED)}{(NIR+RED)+xfactor}$ where xfaxtor=0.16	
5. Visible waveband based vegetation indices	Visible band normalized difference vegetation index1	VBNDVII	$\frac{(GREEN-RED)}{(GREEN+RED)}$	This paper
	Visible band normalized difference vegetation index1	VBNDVI2	$\frac{(GREEN - BLUE)}{(GREEN+BLUE)}$	This paper
	Green band vegetation index1(only for narrow bands)	GRNDVI1	$\frac{(GREEN\ 0.560\ \mu m - GREEN\ 0.575\ \mu m)}{(GREEN\ 0.5\ 60\ \mu m + GREEN\ 0.575\ \mu m)}$	This paper
	Green band vegetation index2(only for narrow bands)	GRNDVI2	$\frac{(GREEN\ 0.525\ \mu m - GREEN\ 0.575 \mu m)}{(GREEN\ 0.525\ \mu m + GREEN\ 0.575\ \mu m)}$	This paper

(Continued)

6. Ultra voilet-early visible (0.350-0.450 μm) and NIR based vegetation index	Ulta voilet-early visible and NIR based normalized difference vegetation index	UNNDVI	(NIR-VISBAN1)where VISBAN1=0.35-0.45 μm (NIR+VISBAN1)	This paper
7. Derivative Green Vegetation Indices across the chlorophyll red edge (0.626-0.795 μm) -narrow band indices	First order derivative greenness vegetation index 1	DGVI1	$\sum_{n} \frac{(\rho'(\lambda_i)-(\rho'(\lambda j)}{\chi_i \quad \Delta\lambda_i}$ Where, I and j are band numbers, λ = center of wavelength, χ_i = 0.626 μm, χ_v = 0.795 μm, ρ′ = first derivative reflectance.	
	Second order derivative greenness vegetation index 2	DGVI2	$\sum_{n} \frac{\lvert(\rho''(\lambda_i)\rvert}{\chi_1 \quad \Delta\lambda_I}$ ρ = second derivative reflectance. Others same as in DGVI1.	
8. Other narrow bands used to compute various indices in groups 1-6 defined above and for computing multilinear regressions	1.43 nanometer wide narrow bands at specified wavelengths (center of the 1.43 nm wavelengths)	NB400, B485 NB525, NB560 NB575, NB678 NB717, NB735 NB850, NB920 and NB970.	0.400 μm, 0.485 μm 0.525 μm, 0.560 μm 0.575 μm, 0.674 μm 0.717 μm, 0.735 μm 0.850 μm, 0.920 μm, and 0.970 μm	This paper
9. Exponential, and power vegetation indices	Exponential indices	EXVI's	$a*e^{bVI}$	
	Power indices	POVI's	$a*VI^{b}$	
10. Growth stage, moisture and biomass sensitivity index in 0.94-1.04 μμ	Near infrared difference index1	NIRDIF1	(maximum value in 0.9-0.92 μm)- (minimum value in 0.96-0.98 μm)	This paper
11. Mid-infrared based vegetation indices[E]	mid-infrared normalized difference vegetation index57	MNDVI57	(TM5-TM7) (TM5+TM7)	This paper
	mid-infrared vegetation index ratio57	MVI5R7	TM5 TM7	This paper

A= a=slope or gain of the soil line; b=intercept or offset of the soil line obtained by plotting NIR and RED bands. The waveband range for BLUE: 0.40-0.50 μm, GREEN: 0.50-0.60 μm, RED: 0.60-0.70 μm, NIR: 0.70-1.3 μm. The exact ranges of these and other wavebands differ from sensor to sensor. For TM bands: TM1 (BLUE): 0.45-0.52μm, TM2 (GREEN): 0.52-0.60 μm, TM3 (RED): 0.63-0.69 μm, TM4 (NIR): 0.76-0.90 μm, TM5 (MIR1): 1.55-1.75 μm, TM7 (MIR2): 2.08-2.35 μm. The new bands are defined as follows: visible band 1(VISBAN1): 0.35-0.40 μm, visible band 2(VISBAN2): 0.35-0.45 μm, visible band 3 (VISBAN3): 0.40-0.50 μm, near infrared band 1 (NIRBAN1): 0.94-1.0 μm, near infrared band 2 (NIRBAN2): 0.94-1.04 μm

B= L=is soil adjustment factor for SAVI as defined by Huete (1988). L is 1.0 when canopy is very low (0-25 percent), 0.75 for canopy cover of 25-50 percent, 0.25 for canopy of 51-75 percent and 0 for canopy cover greater than 75 percent. When canopy cover is not known, L can be decided based on NDVI. For example, lower the NDVI, lower is the canopy cover, and hence higher will be L value and vice versa. Normally L is taken as 0.50.

C = the coefficients of GVI for the first 4 Landsat TM bands were, for example, computed using the principal component analysis (see Mishra and Wheeler 1977). Data points of the 4 TM bands for all land themes were used. The GVI defined above is for n-space.

D = VISBAN1=0.35-0.40 μm, VISBAN2= 0.35-0.45 μm, VISBAN3 = 0.40-0.50 μm, NIRBAN1= 0.94-1.0 μm; and NIRBAN2= in 0.94-1.04 μm.

E= mid infrared vegetation indices are used only for Landsat TM data from satellite based sensor. The hand-held radiometer did not have data in this wavelength.

Figure 51. Contour plot of R^2 values modeling crop biophysical variables using hyperspectral 2-band vegetation indices (TBVIs). Currently, we generate hyperspectral data from multi-temporal images as well (e.g., layerstacking of MODIS images over one year for a river basin). We are in a position to use these advanced vegetation indices, rather than a simple list of vegetation indices, due to advances in computer processing algorithms and frequent availability of high-dimension data. A wide range of biophysical characteristics (e.g., LAI, biomass and growth) of crops and vegetation are modeled using these indices. We expect these indices to play a key role in the study of basin characteristics (e.g., biomass, LAI quantification and degradation-subtle changes)

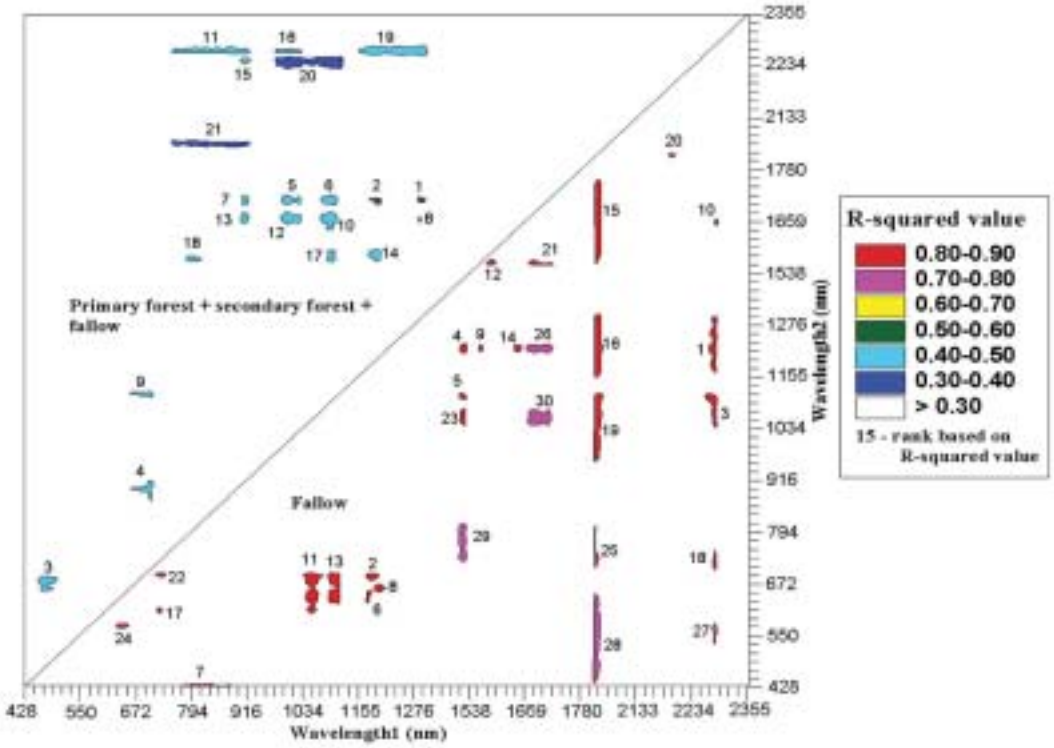

relationship will allow us to derive ET directly from thermal imagery and help us determine a crop by crop and vegetation by vegetation consumptive use.

Realistically, the time frequency of thermal data available from higher resolution imagery is highly inadequate for CU and ET calculations at subbasins. So MODIS 1,000-m imagery is the best option for near real time assessments of surface temperature every 8-16 days.

11.11.5 Crop Stress

Stress per se can be detected and quantified, and is an important parameter in order to assess drought, disease, and yield prediction. Water stress is well detected through absorption feature in 940-1,000 nm range and in the MIR. However, the greatest difficulty has been in detecting the type of stress (e.g., water deficit or excess, pest and disease, and nutrient deficiency). With timely and adequate field sampling backed by near-real-time images this problem can be overcome.

11.11.6 ET

In order to accurately determine — (ET) (evaporation from plants and soils) in every pixel of the basins will require characterizing precisely the plant and soil properties in each pixel. The goal is to characterize surface resistance to latent heat flux or ET. This will require:

1. Characterizing plants: type, species, growth stages, and growth conditions. Maps of LAI and biomass for different crop types or species types at different growth stages and/or conditions will be needed;

2. Characterize soils: moisture in soil needs to be quantified and mapped.

Both above characteristics vary in space and time and, hence, routine maps of above characteristics throughout the season are needed.

11.11.7 Quantitative Geomorphology: Wetland and Inland Valley Characterization

Remote sensing, in general, has great scope in extracting quantitative geomorphologic variables such as basin shape, size, and spatial distribution of drainage network, drainage density, and drainage frequency at basin, subbasin, and watershed levels (e.g., Figure 52). The implication of such ability is multifold. For example, delineating the stream network will help study their LULC patterns separately from rest of the landscape. The lands along the streams have greater moisture and generally have more fertile soils making them unique land units that are ideal for cultivating crops.

Figure 52. Basin quantitative geomorphology. Drainage density, drainage frequency, and spatial distribution of drainage network are rapidly mapped and characterized (e.g., lowland land use) using moderate to fine resolution images.

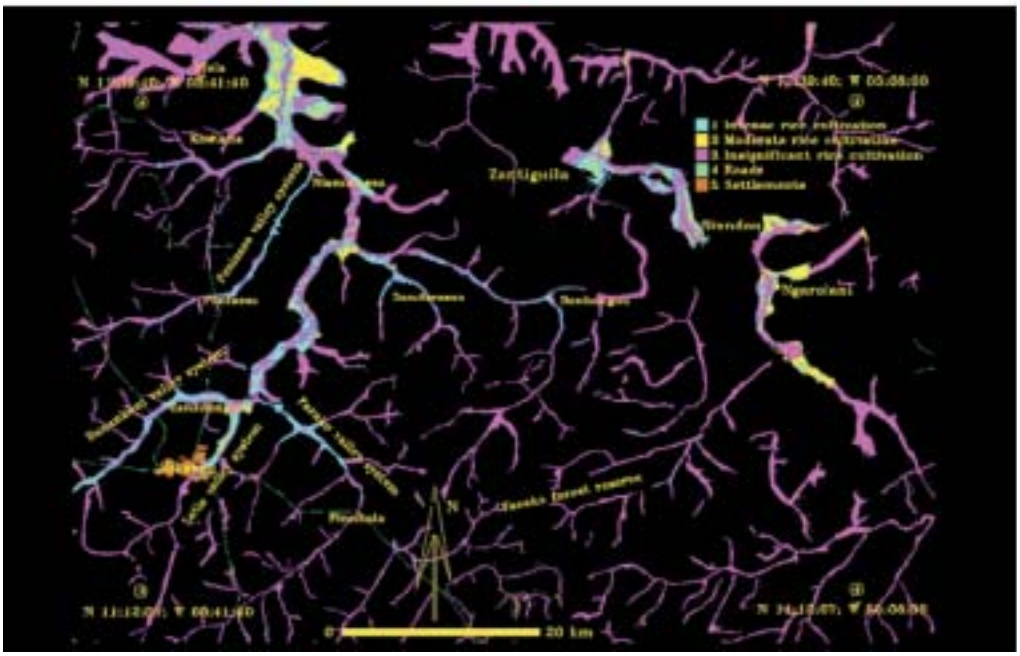

11.11.8 Floods

Basin parameters that impact floods such as quantitative geomorphologic variables, land use patterns, moisture regimes, and rainfall distributions will be established using METEOSAT, SSM/I, AVHRR, and TRMM datasets products.

The aerial extent and depth of floods can be mapped just after or few days after the event using various sources of imagery. Given the large sizes of the CP BBs, MODIS is again the most attractive. Also because MODIS time compositing helps obtain relatively cloud free images. The radar data from Radarsat and ERS will be of much value given their ability to see through the clouds which is crucial during the flooding season.

12.0 Ground Truth Data for Basin Characterization

A well-designed and well-organized ground truthing agenda is a must for mapping, modeling, and accuracy assessment of all the products. The essential components of ground truthing must include quantitative and qualitative measures of biophysical (e.g., LAI and biomass), hydrological (snow occurrences, snow depth, and rainfall amount), and land cover issues (e.g., percentage of cover and type of vegetation).

12.1 Sampling Design

The most efficient, cost-effective, and practical design of sampling framework at all levels (Basin, subbasin and watershed) in the benchmark basins will be:

12.1.1 Stratified-random Sample Design: The framework is stratified by motorable road network or even footpath access where possible. The framework is randomized by locating sites for every 10 minutes of drive.

12.1.2 Stratified-systematic Sample Design: The framework is stratified by motorable road network or even footpath access where possible. The framework is systematic by locating sites every 5 or 10 kilometers of drive along the road network or trek.

Of the total number of sample numbers, about 25 percent will be reserved for accuracy assessment.

Purely random sampling design is most ideal and least practical. Often in projects one comes across these idealistic designs only to be abandoned or compromised once the field activities begin, since such a design is almost impossible to implement, and certainly so at basin and subbasin levels. There may be a possibility of implementing such a design at watershed scales, but this again depends on the complexities of the landscape.

12.2 Sample Size

Congalton (1994) suggests that a rough rule of thumb for accuracy assessment is to use about 50 samples per class. This is feasible for subbasin and watershed studies when higher resolution data

are used. In such a set up, replicating samples in a fairly small area is not difficult. However, for basin level studies, such a large number of samples per class are impractical. It may be appropriate to have something like 10 sample locations per class for accuracy assessments at basin level studies. Lesser the sample size, lesser the precision and vice versa.

12.3 *Sampling Unit*

The sampling units will be pixels. Pixels are point-based sampling units that also have aerial component (Janssen and van der Wel 1994).

Sampling units for the CP BB work will be:

12.3.1 Medium and fine resolution*:* a 3 pixel by 3 pixel areas (90 meters by 90 meters) of a Landsat pixel (30-m) will be the most common sampling unit. This will provide data from nine effective pixels (0.81 hectares) per sample location.

This sample unit will also be used for all finer spatial resolution images. Thereby, for an IKONOS 4-m data, the number of effective pixels in 0.81 hectares will be 506 pixels. For better statistical sampling, in such cases use four sub-blocks within 90 meters by 90 meters area.

12.3.2 Coarse Resolution: For MODIS and AVHRR a 1 by 1 pixel area (e.g., 500 m by 500 m) area will suffice. However, one has to use utmost caution to determine the precise geolocation of the pixel. When one is not absolutely sure about the preciseness of the geolocation a larger number of pixels (3 by 3 pixels) may be needed.

13 Accuracies and Errors in Basin Classification; Parameterization; and Modeling

13.1.1 Accuracy Assessment in CP BB RS Work

All products produced using remote sensing and GIS in the research themes of CP BBs must strive for accuracy assessments. The goal should be to achieve overall accuracy levels of 85 percent. More than one measure of accuracy must be reported. A comprehensive review of literature (see Foody 2002) highlights the centrality of confusion matrix in accuracy assessments with a recommendation for reporting a second measure of accuracy.

Thereby, the essential components of accuracy assessments at all levels of CP BB work must involve (Table 5):

13.1.2 Error Matrix Reporting: overall accuracies, error of omissions, and errors of commissions.

13.1.3 Kappa Coefficient Assessments

The procedure for calculating and reporting such an accuracy assessment has been illustrated in Table 5.

Table 5. Classification matrix of rainforest vegetation using 23 Hyperion narrowbands. Discriminant model used to classify each observation into one of the groups.

Generalized Squared Distance Function: $D_j^2(X) = (X - \bar{X}_j)' COV^{-1} (X - \bar{X}_j)$

Posterior Probability of Membership in each CROPTY: $Pr(j|X) = \exp(-.5\, D_j^2(X)) / \sum_k \exp(-.5\, D_k^2(X))$

Number of Observations and Percent Classified into LULC

From LULC	Fallow (1-3 yr)	Fallow (3-5 yr)	Fallow (5-8 yr)	Primary forest	Disturbed primary forest	Mature secondary forest	Mixed secondary forest	Young secondary forest	Total	Errors of commission (%)
Fallow	5	0	0	0	0	0	0	0	5	
(1-3 yr)	100.00	0.00	0.00	0.00	0.00	0.00	0.00	0.00	100.00	0
Fallow	0	3	0	0	0	0	0	0	3	
(3-5 yr)	0.00	100.00	0.00	0.00	0.00	0.00	0.00	0.00	100.00	0
Fallow	0	0	2	0	0	0	0	0	2	
(5-8 yr)	0.00	0.00	100.00	0.00	0.00	0.00	0.00	0.00	100.00	0
Primary forest	0	0	0	12	0	0	0	1	13	
	0.00	0.00	0.00	92.31	0.00	0.00	0.00	7.69	100.00	8
Disturbed primary	0	0	0	0	3	0	0	0	3	
forest	0.00	0.00	0.00	0.00	100.00	0.00	0.00	0.00	100.00	0
Mature secondary	0	0	0	0	0	4	1	0	5	
Forest	0.00	0.00	0.00	0.00	0.00	80.00	20.00	0.00	100.00	20
Mixed secondary	0	0	0	0	0	0	8	0	8	
Forest	0.00	0.00	0.00	0.00	0.00	0.00	100.00	0.00	100.00	0
Young secondary	0	0	0	0	0	0	0	8	8	
Forest	0.00	0.00	0.00	0.00	0.00	0.00	0.00	100.00	100.00	0
Total	5	3	2	12	3	4	9	9	47	
	10.64	6.38	4.26	25.53	6.38	8.51	19.15	19.15	100.00	
Errors of Omission (%)	0	0	0	0	0	0	11	11	overall accuracy = 95.7 %	

$$K_{hat} = \frac{[N\sum_{i=1}^{r} X_{ii} - \sum_{i=1}^{r} X_{+i}(X_{i+})]}{[N^2 - \sum_{i=1}^{r} X_{i+}(X_{+i})]}$$

where, r is the number of rows in the matrix, X_i is the number of observations in row i and column i, X_{i+} and X_{+i} are the marginal totals of i and column i respectively, and N is the total number of observations.

Thereby, K_{hat} = [(47) (45) – 367] / [(47)^2 – 367] = 0.95; where (5*5) + (3*3) + (2*2) + (12*13) +(3*3) +4*5) + (9*8) + (9*8) = 367

Table 6. Image spectral, spatial, and radiometric characteristics. Image characteristics of hyper-spectral, hyper-spatial, and multi-spectral images of the rainforests of Akok in Cameroon.

Sensor	Spatial	Spectral	Radiometric	Band range (nm)	Band centers (nm)	Bandwidths (nm)	Irradiance
A. Hyper-spectral sensor							
1. Hyperion	30 m	196[a]	16-bit	196 effective Calibrated bands VNIR (band 8 to 57) 427.55 to 925.85 nm SWIR (band 79 to 224) 932.72 to 2395.53 nm	VNIR band centers start at 427.55 nm for VNIR and goes till 925.85 nm SWIR band centers start at 932.72 nm and goes till 2395.53 nm	10 nm wide (approx.) for all 196 bands	See data in Neckel and Labs (1984). Plot it and obtain values for Hyperion bands
B. Hyper-spatial sensor							
1. IKONOS	4 m	4	11-bit	445-516	480	71	9.88 (mW/cm^2)
				506-595	550	89	12.7
				632-698	664	66	9
				757-853	805	96	9.15
C. Multi-spectral sensors							
1. ALI multispectral	30 m	9	16-bit	433-453	443	20	1849.5(W/m^{2}Sr µm)
			450-515	483	65	1985.0714	
		425-605	565	80	1732.1765		
				633-690	660	57	1485.2308
				775-805	790	30	1134.2857
				845-890	868	45	948.36364
				1200-1300	1250	100	439.61905
				1550-1750	1560	200	223.39024
				2080-2350	2225	270	78.072727
2. Landsat-7 ETM+	30 m	6	8-bit	450-515	482	65	1970 (W/m^{2}Sr µm)
				525-605	565	80	1843
				630-690	660	60	1555
				750-900	825	150	1047
				1550-1750	1650	200	227.1
				2090-2350	2220	260	80.53

Note: a = Of the 242 bands, 196 are unique and calibrated. These are: (A) Band 8 (427.55 nm) to band 57 (925.85 nm) that are acquired by visible and near-infrared (VNIR) sensor; and (B) Band 79 (932.72 nm) to band 224 (2395.53 nm) that are acquired by short wave infrared (SWIR) sensor.

In addition:

13.1.4 Fuzzy accuracy assessment: will be included in some studies. The fuzzy approach (Gopal and Woodcock 1994; Woodcock and Gopal 2000) suggests a scale of error severity (e.g., correct, mostly correct, mostly incorrect, incorrect, and somewhat correct) in contrast to a simple correct/ incorrect evaluation. This is indeed an attractive proposition given in real world nothing is really as deterministic and definitive as correct and incorrect.

The accuracy assessment has evolved over the years that is outlined into four distinct stages by Congalton (1994):

a. Basic visual appraisal period: if it looked good it ought to be the right period. This was subjective and had to be abandoned.

b. Reference map comparison period: where an aerial extent of a class mapped was compared to a reference map. This approach was basically flawed due to uncertainties involved with the reference map. Often the reference map was historic.

c. Error matrix evaluation period: this is still at the heart of accuracy assessment today and involves the use of ground measured observations in accuracy assessments. The technique is solid, if the approach is solid. For example, the reference data if collected on a real or near-real time to mapping project then the relevance of accuracy matrix increases. Further, the accuracy assessment should not be limited to assessments of overall accuracies and errors alone

d. Improved error matrix approaches: involving techniques such as fuzzy and probabilistic logic applications (Congalton, 1994; Congalton and Green1999).

13.2 *Points to Reflect in Accuracy Assessments*

There are two myths in accuracy assessments that need attention in benchmark basin work.

First, a fundamental flaw in most accuracy assessments has been to compare a product produced with a reference map source that is either outdated or produced using a different set of definitions and primary datasets. In every accuracy assessment there is an inherent assumption that the reference map is more correct than the product produced. This is a myth.

A second, fundamental flaw has been to assume that all ground truth data are more accurate than the satellite derived products. This can be true, but is not necessarily true. Often ground truth data suffers from imprecise definition, incorrect labeling, imprecise quantification, errors in laboratory experimentation, and numerous other factors leading to more errors than remotely sensed data (Bauer et al. 1994; Bowers and Rowan, 1996; Merchant et al. 1994). Yet, ground truth data are always “supposed” to be the truth to which the satellite imagery is referred to check. This again is a myth.

13.3 *Sources of Error*

Measures need to be adopted to reduce the sources of errors in characterization, mapping, and modeling using spatial datasets at all levels of work in the benchmark. One cannot over-emphasize

the need for quality control at every level, so that the products have minimum chances of accumulative errors. Some common sources of errors include:

1. Misregistration: image misregistration, specifically in multidate images is common;

2. Ground truthing: mislabeling, wrong location, and wrong measurements;

3. Data entry: a common source of error often overlooked;

4. Classification techniques: classifying and labeling classes based on pixel-based classifiers, often leads to a single deterministic class. In reality every class is mixed and dynamic. Modern remote sensing datasets, analysis techniques, and computer hardware and software capabilities facilitate addressing these issues;

5. Interpreter consensus: degree of consensus is known to vary among image interpreters (even in automated classifications, this cannot be avoided completely).

13.4 Limitations of All Methods of Accuracy Assessments

The accuracy assessment methods are difficult to apply for coarse resolution AVHRR 1 or 8-km or MODIS 250 to 1,000-m pixels due to difficulties involved in ground-truthing and accurately characterizing and quantifying such large pixel areas. Thereby, there has been very little accuracy assessments of these global datasets.

The IGBP global LULC classes have a weighted accuracy of 66.9 percent, which is significantly less than the desired standard of 85 percent.

13.5 The Potential to Achieve Better Classification Accuracies in the CP BBs

There are many reasons why we should achieve better classification accuracies in the CP BBs. These include:

1. Focus on BBs: At all levels (basin, subbasin, and watershed) by focusing on CP BBs one will be able to classify far more classes than any global efforts. We will put substantial efforts in fieldwork that will help us better classify and achieve better classification accuracies.

2. Advanced sensor data: We will use datasets from MODIS, ASTER and other advanced sensors which have more number of bands and greater frequency of acquisition than ever before;

3. Cloud/haze cleaning algorithms: The advances made in providing the user with 8-16 day time composited images with sophisticated processing for cloud, haze, and other effects make the imagery far more attractive to accurate analysis than even before.

4. Advance methods and techniques: Advances in numerous methods and techniques involving sub-pixel classifications, multi-date and multi-sensor data processing, and availability of finer resolution data for ground truthing coarser resolution imagery must facilitate greater accuracies in classes mapped.

14.0 Summary and Discussions

The working paper provides a comprehensive framework on approaches and methods required to handle satellite sensor data from various eras for large CP BBs. The issues of data types, access, volumes, formats, exchange mechanisms, analysis techniques, calibrations, atmospheric corrections, and capacities (e.g., hardware, software, data, and expertise) have been discussed in detail. An automated operational system for generating continuous stream of satellite sensor based data, products, and science applications for the nine Challenge Program Benchmark river basins of the World has been advocated and a strategy for implementing the same has been discussed.

A. The First Step: The Data Banks

The very first step in this great challenge will be in populating science quality data sets. The complexity and challenge of populating the remote sensing data for the challenge program benchmark basins (CP BBs) is huge in terms of data types (see various sub-sections in section 4.0), data volumes (Table 8 through 10), data transfer rates, archival, and distribution mechanisms. The total volumes of data for all river basins will be in terabytes (Table 8 through 10). From all CP BBs and their associate basins, the MODIS data alone will have 40 tiles (Table 8a) consuming an estimated 797.4 GB (Table 8b) for 200-2003. The specific Landsat TM geocover tiles and AVHRR tiles for the CP basins and their estimated data volumes are listed in Table 9 and Table 10, respectively.

The recent advances in computing power and storage capacities (e.g., USB drives and RAID drives running to 100s of GB) have made it possible to handle huge data volumes. The working paper conceptualizes the development and integration of a seamless data bank that takes into consideration harmonizing and synthesizing satellite sensor data from a wide range of sensors providing data in various pixel resolutions, band widths, waveband range and number, and radiometry.

B. The Second Step: Knowledge Banks

The following product line (see Tables 11 and 12) is conceptualized by harmonizing and synthesizing satellite sensor data from the: (1) The Earth Observing System (EOS) era of MODIS-Terra/Aqua and Landsat-7, (2) The New Millennium era of the test of concept satellites such as Earth Observing-1 (EO-1), and (3) the older generation Landsat era:

1. Continuous streams of data products on a monthly time scale starting January 2004;

2. Baseline datasets, products, and indices for 2000-2003 from MODIS 500-m 7-band data;

3. Historical datasets, products, and indices for last 20-years using NOAA AVHRR data;

4. All of above at subbasin and watershed-levels at finer-scales using Landsat-7 and other data from high-spectral and high-spatial resolution sensors.

C. Third Step: Science Goals

Monthly, continuous streams of data and products (Tables 11 and 12) will be generated mainly from MODIS 500-m 7-band Land data every 8-16 days to produce land-use/land-cover (LULC),

Table 7. Characteristics of satellite sensor data at basin, sub-basin, and watershed level.

Code RS_Spectral Properties _ID	Number	Spectral Range	Unit Pol	Spectral Range Name	Ground Resolution	Res Name	Image Size km	Dynamic Range _bits	Application
1.0 Characteristics of basin level satellite sensor data									
1MODIS-Terra	1	620-670	µ m	Red (VIS)	250 m, 500 m, 1000m	2330	1000*1000		Absolute Land Cover Transformation, Vegetation Chlorophyll
-Aqua	2	841-876	µ m	Near infrared (NIR)	250 m, 500 m, 1000m	2330	1000*1000	8	Cloud Amount, Vegetation Land Cover Transformation
	3	459-479	µ m	Blue (VIS)	250 m, 500 m, 1000m	2330	1000*1000	8	Soil/Vegetation Differences
	4	545-565	µ m	Green (VIS)	250 m, 500 m, 1000m	2330	1000*1000	8	Green Vegetation
	5	1230-1250	µ m	Later NIR 1	250 m, 500 m, 1000m	2330	1000*1000	8	Leaf/Canopy Differences
	6	1628-1652	µ m	Early mid infrared 1 (EMIR 1)	250 m, 500 m, 1000m	2330	1000*1000	8	Snow/Cloud Differences
	7	2105-2155	µ m	Late mid infrared 1 (LMIR 1)	250 m, 500 m, 1000m	2330	1000*1000	8	Cloud Properties, Land Properties
	8	405-420	µ m	Blue 2	250 m, 500 m, 1000m	2330	1000*1000	8	Chlorophyll
			µ m		250 m, 500 m, 1000m	2330	1000*1000	8	
	9	438-448	µ m	Blue 3	250 m, 500 m, 1000m	2330	1000*1000	8	Chlorophyll
	10	483-493	µ m	Blue 4	250 m, 500 m, 1000m	2330	1000*1000	8	Chlorophyll
	11	526-536	µ m	Green 1	250 m, 500 m, 1000m	2330	1000*1000	8	Chlorophyll
	12	546-556	µ m	Green 2	250 m, 500 m, 1000m	2330	1000*1000	8	Sediments
	13h	662-672	µ m	Red 1	250 m, 500 m, 1000m	2330	1000*1000	8	Atmosphere, Sediments
	13l	662-672	µ m	Red 2	250 m, 500 m, 1000m	2330	1000*1000	8	Atmosphere, Sediments
	14h	673-683	µ m	Red 3	250 m, 500 m, 1000m	2330	1000*1000	8	Chlorophyll Fluorescence
	14l	673-683	µ m	Red 4	250 m, 500 m, 1000m	2330	1000*1000	8	Chlorophyll Fluorescence
	15	743-753	µ m	NIR 1	250 m, 500 m, 1000m	2330	1000*1000	8	Aerosol Properties
	16	862-877	µ m	NIR 2	250 m, 500 m, 1000m	2330	1000*1000	8	Aerosol Properties, Atmospheric Properties
	17	890-920	µ m	NIR 3	250 m, 500 m, 1000m	2330	1000*1000	8	Atmospheric Properties, Cloud Properties
	18	931-941	µ m	NIR post peak 1	250 m, 500 m, 1000m	2330	1000*1000	8	Atmospheric Properties, Cloud Properties
	19	915-965	µ m	Moisture sensitive NIR (MSNIR)	250 m, 500 m, 1000m	2330	1000*1000	8	Atmospheric Properties, Cloud Properties
	20	3.660-3.840	µ m	TIR 1	250 m, 500 m, 1000m	2330	1000*1000	8	Sea Surface Temperature
	21	3.929-3.989	µ m	TIR 2	250 m, 500 m, 1000m	2330	1000*1000	8	Forest Fires & Volcanoes
	22	3.929-3.989	µ m	TIR 3	250 m, 500 m, 1000m	2330	1000*1000	8	Cloud Temperature, Surface Temperature
	23	4.020-4.080	µ m	TIR 4	250 m, 500 m, 1000m	2330	1000*1000	8	Cloud Temperature, Surface Temperature
	24	4.433-4.498	µ m	TIR 5	250 m, 500 m, 1000m	2330	1000*1000	8	Cloud Fraction, Troposphere Temperature
	25	4.482-4.549	µ m	TIR 6	250 m, 500 m, 1000m	2330	1000*1000	8	Cloud Fraction, Troposphere Temperature
	26	1.360-1.390	µ m	EMIR 2	250 m, 500 m, 1000m	2330	1000*1000	8	Cloud Fraction (Thin Cirrus), Troposphere Temperature
	27	6.535-6.895	µ m	TIR 7	250 m, 500 m, 1000m	2330	1000*1000	8	Mid Troposphere Humidity
	28	7.175-7.475	µ m	TIR 8	250 m, 500 m, 1000m	2330	1000*1000	8	Upper Troposphere Humidity
	29	8.400-8.700	µ m	TIR 9	250 m, 500 m, 1000m	2330	1000*1000	8	Surface Temperature
	30	9.580-9.880	µ m	TIR 10	250 m, 500 m, 1000m	2330	1000*1000	8	Total Ozone
	31	10.780-11.280	µ m	TIR 11	250 m, 500 m, 1000m	2330	1000*1000	8	Cloud Temperature, Forest Fires & Volcanoes, Surface Temp.
	32	11.770-12.270	µ m	TIR 12	250 m, 500 m, 1000m	2330	1000*1000	8	Cloud Height, Forest Fires & Volcanoes, Surface Temperature
	33	13.185-13.485	µ m	TIR 13	250 m, 500 m, 1000m	2330	1000*1000	8	Cloud Fraction, Cloud Height
	34	13.485-13.785	µ m	TIR 14	250 m, 500 m, 1000m	2330	1000*1000	8	Cloud Fraction, Cloud Height
	35	13.785-14.085	µ m	TIR 15	250 m, 500 m, 1000m	2330	1000*1000	8	Cloud Fraction, Cloud Height
	36	14.085-14.385	µ m	TIR 16	250 m, 500 m, 1000m	2330	1000*1000	8	Cloud Fraction, Cloud Height
2 AVHRR	1	0.58-0.68	µ m	Blue-green region	1000 m	2400	Global	8	Chlorophyll absorption of healthy vegetation

(Continued)

	2	0.725-1.1	µ m		1000 m	2400	Global	8	Sensitive to varying vegetation biomass and emphasizes soil/crop and land/water boundaries
	3	3.55-3.93	µ m		1000 m	2400	Global		detects both reflected sunlight and earth-emitted radiation and is useful for snow/ice discrimination and forest fire detec
	4	10.30-10.95	µ m		1000 m	2400	Global	8	Crop stress detection and locating/monitoring geothermal activity. This channel is also commonly used for water surface temperature measurements
	5	10.95-11.65	µ m		1000 m	2400	Global	8	Similar to band 4, this channel is often used in combination with band 4 to better account for the effects of atmospheric absorption, scattering and emission
2.0 characteristics of sub-basin level satellite sensor data									
3 ASTER	1	0.52-0.63	µ m		15 m	60	60 x 60	8	green reflectance of healthy vegetation
	2	0.63-0.69	µ m		15 m	60	60 x 60	8	chlorophyll absorption
	3	0.76-0.86	µ m		15 m	60	60 x 60	8	vegetation discrimination because of red chlorophyll absorption
	4	0.76-0.86	µ m		15 m	60	60 x 60	8	vegetation discrimination because of red chlorophyll absorption
	5	1.6-1.7	µ m		30 m	60	60 x 60	8	Reflectance peak 1 in MIR. Sensitive to lignin, biomass, starch.
	6	2.145-2.185	µ m		30 m	60	60 x 60	8	Cloud Properties, Land Properties
	7	2.185-2.225	µ m		30 m	60	60 x 60	8	
	8	2.235-2.285	µ m		30 m	60	60 x 60	8	
	9	2.295-2.365	µ m		30 m	60	60 x 60	8	
	10	2.360-2.430	µ m		30 m	60	60 x 60	8	
	11	8.125-8.475	µ m		90 m	60	60 x 60	12	
	12	8.475-8.825	µ m		90 m	60	60 x 60	12	Surface Temperature
	13	8.925-9.275	µ m		90 m	60	60 x 60	12	
	14	10.25-10.95	µ m		90 m	60	60 x 60	12	Crop stress detection and locating/monitoring geothermal activity. This channel is also commonly used for water surface temperature measurements
	15	10.95-11.65	µ m		90 m	60	60 x 60	12	This channel is often used in combination with band 4 to better account for the effects of atmospheric absorption, scattering and emission
4 ETM+	1	0.45 - 0.515	µ m	Blue (VIS)	30 m	85	170 x 170	8	Water penetration, land use , vegetation characteristics, sediment
	2	0.525 - 0.605	µ m	Green (VIS)	30 m	185	170 x 170	8	Green reflectance of healthy vegetation
	3	0.630 - 0.690	µ m	Red (VIS)	30 m	185	170 x 170	8	Vegetation discrimination because of red chlorophyll absorption
	4	0.500 - 0.750	µ m	Panchromatic (PAN)	15 m	185	170 x 170	8	Mapping, land use, geography
	5	0.750-0.900	µ m	Near infrared (NIR)	30 m	185	170 x 170	8	plant turgidity, droughts, clouds, snow-ice discrimination
	6	1.550 - 1.75	µ m	Short wave infrared (SWIR1)		30 m	185	170 x 170	8 plant turgidity, droughts, clouds, snow-ice discrimination
	7	2.09 - 2.35	µ m	Short wave infrared (SWIR2)		30 m	185	170 x 170	8 Relative temperature, themal discharges, vegetation classification, surface moisture layer
	8	10.0 - 12.5	µ m	Thermal infrared (TIR)	60 m	185	170 x 170	8	Snow cover, vegetation water content
8 Advanced Land Imager: ALI	1	0.433-0.453	µ m		30 m	60	60 x 60	16	
	2	0.450-0.515	µ m		30 m	60	60 x 60	16	
	3	0.425-0.605	µ m		30 m	60	60 x 60	16	
	4	0.633-0.690	µ m		30 m	60	60 x 60	16	
	5	1.134-2.857	µ m		30 m	60	60 x 60	16	
	6	0.845-0.890	µ m		30 m	60	60 x 60	16	
	7	1.200-1.300	µ m		30 m	60	60 x 60	16	
	8	1.550-1.750	µ m		30 m	60	60 x 60	16	
	9	2.080-2.350	µ m		30 m	60	60 x 60	16	
		Pan	µ m	10 m		60	60 x 60	16	
5 SPOT	Pan	0.51-0.73	µ m	10 m		60	60 x 60	8	Isual interpretation, digitally sharpening lower-resolution

(Continued)

									multi-spectral data, and generation of stero pairs		
	1	0.50-0.59	µ m			20 m		60	60 x 60	8	Chlorophyll reflectance of healthy vegetation
	2	0.61-0.68	µ m			20 m		60	60 x 60	8	Distinguishing plant species, soil and geologic boundaries.
	3	0.79-0.89	µ m			20 m		60	60 x 60	8	Varying vegetation biomass and emphasizes soil/crop and land/water boundaries.
	4	1.5-1.75	µ m			20 m		60	60 x 60	8	Band has a high degree of sensitivity to soil and leaf moisture
6Landsat TM	1	0.45-0.52	µ m		30 m		185	185x170	8		
	2	0.52-0.60	µ m			30 m		185	185x170	8	
	3	0.63-0.69	µ m			30 m		185	185x170	8	
	4	0.76-0.90	µ m			30 m		185	185x170	8	
	5	1.55-1.74	µ m			30 m		185	185x170	8	
	6	10.4-12.5	µ m			30 m		185	185x170	8	
	7	2.08-2.35	µ m			30 m		185	185x170	8	
7 Landsat MSS	1	0.5-0.6	µ m		56 x 79 m		185	185x170	6		
	2	0.6-0.7	µ m			56 x 79 m		185	185x170	6	
	3	0.7-0.8	µ m			56 x 79 m		185	185x170	6	
	4	0.8-1.1	µ m			56 x 79 m		185	185x170	6	
3 JERS1	1	23.50	c m	L	Microwave			12.5,100,500	75 x 75	8	
3.0 characteristics of watershed level satellite sensor data											
9 IKONOS	1	0.445-0.516	µ m			4 m		10	10 x 10	11	Best data for mapping depth/detail of water covered areas
	2	0.506-0.595	µ m			4 m		10	10 x 10	11	Green reflectance of chlorophyll in healthy vegetation
	3	0.632-0.698	µ m			4 m		10	10 x 10	11	Distinguishing plant species, soil and geologic boundaries
	4	0.757-0.853	µ m			4 m		10	10 x 10	11	Sensitive to varying vegetation biomass. It also emphasizes soil/crop and land/water
boundaries											
	Pan	0.45-0.90	µ m			1 m		10	10 x 10	11	Visual interpretation and for digitally sharpening lower-resolution multi-spectral data
11 Quickbird-2		0.445-0.516	µ m			2.44 m		25	25 x 25	11	
		0.506-0.595	µ m			2.44 m		25	25 x 25	11	
		0.632-0.698	µ m			2.44 m		25	25 x 25	11	
		0.757-0.853	µ m			2.44 m		25	25 x 25	11	
	Pan	0.45-0.90	µ m			0.61 m		25	25 x 25	11	
2 Radarsat	1	50000.00	µ m	vv	Microwave - short wave	8X8	Fine		12.5 to 100	16	Melting snow, soil moisture, water-land boundaries
	2	50000.00	µ m	vv	Microwave - short wave		100X100	SwathSAR			
	3	50000.00	µ m	vv	Microwave - short wave		25x25	ScanSar			
	4	50000.00	µ m	vv	Microwave						

Need to have groups of sensor characteristics indexed by number for each sensor
NB Spectral bands ranges, and definitions vary from sensor to sensor.
Radar must have polarisations
SAR such as Radarsat has variable resolution options Have conventional names for bands, X,C,L,P
Sensors such as ASTER and Radarsat are pointable.

Table 8a. MODIS 500-m and 250-m tile X,Y and the number of tiles required for each Challenge Program Benchmark Basins (CP BBs).

Basin	Basin	Tile X-Y (area)[4,5]	Tile X-Y (area)[4,5]	Tile X-Y (area)[4,5]	Tile X-Y (area)[4,5]	Tile X-Y (area)[4,5]	Tile X-Y (area)[4,5]	Tile X-Y (area)[4,5]	Tile X-Y (area)[4,5]	Tile X-Y (area)[4,5]	Total Unique tiles
#	Name	X-Y (%)	X-Y (%)	X-Y (%)	X-Y (%)	X-Y (%)	X-Y (%)	X-Y (%)	X-Y (%)	X-Y (%)	#
1	Sao Francisco	13-10 (57)	13-11 (35)	13-9 (5)	14-9 (5)	14-10 (3)					3
2	Limpopo	20-11 (92)	20-10 (5)	21-11 (3)							3
3	Nile	20-7 (30)	21-7 (25)	20-6 (25)	20-5 (3)	21-6 (4)	20-8 (15)	21-8 (15)	20-9 (4)	21-9 (4)	9
4	Volta[1]	18-7 (70)	18-8 (25)	17-7 (5)							3
5	Indus	24-6(40)	24-5(25)	25-6(25)	23-6 (5)	23-5 (5)					5
6	Ganges	25-6 (60)	25-5(10)	24-6 (20)	24-5 (10)						1
7	Yellow River	27-5 (40)	27-4 (10)	26-5 (12)	28-5 (5)	27-6(5)	26-6 (5)				6
8	Mekong	27-7(35)	28-7 (30)	27-6 (21)	26-6 (10)	27-7 (2)	27-8 (2)				4
9	Karkey	22-5(70)	22-6(20)	21-5(10)							3
10	Virtual Andes[2.3]	10-9 (70)	10-8 (30)								2
11	Krishna[1]	25-7 (100)									1
							Total MODIS tiles from all basins				40

Note: 1 = is an associate basin
2 = is not a real basin with basin boundary, but covers basins or subbasins of different rivers in the Andes.
3 = 1 and 2
4 = MODIS path (X) and row (Y) and the estimated area of basin covered by the tile within the bracket
5 = the tiles highlighted are the unique tiles not repeated in any other basin. Tiles not highlighted are already covered in another basin.

Table 8b. Estimated storage volume for the MODIS 500-m and 250-m primary data for the Challenge Program Benchmark Basins[1,2].

MODIS data (m)	Total tiles for all basins #	per tile hdf MB	per tile Sinousoidal MB	per tile UTM MB	per tile 7 bands Sinousoidal MB	per tile 7bands UTM MB	# of tiles per year #	Total volume per year GB	Total volume for 2000-2003 GB	Total volume per year GB	Total volume for 2000-2003 GB
500 [3]	40	163	158	158	95	95	45	293.4	880.2	171	513
250 [4]	40	135	158	158	158	158	45	243	243	284.4	284.4
				USB drives: basins1, basins2, basins3, basins4, basins5 [5]							797.4
				USB drives: basins1B, basins2B, basins3B, basins4B, basins5B [6]							797.4

Note: 1 = MODIS 13 band data is reduced to 7 band data and reprojected to sinosoidal or UTM for archive
2 = before archiving the data will be moasicked into basins and only the data falling within basin boundary will be retained
3 = The 500 meter data is available for 2001, 2002, and 2003 (data for 2000 will not be used). Highlighted figures are used for volume calculations.
4 = The 250 meter data is available for 2003 (data prior to that, if any, will not be used). Highlighed figures are used for volume calculations.
5 = Main drive names
6 = mirror drive names

Table 9a. Landsat TM 3-band and 7-band mosaics of the Challenge Program Benchmark Basins (CP BBs).

Basin #	Basin Name	Tile X-Y (area)[4, 5] X-Y (%)	Tile X-Y (area)[4, 5] X-Y (%)	Tile X-Y (area)[4, 5] X-Y (%)	Tile X-Y (area)[4, 5] X-Y (%)	Tile X-Y (area)[4, 5] X-Y (%)	Tile X-Y (area)[4, 5] X-Y (%)	Tile X-Y (area)[4, 5] X-Y (%)	Tile X-Y (area)[4, 5] X-Y (%)	Tile X-Y (area)[4, 5] X-Y (%)	Total Unique tiles #	
1	Sao francisco											7
2	Limpopo											4
3	Nile	N-36-30(3)	N-35-30(2)	N-36-25(5)	N-35-25(4)	N-36-20(8)	N-35-20(6)	N-37-20(3)	N-36-15(8)	N-35-15(7)	N-37-15(4)	22
		N-36-10(9)	N-35-10(7)	N-37-10(6)	N-38-10(1)	N-34-10(3)	N-34-15(2)	N-37-5(4)	N-36-5(4)	N-35-5(4)N-34-5(3)N-35-0(4)	N-36-0 (4)	
4	Volta[1]											4
5	Indus	N-42-25(30)N-43-30(21)N-42-30 (12)N43-25(12)N-42-20(8)N-44-30(3)N-42-25(2)N-42-30(3)N-42-35(3)N43-35(3)N-44-35 (3)										11
6	Ganges	N-44-25 (20)N-43-30 (15)N-43-25 (14)N-45-25(14)N-45-20(14)N-44-20(8)N-45-20(7)N-43-20(4)N-44-30 (4)										4
7	Yellow river	N-48-35(7)N-48-40(10)N-48-45(10)N-49-35(7)N-49-40(8)N-49-45(9)N-50-35(5)N-50-40(6)N-50-45(5)N-47-35(6)N-47-40(9)N-47-45(4)N-47-30(4)N-48-30(5)N-49-30(4)N-50-30 (1)										16
8	Mekong	N-49-10(12)N-48-05(2)N-47-10(4)N-48-15(10)N-47-15(9)N-49-15(2)N-47-20(10)N-47-25(10)N-47-30(10)B-48-20(6)N-46-20(5)N-48-25(6)N-46-25 (7)N-46-30(4)N-48-30 (3)										12
9	Karkey	N-39-30(82)N-38-30(15)N-39-25(3)										3
10	Virtual Andes[2,3]											6
11	Krishna[1]	N-43-15(40)N-44-14(40)N-44-10(5)N-44-20(5)N-45-15(2)N-44-20(5)N-45-20 (3)										4
										Total Landsat Geocover mosaics from all basins		93

Note: 1 = is an associate basin

2 = is not a real basin with basin boundary, but covers basins or subbasins of different rivers in the Andes. 3

= 1 and 2

4 = Landsat TM Geocover mosaic shown by North (or south)-UTM Zone-Minimum latitude (a rough estimate of the percent area of basin)

5 = the tiles highlighted are the unique tiles not repeated in any other basin. Tiles not highlighted are already covered in another basin.

Table 9b. Estimated storage volume for the 3-band and 7-band Geocover Landsat TM 1990 primary data for the challenge program benchmark basins[1,2].

Landsat Geocover (m)	Total tiles for all basins #	per tile UTM MB	Total volume of Data GB	Ganges-Indus 134	Karkeh 196	Mekong 12	Nile 69	Olifats 252	Sao Francisco 36	53	Volta 5	Yellow River 34	95
3-band	93	55	5.115	21	31	2	11	40	6	8	5	15	
7-band	930	158	146.94										
		USB drives: basedata[4]	1										
		USB drives: basedata1B[5]	1										

Note: 1 = This is an estimate and not a perfect figure.

2 = before archiving the data will be moasicked into basins and only the data falling within basin boundary will be retained

3 = The 7-band data is estimated based on a nominal coverage of 10 TM scenes per 5 degree latitude and 6 degree logitude tile. This figure may slightly vary.

4 = Main drive names

5 = mirror drive names

Table 10a. AVHRR 8-km tiles for the Challenge Program Benchmark Basins (CP BBs).

Basin	Basin Name	Tile X-Y (area)[4, 5] X-Y (%)	Tile X-Y (area)[4, 5] X-Y (%)	Tile X-Y (area)[4, 5] X-Y (%)	Tile X-Y (area)[4, 5] X-Y (%)	Tile X-Y (area)[4, 5] X-Y (%)	Tile X-Y (area)[4, 5] X-Y (%)	Tile X-Y (area)[4, 5] X-Y (%)	Tile X-Y (area)[4, 5] X-Y (%)	Tile X-Y (area)[4, 5] X-Y (%)		Total Unique tiles #
1	Sao francisco	14-10 (70)	14-9 (10)	15-9 (10)	14-11 (5)	15-10 (5)						5
2	Limpopo	22-10 (40)	22-11 (30)	23-10 (15)	23-11 (15)							4
3	Nile	23-8 (17)	23-7 (17)	23-6 (17)	23-5 (12)	22-8 (5)	22-7 (9)	22-6 (8)	22-5 (6)	24-7 (5)	24-6 (4)	10
4	Volta[1]	20-7 (80)	19-7 (9)	20-6 (4)	19-6 (4)	21-7 (3)						5
5	Indus	27-5 (45)	27-4 (16)	27-6 (8)	28-5 (14)	28-4 (7)	26-5 (6)	26-4 (4)				5
6	Ganges	28-5 (46)	27-5 (18)	29-5 (17)	28-6 (14)	29-6 (5)						4
7	Yellow river	30-4 (36)	29-4 (10)	31-4 (6)	30-5 (15)	29-5 (7)	31-5 (7)	30-3 (7)	29-3 (7)	31-3 (5)		9
8	Mekong	31-7 (40)	30-7 (5)	30-6 (35)	30-7 (4)	30-5 (8)	29-6 (8)					6
9	Karkey	25-5 (75)	25-4 (15)	24-4 (5)	24-5 (5)							4
10	Virtual Andes[2,3]	12-9 (40)	11-9 (30)	11-8 (15)	12-8 (15)							4
11	Krishna[1]	28-6 (80)	28-7 (15)	27-6 (5)								3
										Total tiles from all basins		59

Note: 1 = is an associate basin
2 = is not a real basin with basin boundary, but covers basins or subbasins of different rivers in the Andes.
3 = 1 and 2
4 = AVHRR tile numbers X-Y (area in percent of total basin areas covered by the tile). This is a rough estimate.
5 = the tiles highlighted are the unique tiles not repeated in any other basin. Tiles not highlighted are already covered in another basin.

Table 10b. Estimated storage volume for the AVHRR primary data for the Challenge Program Benchmark Basins[1,2].

AVHRR images (m)	Total tiles for all basins #	per tile MB	Total volume tiles for 1981-2001 GB
monthly	59	0.007	0.104076
10-day	59	0.007	0.312228
		USB drives: avhrr8km[4]	1
		USB drives: avhrr8kmB[5]	1

Note: 1 = This is an estimate and not a perfect figure.
2 = before archiving the data will be moasicked into basins and only the data falling within basin boundary will be retained
3 = The monthly data is available for the 1981 to 2001 period and the 10-day is also available for the same period.
4 = Main drive names
5 = mirror drive names

LULC change, snow cover, snow frequency, snow depth, land degradation, evapotranspiration, evaporative fraction, biomass, leaf area index, droughts (agricultural) and vegetation condition index, top of atmosphere reflectance, and surface reflectance. These products are expected to routinely feed into hydrological, biophysical, and econometric models. Continuous streams will be compared to baseline and historical datasets to infer global changes in terrestrial systems over space and time. Data and products will be delivered via web access and DVDs on a near-real-time basis for decision support for every basin.

D. Final Word: The First Challenge of Challenge Program for Food and Water

Finally, this working paper highlights one of the first challenges of the challenge program for Water and Food (CPWF) addressing the issue of populating and operationalzing enormously complex satellite sensor based data banks as knowledge banks available to answer a multitude of science questions.

Table 11. Possible "test of concept" continous stream of remote sensing products for CP basins for the November baseline conference.

Primary data used	Period for which products are produced	frequency of products	Type of products	Product form	which CP basins
1. MODIS 500-m	January, 2001-August, 2003	monthly	1. land use/land cover	digital images, some hard copies	all CP basins
	January, 2001-August, 2003	monthly	2. vegetation dynamics	digital images, some hard copies	all CP basins
	January, 2001-August, 2003	monthly	3. snow cover	digital images, some hard copies	Ganges, Indus, Yellow river
	January, 2001-August, 2003	monthly	4. snow depth	digital images, some hard copies	Ganges, Indus, Yellow river
	January, 2001-August, 2003	monthly	5. water spread area (reservoir, lakes, tanks)	digital images, some hard copies	all CP basins
	January, 2001-August, 2003	monthly	6. change vector (change magnitude, direction, type)	digital images,graphs/plots,hard copies	all CP basins
	January, 2001-August, 2003	monthly	7. forest maps and change	digital images, some hard copies	all CP basins
	January, 2001-August, 2003	monthly	8. basin agricultural cropped area	digital images, some hard copies	all CP basins
	January, 2001-August, 2003	monthly	9. vegetation condition index (VCI)	digital images, some hard copies	all CP basins
	January, 2001-August, 2003	monthly	10. temperature condition index (TCI)	digital images, some hard copies	all CP basins
	January, 2001-August, 2003	monthly	11. begin green-up, green peak month,	graphs, plots	all CP basins
			end of green, lowest green month		all CP basins
2. MODIS 250-m	January, 2003-August, 2003	monthly	1. land use/land cover	digital images, some hard copies	all CP basins
	January, 2003-August, 2003	monthly	2. vegetation dynamics	digital images, some hard copies	all CP basins
	January, 2003-August, 2003	monthly	3. snow cover	digital images, some hard copies	Ganges, Indus, Yellow river
	January, 2003-August, 2003	monthly	4. snow depth	digital images, some hard copies	Ganges, Indus, Yellow river
	January, 2003-August, 2003	monthly	5. water spread area (reservoir, lakes, tanks)	digital images, some hard copies	all CP basins
	January, 2003-August, 2003	monthly	6. change vector (change magnitude, direction, type)	digital images,graphs/plots,hard copies	all CP basins
	January, 2003-August, 2003	monthly	7. forest maps and change	digital images, some hard copies	all CP basins
	January, 2003-August, 2003	monthly	8. basin agricultural cropped area	digital images, some hard copies	all CP basins
	January, 2003-August, 2003	monthly	9. vegetation condition index (VCI)	digital images, some hard copies	all CP basins
	January, 2003-August, 2003	monthly	10. temperature condition index (TCI)	digital images, some hard copies	all CP basins
	January, 2003-August, 2003	monthly	11. begin green-up, green peak month,	graphs, plots	all CP basins
	January, 2003-August, 2003	monthly	end of green, lowest green month		all CP basins

(Continued)

3. Landsat-28.5 m basemap	1990 (nominal)	one snap shot baseline product 1. basin base map (FCC:7,4,2)		digital images, some hardcopies	all CP basins
	1990 (nominal)	one snap shot baseline product 2. basin 1990 land use/land cover		digital images, some hardcopies	all CP basins
	1990 (nominal)	one snap shot baseline product 3. basin vegetation index		digital images, some hardcopies	all CP basins
	1990 (nominal)	one snap shot baseline product 4. basin snow spread area		digital images, some hardcopies	Ganges, Indus, Yellow river
	1990 (nominal)	one snap shot baseline product 5. basin forest cover		digital images, some hardcopies	all CP basins
	1990 (nominal)	one snap shot baseline product 6. basin agricultural crop area		digital images, some hardcopies	all CP basins
4. NOAA AVHRR 8-km 1982-2000		monthly	1. land use/land cover	digital images, some hardcopies	all CP basins
		1981, 1985, 1990,	2. land use/land cover change	digital images, some hardcopies	all CP basins
			2. vegetation dynamics	digital images, some hardcopies	all CP basins
			11. begin green-up, green peak month, end of green, lowest green month	graphs, plots	all CP basins

Table 12. Secondary remote sensing derived and GIS data products for CP basins for the November baseline conference.

Secondary data	Period for which products are produced	Frequency of products	Type of products	Product form	Which CP basins
1. basin boundary	one time	one time	boundary vector	digital, hard copy	all CP basins
2. basin DEM	one time	one time	elevation	digital, hard copy	all CP basins
3. basin drainage	one time	one time	streams	digital, hard copy	all CP basins
4. MODIS land use/ land cover	2000-2001	one time	17 IGBP type classes	digital, hard copy	all CP basins
5. USGS Land use/ land cover	1992-1993	one time	24 USGS classes	digital, hard copy	all CP basins
6. IGBP Land use/ land cover	1992-1993	one time	17 IGBP LULC classes	digital, hard copy	all CP basins
7. USGS seasonal land use/land cover	1992-93	one time	253 USGS LULC classes	digital, hard copy	all CP basins
8. Olson ecoregionsf of the World		one time	100 USGS LULC classes	digital, hard copy	all CP basins
9. forest cover	1992-1993; 2001(modis)	one time	5 forest classes	digital, hard copy	all CP basins
10. forest density	1992-1993; 2001 (modis)	one time	0-100 percent	digital, hard copy	all CP basins

LIST OF PARTICIPANTS
DATA AND INFORMATION MANAGEMENT WORKSHOP
IWMI HQ, COLOMBO, SRI LANKA – 19 TO 23 MAY 2003

Advisory Panel	Enrica Porcari
	Glenn Hyman
	Pedro J. Restrepo
	Robert Zomer
	Richard Labelle
	Kate Wild
Themes	Theme 1: Crop Water Productivity Improvement
	Blesilda Albano
	International Rice Research Istitute (IRRI)
	Theme 1: Crop Water Productivity Improvement
	John Bennett
	International Rice Research Institute (IRRI)
	Philippines
	Theme 2: Multiple Use of Upper Catchments
	Simon Cook
	Centrol Internacional de Agricultura Tropical (CIAT)
	Colombia
	Theme 4: Integrated Basin Water Management Systems
	Francis Gikuchi
	International Water Management Institute (IwMI)
	Theme 5: The Global and National Food and Water System
	Claudia Ringler
	International Food Policy Research Institute (IFPRI)
Benchmark Basins	Indo Gangetic
	A.K. Sikka
	Indian Council of Agricultural Research (ICAR), India
	Indo Gangetic
	N. Subash
	Indian Council of Agricultural Research (ICAR), India
	Kharkheh
	Shahram Ashrafi
	Agricultural Research, Education and Extension (AEERO)
	Iran
	Kharkheh
	Nahid Takapouy
	Agricultural Research, Education and Extension (AEERO)
	Iran
	Limpopo
	Adriaan Louw

	Agricultural Research Council (ARC), South Africa
	Limpopo
	Hein Beukes
	Agricultural Research Council (ARC), South Africa
	Mekong
	Gunhild Garsdal
	Mekong River Commission, Cambodia
	Mekong
	Ulf Hedland
	Mekong River Commission, Cambodia
	Nile
	Gamal Shaker
	National Water Research Center (NWRC), Egypt
	Nile
	Nagy Yakoub
	National Water Research Center (NWRC), Egypt
	São Francisco
	Ricardo A.L. Brito
	Brazilian Agricultural Research Corp. (EMBRAPA), Brazil
	São Francisco
	Gisella Avellar
	Brazilian Agricultural Research Corp. (EMBRAPA), Brazil
Associated Basin	Volta
	Winston Andah
	CSIR Water Research Institute, Ghana
Challenge Program for	Ania Grobicki
Water and Food	Coordinator
	Jonathan Woolley
	Competitive Fund Coordinator
	Nishath Yapa
	Database Administrator
	Nedumaran Balakrishnan
	Web Developer
International Water	Wolfgang Flügel
Management Institute	Hugh Turral
	Prasad Thenkabail
	Riazzi Ziard
	Mohideen Sadir
	Zhongping Zhu
	Asad Qureshi
	Ian Makin
Jena University, Germany	Karsten Busch

Appendix 1

Remote Sensing Datasets for Potential Use in CP Basins

Datasets, time-periods, scales, and resolutions

1.0 Global level

1.1 8-km AVHRR data monthly (available at IWMI)

- 1981-2001 monthly NDVI
- 1981-2001 monthly Band 4
- 1981-2001 monthly Band 1
- 1981-2001 monthly Band 2

1.2 8-km AVHRR data 10-day (available at IWMI)

- 1981-2001 10-day NDVI
- 1981-2001 10-day Band 4
- 1981-2001 10-day Band 1
- 1981-2001 10-day Band 2

1.3 1-km AVHRR data (available at IWMI)

- 1992 (April-December)…….every 10 days
- 1993 (January-September)…….every 10 days
- 1995 (February-September)……...every 10 days

Note: thermal data can be downloaded as well, if needed

2.0 Continental and sub-continental level

2.1 500-m MODIS data (available at IWMI for India, Pakistan, Sri Lanka)

- 500-m MODIS data 7-band reflectance, version 3, level 3 and/or
- 500-m MODIS data NDVI and EVI, version 3, level 3

2.2 250-m MODIS data (available at IWMI for India, Pakistan, Sri Lanka)

- 250-m MODIS data 2-band reflectance, version 3, level 3 and/or
- 250-m MODIS data NDVI and EVI, version 3, level 3

Note: 188-m IRS WIFS can be considered as well

3.0 Region or watershed/basin level (some data at IWMI)

- 15-90 meter ASTER data, 15 bands (4 VNIR, 6 MIR, 5 TIR)
- 15-60-m ETM+ data, 8 bands (1 Pan, 6 non-thermal, 1 thermal)
- 5-23.6-m IRS-1c/1d data, 3 bands (1 Pan, 2 multispectral)
- 30-m Hyperion data, 196 calibrated bands, 16-bit
- 10-30 m ALI data, 10 bands (1 Pan and 9 multispectral, 16-bit)

4.0 Local or micro-watershed/subbasin level (some data at IWMI)

- 1-4 meter IKONOS data 4 (1 Pan, 3 multispectral), 11-bit
- 0.61-2.44 m Quickbird data (1 Pan, 3 multispectral), 11-bit

Appendix 2

LULC description, legend, and header file

1.0 Overview of the USGS global land cover characteristics (GLCC) database (Version 2.0)

Description:

The global land cover characteristics database was developed on a continent-by-continent basis. All continental databases share the same map projections (Interrupted Goode Homolosine and Lambert Azimuthal Equal Area), have 1-km nominal spatial resolution, and are based on 1-km Advanced Very High Resolution Radiometer (AVHRR) data spanning April 1992 through March 1993.

Accuracy:

Sample point accuracy 59.4 percent
Area-weighted accuracy 66.9 percent
Majority Rule Accuracy 73.5 percent
Area Weighted Majority Rule 78.7 percent

Reference:

Brown, J.F., Loveland, T.R., Merchant, J.W., Ohlen, D.O., Reed, B.C., and Zhu, J, Yang, L., 2000. Development of a Global Land Cover Characteristics Database and IGBP Discover from 1-km AVHRR Data. International Journal of Remote Sensing, v. 21, no. 6/7, p. 1,303-1,330.

Download site:

http://edcdaac.usgs.gov/glcc/globe_int.html

Contact:

lcac@usgs.gov

Credits:

U.S. Geological Survey (USGS)
University of Nebraska-Lincoln (UNL), and
European Commission's Joint Research Centre (JRC)

1.1 Legend of the USGS global land cover characteristics (GLCC) database (Version 2.0)

Class #	Unique code	Class name
1	100	Urban and Built-Up Land
2	211	Dry land Cropland and Pasture
3	212	Irrigated Cropland and Pasture
4	213	Mixed Dry land/Irrigated Cropland and Pasture
5	280	Cropland/Grassland Mosaic
6	290	Cropland/Woodland Mosaic
7	311	Grassland
8	321	Shrub land
9	330	Mixed Shrub land/Grassland
10	332	Savanna
11	411	Deciduous Broadleaf Forest
12	412	Deciduous Needle leaf Forest
13	421	Evergreen Broadleaf Forest
14	422	Evergreen Needle leaf Forest
15	430	Mixed Forest
16	500	Water Bodies
17	620	Herbaceous Wetland
18	610	Wooded Wetland
19	770	Barren or Sparsely Vegetated
20	820	Herbaceous Tundra
21	810	Wooded Tundra
22	850	Mixed Tundra
23	830	Bare Ground Tundra
24	900	Snow or Ice
100	-	NO DATA

1.2 Header information of the USGS global land cover characteristics (GLCC) database (Version 2.0)

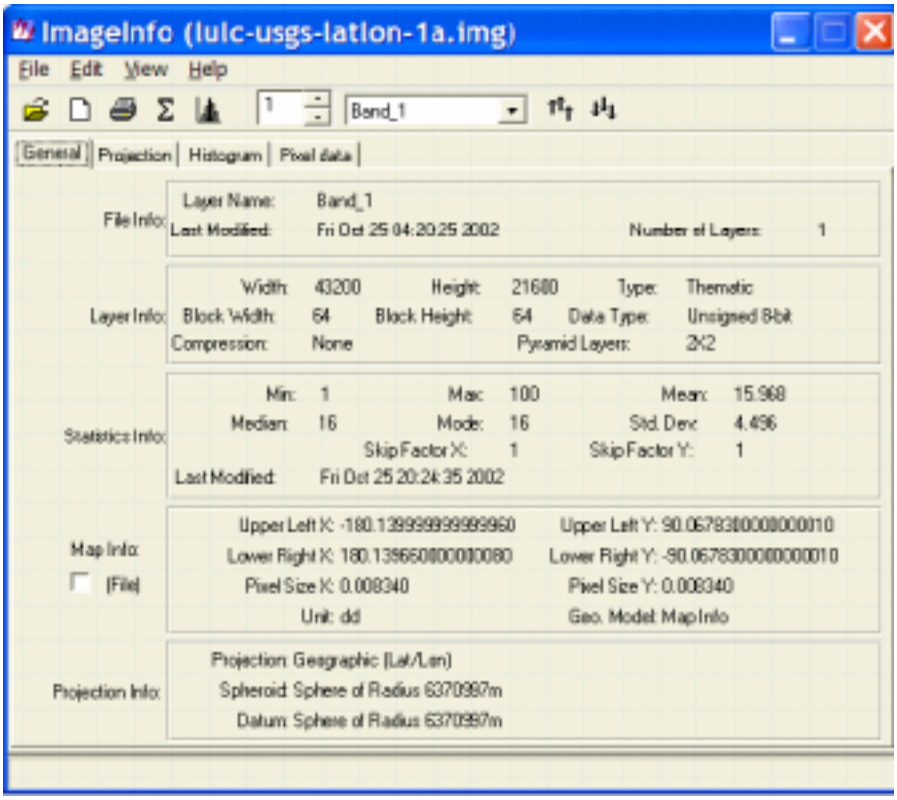

2.0 Overview of the International Geospere-Biosphere Program (IGBP) LULC (Version 2.0)

Description:

The global land cover characteristics database was developed on a continent-by-continent basis. All continental databases share the same map projections (Interrupted Goode Homolosine and Lambert Azimuthal Equal Area), have 1-km nominal spatial resolution, and are based on 1-km Advanced Very High Resolution Radiometer (AVHRR) data spanning April 1992 through March 1993.

Accuracy:

Sample point accuracy 59.4 percent
Area-weighted accuracy 66.9 percent
Majority Rule Accuracy 73.5 percent
Area Weighted Majority Rule 78.7 percent

Reference:

Brown, J.F., Loveland, T.R., Merchant, J.W., Ohlen, D.O., Reed, B.C., and Zhu, J, Yang, L., 2000. Development of a Global Land Cover Characteristics Database and IGBP Discover from 1-km AVHRR Data. International Journal of Remote Sensing, v. 21, no. 6/7, p. 1,303-1,330.

Download site:

http://edcdaac.usgs.gov/glcc/globe_int.html

Contact:

lcac@usgs.gov

Credits:

U.S. Geological Survey (USGS)
University of Nebraska-Lincoln (UNL), and
European Commission's Joint Research Centre (JRC)

2.1 Legend of the International Geosphere-Biosphere Program (IGBP) LULC Version 2.0

1 Evergreen needleleaf forest
2 Evergreen broadleaf forest
3 Ddeciduous needleleaf forest
4 Deciduous broadleaf forest
5 Mixed forests
6 Closed shrub lands
7 Open shrub lands
8 Woody savannas
9 Savannas
10 Grasslands
11 Permanent wetlands
12 Croplands
13 Urban and built-up
14 Cropland/natural vegetation mosa
15 Snow and ice
16 Barren or sparsely vegetated
17 Water bodies
18 No data

2.2 Header information of the International Geosphere-Biosphere Program (IGBP) LULC Version 2.0

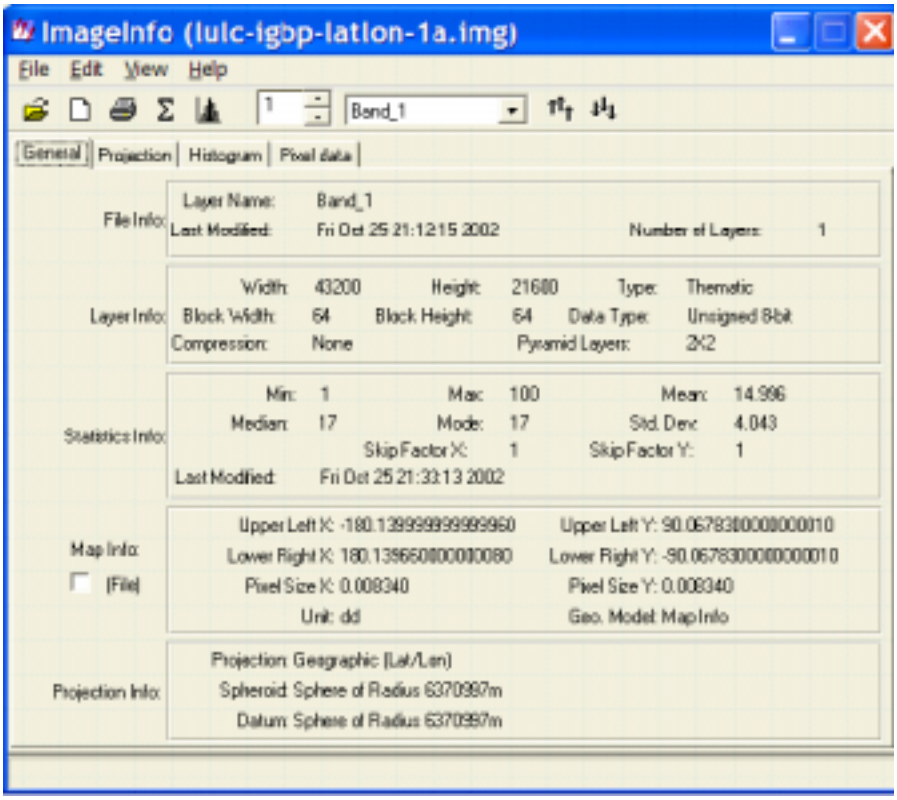

3.0 Overview of the USGS Seasonal global land cover characteristics (GLCC)

Seasonal LULC database (Version 2.0)

Description:

The global land cover characteristics database was developed on a continent-by-continent basis. All continental databases share the same map projections (Interrupted Goode Homolosine and Lambert Azimuthal Equal Area), have 1-km nominal spatial resolution, and are based on 1-km Advanced Very High Resolution Radiometer (AVHRR) data spanning April 1992 through March 1993.

The seasonal land cover regions are then translated into the Global Ecosystem framework (1994a, 1994b). Olson has defined 94 ecosystem classes that are based on their land cover mosaic, floristic properties, climate, and physiognomy. The Global Ecosystem framework provides a mechanism for tailoring data to the unique landscape conditions of each continent, while still providing a means for summarizing the data at the global level.

Accuracy:

Sample point accuracy 59.4 percent
Area-weighted accuracy 66.9 percent

Majority Rule Accuracy 73.5 percent
Area Weighted Majority Rule 78.7 percent

Reference:

Brown, J.F., Loveland, T.R., Merchant, J.W., Ohlen, D.O., Reed, B.C., and Zhu, J, Yang, L., 2000. Development of a Global Land Cover Characteristics Database and IGBP DISCover from 1-km AVHRR Data. International Journal of Remote Sensing, v. 21, no. 6/7, p. 1,303-1,330.

Download site:

http://edcdaac.usgs.gov/glcc/globe_int.html

Contact:

lcac@usgs.gov

Credits:

U.S. Geological Survey (USGS)
University of Nebraska-Lincoln (UNL), and
European Commission's Joint Research Centre (JRC)

3.1 Legend of the USGS Seasonal global land cover characteristics (GLCC) Seasonal LULC database (Version 2.0)

SLCR2.0	SLCR 2.0 LABEL
1	Transitional Boreal Conifer (Pine and Spruce) Forest
2	Boreal Forest (Spruce, Birch, Pine, Larch)
3	Temperate Alpine Conifer Forest
4	Highland Meadow/Conifer Forest (Fir, Spruce)
5	Boreal Forest (Spruce, Pine)
6	Boreal Forest (Spruce, Fir, Alder)
7	Pine Dominated Forest
8	Boreal Forest (Spruce, Birch, Alder)
9	Conifer Forest (Larch, Fir)
10	Spruce, Pine, and Birch Forest with Cropland
11	Evergreen Needle leaf Forest with Rice Paddies
12	Northern Pine and Fir Forest
13	Pine Forest with Cropland (Maize and Vineyards)
14	Tropical Forest
15	Fragmented Monsoon Tropical Broadleaf Forest
16	Evergreen Broadleaf Forest with Shrub land
17	Evergreen Broadleaf Forest with Grassland
18	Broadleaf Evergreen Monsoon Forest
19	Tropical Evergreen Rain forest
20	Boreal Larch, Birch, Spruce Forest
21	Boreal Forest (Larch, Spruce)
22	Boreal Forest (Larch, Birch, Elder)

23 Larch Forest
24 Larch Forest
25 Boreal Forest (Larch/Birch/Aspen)
26 Mixed Boreal Forest (Larch, Birch, Poplar)
27 Montane, Monsoon Deciduous Rain Forest
28 Broadleaf Deciduous Forest (Ash, Elm, Birch, Basswood)
29 Oak Woodland
30 Deciduous Broadleaf Woodland/Shrub land
31 Agriculture and Plantations (Rubber, Coconut)
32 Tropical Fruit Plantations
33 Deciduous Forest (Hornbeam, Beech, Oak) with Crops
34 Deciduous Broadleaf Forest
35 Deciduous Monsoon Forest
36 Disturbed Deciduous Monsoon Forest
37 Closed and Open Deciduous Broadleaf Forest with Cropland
38 Montane Deciduous Monsoon Forest
39 Woodland (Oak, Beech, Maple, Pine, Fir)
40 Open Boreal Forest (Larch/Birch)
41 Open Boreal Forest (Larch/Birch)
42 Woodland (Beech, Hornbeam, Oak)
43 Mixed Forest
44 Lowland Larch/Birch/Pine Forest
45 Transitional Boreal Mixed Forest
46 Forested Wetland (Larch, Birch, Pine)
47 Larch Forest/Woodland
48 Northern Boreal Mixed Forest (Spruce, Pine, with Birch, Poplar)
49 Boreal Forest (Pine, Birch) with Marshes and Bogs
50 Larch, Birch, Bogs
51 Boreal Forest (Spruce, Pine, Birch)
52 Birch, Larch, Pine, Spruce
53 Birch Woodland/Marsh
54 Mixed Forest with Grassland
55 Mixed Southern Boreal Woodland (Larch, Pine, Birch, Oak)
56 Mixed Boreal Forest (Birch/Pine)
57 Mixed Boreal Forest (Birch, Spruce, Pine)
58 Forest (Beech, Birch, Cedar Mixed with Pine and Larch)
59 Larch, Birch, Pine Boreal Forest
60 Mixed Forest (Birch, Maple, Poplar, Spruce)
61 Mixed Forest (Pine, Birch)
62 Woodland (Pine, Larch, Oak) with Cropland (Wheat, Grains)
63 Mixed Forest (Larch, Pine, Oak, Aspen)
64 Mixed Forest (Aspen, Beech, Oak, Poplar, Spruce)
65 Mixed Forest
66 Mixed Forest (Larch, Beech, Aspen, Oak)
67 Mixed Pine and Broadleaf Forest
68 Fragmented and Degraded, Open Forest

69 Oak/Pine Mixed Forest with Cropland
70 Mixed Evergreen Forest (Pine, Live Oak)
71 Evergreen Broadleaf and Needle leaf Forest
72 Evergreen Needle leaf and Broadleaf Forest
73 Arctic Heath
74 Sparse Trees, Bogs (Heath, Shrub Tundra)
75 Deciduous Shrub land
76 Boreal Shrub land (Birch, Alder) with Spruce
77 Pine and Evergreen Shrubs
78 Woodland, Shrub land with Cropland (Cotton, Wheat)
79 Temperate Broadleaf Shrub land
80 Dense Sclerophyllous Oak Woodland
81 Alpine Tundra
82 Desert
83 Alpine Semidesert Shrub
84 Sparse, Dwarf Trees, Willows, Bogs
85 Sparsely Vegetated Desert Shrub
86 Sparsely Vegetated Desert
87 Tundra/Shrub land
88 Alpine Tundra
89 Arctic Shrub Tundra (Birch, Willow)
90 Semi-Arid Grassland/Shrub land
91 Woody Tundra (Dwarf Shrubs/Willows)
92 Semi-Arid Grassland/Shrub land
93 Short Grass and Sparse Shrub
94 Sparse Taiga (Dwarf Trees, Larch)
95 Dwarf Trees (Willows, Shrubs)
96 Woody Tundra/Transitional Taiga (Dwarf Trees)
97 Arid Shrub land
98 Shrub land with Crops
99 Alpine Shrub land
100 Woody Tundra
101 Woody Tundra (Birch/Willow)
102 Sparsely Vegetated Shrub land/Grassland
103 Desert Grassland/Shrub land
104 Tundra/Shortgrass/Cedar, Birch Forest
105 Grassland/Boreal Forest Mosaic
106 Grass and Shrub Mosaic
107 Open Woodland and Grassland
108 Pine/Bamboo and Oak Woodland with Cropland (Grains)
109 Deciduous Woodland/Shrub land with Agriculture
110 Woodland (Pine, Oak, Gum)
111 Deciduous Broadleaf Woodland
112 Oak Woodland/Grassland
113 Deciduous Woodland/Shrub land with Agriculture
114 Grassland with Cropland

115 Sparse Short Grassland
116 Herbaceous Tundra
117 Short Montane Grassland
118 Deciduous Shrubs and Tall Grass
119 Shrub land/Short Grassland
120 Alpine Meadows/Grassland
121 Grassland with Dryland Crops
122 Grassland with Winter Wheat
123 Alpine Shrub land/Grassland
124 Alpine Short Grassland
125 Alpine Grassland/Meadow
126 Grassland, Meadow
127 Short Grassland
128 Short Grassland with Shrubs
129 Alpine Meadow/Grassland
130 Short Grassland
131 Grassland with Cropland
132 Alpine Grassland/Meadow
133 Grassland, Meadow
134 Grassland/Shrub land
135 Grassland
136 Grassland/Meadow with Cropland
137 Alpine Grassland/Meadow
138 Grassland with Pine
139 Alpine Meadow with Coniferous Trees
140 Alpine Meadow
141 Alpine Meadow with Shrubs
142 Sparse Trees, Bogs
143 Wetland/Bog/Deciduous Woody Tundra
144 Lowland Bogs and Transitional Boreal Forest (Woody Tundra, Larch)
145 Blanket Bogs, Heath
146 Grass Wetland/Marsh
147 Mangrove
148 Cropland (Small Grains)
149 Cropland (Small Grains) with Grassland
150 Cropland (Spring Wheat, Small Grains)
151 Cropland (Small Grains) with Grassland
152 Cropland (Cotton, Grains) with Shrubs
153 Cropland (Rice)
154 Cropland (Millet, Wheat, Maize)
155 Irrigated Cropland
156 Dry Cropland (Wheat, Soybeans)
157 Cropland (Spring Wheat, Other Grains)
158 Cropland (Rice)
159 Cropland (Winter Wheat)
160 Cropland (Wheat) with Woodland

161 Cropland (Rice, Cotton)
162 Cropland (Winter Wheat, Small Grains)
163 Irrigated Cropland/Cotton
164 Cropland (Millet, Soybean, Rice)
165 Cropland (Rice, Wheat) with Woodland
166 Cropland (Rice, Grains)
167 Cropland (Grains)/Grassland/Bamboo Mosaic
168 Dry land Cropland (Wheat, Maize, Soybeans)
169 Cropland (Corn, Wheat) with Woodland
170 Cropland (Spring Wheat, Soybeans)
171 Cropland (Small Grains)
172 Cropland (Winter Wheat)
173 Dry land Crops/Orchards/Vineyards
174 Cropland (Rice, Wheat)
175 Mixed Cropland (Small Grains, Corn, Soybeans, Rice) with Woodland
176 Cropland (Grains, Soybeans, Rice, Cotton)
177 Dry land Crops (Millet, Soybeans, Oats, Cotton)
178 Irrigated Cropland (Rice, Wheat)
179 Cropland (Rice)
180 Irrigated Cropland (Cotton, Rice, Sugarcane)
181 Cropland (Rice)
182 Irrigated Cropland (Double Crop Rice)
183 Cropland (Rice)
184 Cropland (Rice, Wheat)
185 Small Grains (Barley, Wheat) with Grassland
186 Cropland (Small Grains) and Pasture
187 Cropland (Rice, Cotton)
188 Cropland (Corn, Wheat) with Woodland
189 Cropland (Wheat, Orchards)
190 Cropland (Wheat, Barley, Corn)
191 Pasture/Cropland/Orchards
192 Irrigated Crops (Rice)
193 Cropland (Rye, Small Grains) with Mixed Forest
194 Cropland (Small Grains, Sugar Beets, Orchards)/Pasture
195 Irrigated Cropland (Rice, Wheat)
196 Irrigated Crops (Rice)
197 Cropland (Rice)
198 Cropland (Double Crop Rice, Wheat, Grains, Peanuts)
199 Cropland (Double Crop Rice, Wheat) with Deciduous Woodland
200 Pasture/Cropland/Orchards
201 Cropland (Rice) with Woodlands
202 Cropland
203 Pasture/Cropland (Wheat, Barley)
204 Irrigated Cropland (Rice, Wheat)
205 Cropland (Double Crop Rice/Wheat, Cotton)
206 Cropland and Pasture (Wheat, Orchards, Vineyards) with Woodland

207 Cropland/Open Woodland
208 Cropland (Cereals)
209 Cropland/Pasture with Woodland (Oak, Beech)
210 Pasture/Cropland
211 Grassland/Cropland (Small Grains) Mosaic
212 Short Grassland/Oak Woodland/Cropland
213 Woodland/Cropland Mosaic
214 Grassland/Irrigated Cropland
215 Cropland/Woodland Mosaic
216 Cropland (Spring Wheat)/Grassland Mosaic
217 Cropland (Spring Wheat, Barley)/Birch Woodland Mosaic
218 Grassland/Cropland (Small Grains) Mosaic
219 Cropland (Grains)/Grassland/Bamboo Mosaic
220 Cropland/Shrub land Mosaic
221 Cropland/Woodland Mosaic
222 Grassland/Cropland (Corn, Wheat) Mosaic
223 Cropland/Grassland Mosaic
224 Cropland (Rice, Cotton)/Woodland Mosaic
225 Cropland (Corn, Barley)/Grassland Mosaic
226 Cropland (Small Grains) and Woodland Mosaic
227 Cropland (Wheat)/Grassland Mosaic
228 Cropland (Small Grains)/Mixed Forest Mosaic
229 Cropland, Orchards, Vineyards/Shrub Mosaic
230 Cropland (Wheat, Cotton)/Meadows Mosaic
231 Cropland (Small Grains)/Woodland Mosaic
232 Deciduous Broadleaf Woodland/Dry Cropland Mosaic
233 Mixed Forest/Cropland (Winter Wheat) Mosaic
234 Dry land Crops (Rice)/Grassland/Shrub land Mosaic
235 Shrub land/Cropland Mosaic
236 Woodland/Cropland/Pasture Mosaic
237 Woodland/Cropland/Grassland Mosaic
238 Oak Woodland/Cropland (Small Grains, Orchards)/Pasture
239 Cropland (Rice)/Grassland
240 Cropland/Shrub land Mosaic
241 Cropland (Irrigated)/Conifer Forest (Pine, Fir, Bamboo)
242 Grassland Meadow/Cereal Crops/Hay with Oak Woodland
243 Cropland (Rice)/Forest Mosaic
244 Fragmented Forest/Shifting Agriculture
245 Grassland/Woodland/Cropland Mosaic
246 Snow and Ice
247 Barren Polar Desert
248 Barren
249 Arctic Tundra
250 Sparsely Vegetated
251 Lowland Barren/Sparse Vegetation
252 Inland Water
253 Ocean

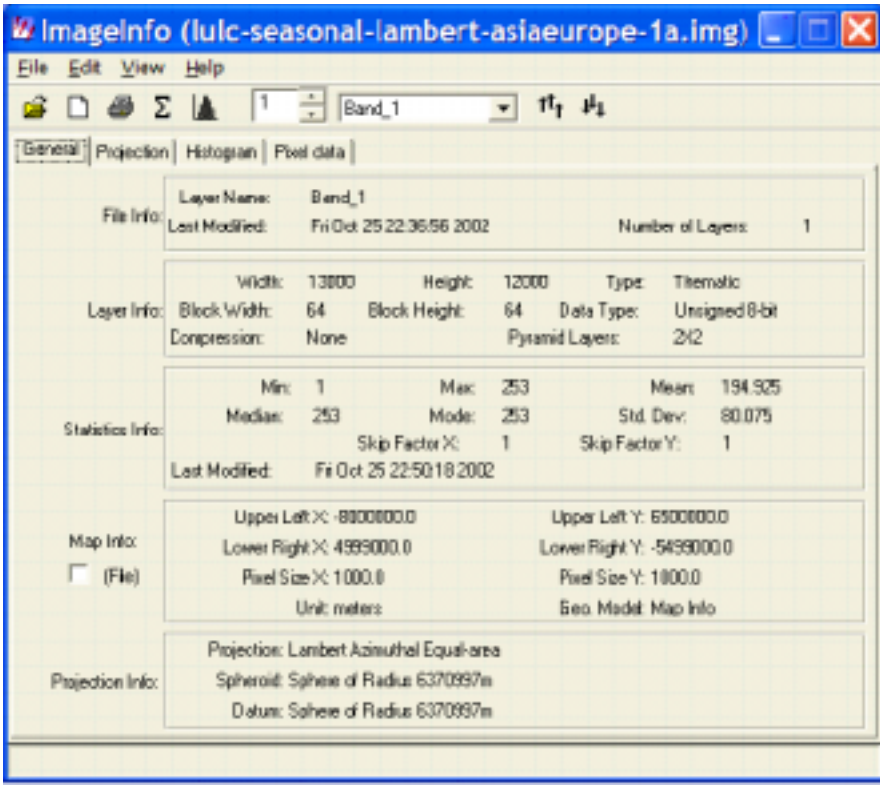

3.2 Header information on the USGS seasonal global land cover characteristics (GLCC) Seasonal LULC database (Version 2.0)

4.0 Overview of the Olson Global Ecosystems of the World

Description:

Olson has defined 94 ecosystem classes that are based on their land cover mosaic, floristic properties, climate, and physiognomy. The Global Ecosystem framework provides a mechanism for tailoring data to the unique landscape conditions of each continent, while still providing a means for summarizing the data at the global level. The Global Ecosystem types have been cross-referenced to land cover classes in the Simple Biosphere Model (SIB), Simple Biosphere 2 Model, the Biosphere Atmosphere Transfer Scheme (BATS), International Geosphere Biosphere Programme (IGBP), and USGS/Anderson (see Table 1).

Table 1. Example translation table to derived data legends.

Cluster Label	Global Ecosystem	BATS Scheme	SiB Scheme	IGBP Scheme
Pine forest	Coniferous Evergreen Forest	Evergreen Needleleaf Tree	Evergreen Needleleaf Trees	Evergreen Needleleaf Forest
Oak/pine mixed forest	Mixed Forest	Mixed Deciduous Conifer Forest	Deciduous and Evergreen Trees	Mixed Forest

Accuracy:

None. User need to determine this.

Reference:

Olson, J.S., 1994. Global Ecosystem Framework: Definitions. USGS EROS Data Center Internal Report, Sioux Falls, SD, 37 p.
Olson, J.S., 1994. Global Ecosystem Framework: Translation Strategy. USGS EROS Data Center Internal Report, 39 p.

Download site:

http://edcdaac.usgs.gov/glcc/globe_int.html

Contact:

lcac@usgs.gov

Credits:

U.S. Geological Survey (USGS)
University of Nebraska-Lincoln (UNL), and
European Commission's Joint Research Centre (JRC)

4.1 Legend of the Olson Ecosystems of the World

Global Ecosystems Legend

Value	Description
1	Urban
2	Low Sparse Grassland
3	Coniferous Forest
4	Deciduous Conifer Forest
5	Deciduous Broadleaf Forest
6	Evergreen Broadleaf Forests
7	Tall Grasses and Shrubs
8	Bare Desert
9	Upland Tundra
10	Irrigated Grassland
11	Semi Desert
12	Glacier Ice
13	Wooded Wet Swamp
14	Inland Water
15	Sea Water
16	Shrub Evergreen
17	Shrub Deciduous
18	Mixed Forest and Field
19	Evergreen Forest and Fields
20	Cool Rain Forest
21	Conifer Boreal Forest
22	Cool Conifer Forest

23 Cool Mixed Forest
24 Mixed Forest
25 Cool Broadleaf Forest
26 Deciduous Broadleaf Forest
27 Conifer Forest
28 Montane Tropical Forests
29 Seasonal Tropical Forest
30 Cool Crops and Towns
31 Crops and Town
32 Dry Tropical Woods
33 Tropical Rain forest
34 Tropical Degraded Forest
35 Corn and Beans Cropland
36 Rice Paddy and Field
37 Hot Irrigated Cropland
38 Cool Irrigated Cropland
39 Cold Irrigated Cropland
40 Cool Grasses and Shrubs
41 Hot and Mild Grasses and Shrubs
42 Cold Grassland
43 Savanna (Woods)
44 Mire, Bog, Fen
45 Marsh Wetland
46 Mediterranean Scrub
47 Dry Woody Scrub
48 Dry Evergreen Woods
49 Volcanic Rock
50 Sand Desert
51 Semi Desert Shrubs
52 Semi Desert Sage
53 Barren Tundra
54 Cool Southern Hemisphere Mixed Forests
55 Cool Fields and Woods
56 Forest and Field
57 Cool Forest and Field
58 Fields and Woody Savanna
59 Succulent and Thorn Scrub
60 Small Leaf Mixed Woods
61 Deciduous and Mixed Boreal Forest
62 Narrow Conifers
63 Wooded Tundra
64 Heath Scrub
65 Coastal Wetland, NW
66 Coastal Wetland, NE
67 Coastal Wetland, SE
68 Coastal Wetland, SW

69	Polar and Alpine Desert
70	Glacier Rock
71	Salt Playas
72	Mangrove
73	Water and Island Fringe
74	Land, Water, and Shore (see Note 1)
75	Land, Water, and Rivers (see Note 1)
76	Crop and Water Mixtures
77	Southern Hemisphere Conifers
78	Southern Hemisphere Mixed Forest
79	Wet Sclerophylic Forest
80	Coastline Fringe
81	Beaches and Dunes
82	Sparse Dunes and Ridges
83	Bare Coastal Dunes
84	Residual Dunes and Beaches
85	Compound Coastlines
86	Rocky Cliffs and Slopes
87	Sandy Grassland and Shrubs
88	Bamboo
89	Moist Eucalyptus
90	Rain Green Tropical Forest
91	Woody Savanna
92	Broadleaf Crops
93	Grass Crops
94	Crops, Grass, Shrubs
95	Evergreen Tree Crop
96	Deciduous Tree Crop
99	Interrupted Areas (Goodes Homolosine Projection)
100	Missing Data

Level I	Level II
1. Urban or Built-up Land	11. Residential.
	12 Commercial and Services.
	13. Industrial.
	14. Transportation, Communications, and Utilities.
	15. Industrial and Commercial complexes.
	16. Mixed Urban or Built-up Land.
	17. Other Urban or Built-up Land.
2. Agricultural Land	21. Cropland and Pasture.
	22. Orchards, Groves, Vineyards, Nurseries, and Ornamental Horticultural Areas.
	23. Confined Feeding Operations.
	24. Other Agricultural Land.
3. Rangeland	31. Herbaceous Rangeland.
	32. Shrub and Brush Rangeland.
	33. Mixed Rangeland.
4. Forest Land	41. Deciduous Forest Land.
	42. Evergreen Forest Land.
	43. Mixed Forest Land.
5. Water	51. Streams and Canals.
	52. Lakes.
	53. Reservoirs.
	54. Bays and Estuaries.
6. Wetland	61. Forested Wetland.
	62. Non-forested Wetland.
7. Barren Land	71. Dry Salt Flats.
	72. Beaches.
	73. Sandy Areas other than Beaches.
	74. Bare Exposed Rock.
	75. Strip Mines, Quarries, and Grave Pits
	76. Transitional Areas.
	77. Mixed Barren Land.
8. Tundra	81. Shrub and Brush Tundra.
	82. Herbaceous Tundra.
	83. Bare Ground Tundra.
	84. Wet Tundra.
	85. Mixed Tundra.
9. Perennial Snow or Ice	91. Perennial Snowfields.
	92. Glaciers.

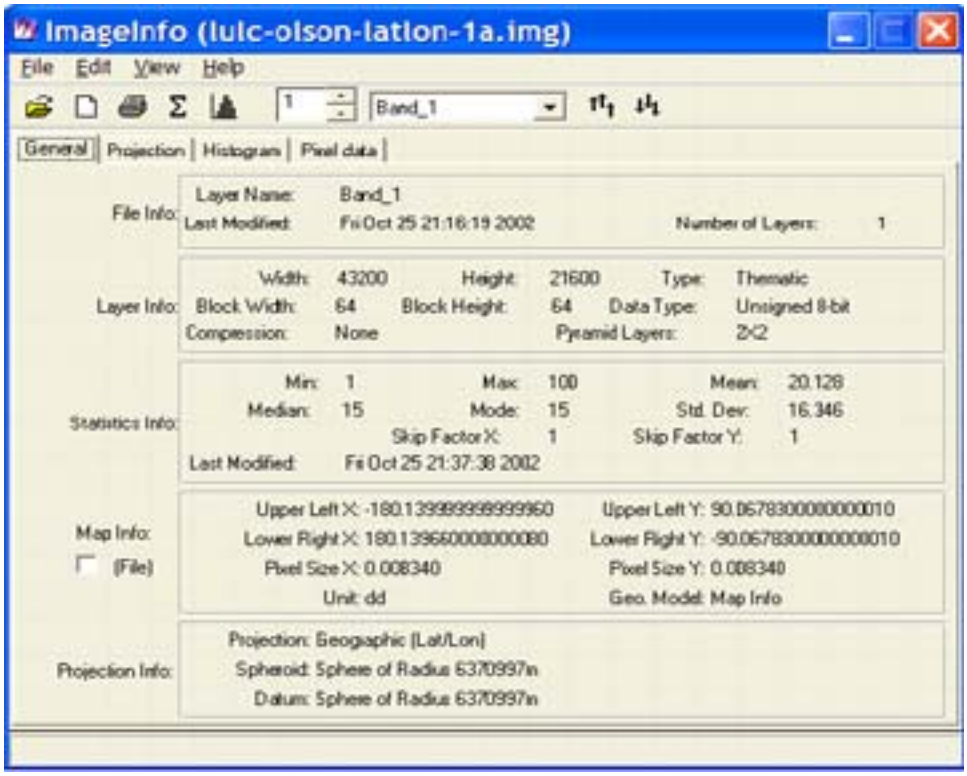

4.3 Header information of the Olson Ecosystems of the World

5.0 Overview of the MODIS LULC database (Period 10/15/00 to 10/15/01)

Description:

The 2000289 product was made from MODIS data from the period 10/15/00 to 10/15/01. It is designated as "provisional," meaning that it contains useful science data but is subject to further improvement. This product was used as the base layer of a centerfold map and on line shockwave file by Time magazine on 26 August, 2002. We appreciate notice of the uses to which our products contribute.

Accuracy:

None, so far. It is for the user to evaluate the accuracies and errors.

Reference:

Borak, J., Friedl, M., Gopal, S., Lambin, E., Moody, A. Muchoney, D., and Strahler, A. MODIS Land Cover Product Algorithm Theoretical Basis Document (ATBD). Version 5.0. MODIS Land Cover and Land-Cover Change Team, Boston University.

Download site:

http:// modis.gsfc.nasa.gov

Contact:

Credits:

Boston University
Université Catholique du Louvain
University of North Carolina

5.1 Legend of the MODIS LULC database (period 10/15/00 to 10/15/01)

0	Water
1	Evergreen Needleleaf Forest
2	Evergreen Broadleaf Forest
3	Deciduous Needleleaf Forest
4	Deciduous Broadleaf Forest
5	Mixed Forests
6	Closed Shrub lands
7	Open Shrub lands
8	Woody Savannas
9	Savannas
10	Grasslands
11	Permanent Wetlands
12	Croplands
13	Urban and Built-Up
14	Cropland/Natural Vegetation M
15	Snow and Ice
16	Barren or Sparsely Vegetated
17	IGBP Water Bodies, recoded

5.2 The header information on the MODIS LULC database (period 10/15/00 to 10/01)

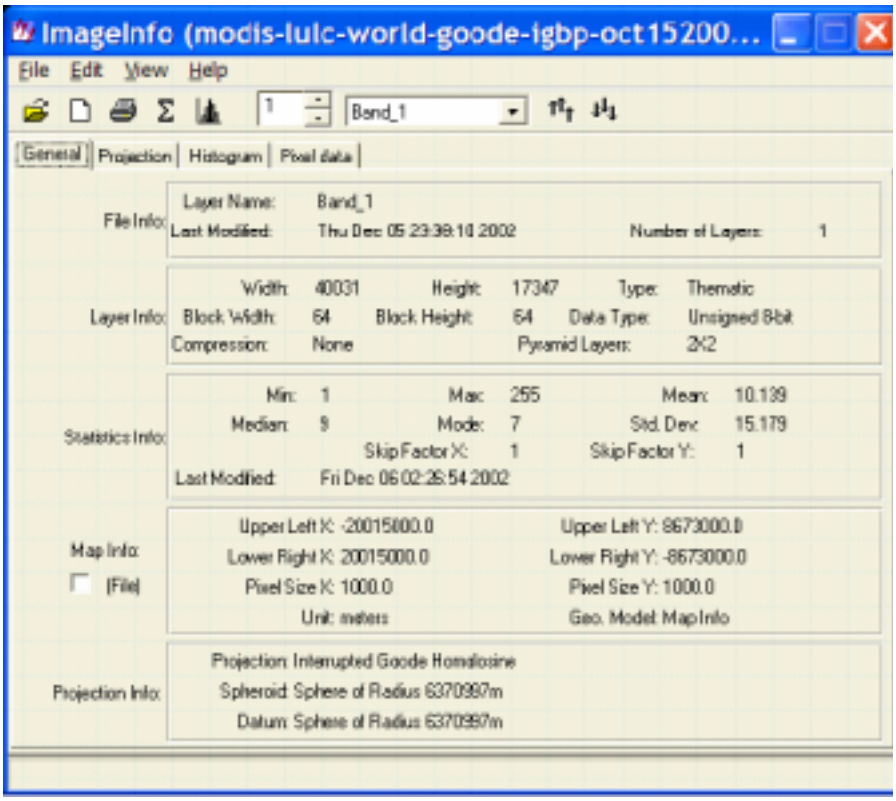

6.0 Globalland cover 2000 legend

Domain	I. Aggregation Global Classes (mandatory)	II. Suggestion for regional and subregional classes (additional classes may be added if consistently achievable)	<< corresponding LCCS codes and classifiers (examples - not exhaustive)	General comments
Forest types	1.Tree Cover, broadleaved, evergreen (LCCS >15% tree cover, tree height >3m)	1.1 -closed > 40% tree cover (LCCS >65% and >40-65% r)	2*& A3, A10,A11+A12, D1, E1,	· GLC forest definition overlaps in terms of definition Partly with IGBP Woody Savannas and Savannas
		1.2 -.open 5-40% tree cover ·	2*& A3, A11+A13, D1, E	
	2.Tree Cover, broadleaved, deciduous	2.1 - closed	2*& A3, A10,A11+A12, D1, E2	· GLC Forest is close to FAO definitions, recommended By definitions workshop also for 'Kyoto forests'
		2.2 - open	2*& A3, A11+A13, D1, E2	
	3.Tree Cover, needle-leaved, evergreen	3.1 - closed	2*& A3, A10,A11+A12, D2, E1	
		3.2 - open	2*& A3, A11+A13, D2, E1	
	4.Tree Cover, broadleaved, deciduous	4.1 - closed	2*& A3, A10,A11+A12, D2, E2	
		4.2 - open	2*& A3, A11+A13, D2, E2	
Flooded and inundated forest types	5.Tree Cover, mixed phenology or leaf type	5.1 - closed	2*& A3, A10,A11+A12, D1+// D2 or E1//E2	
		5.2 - open	2*& A3, A11+A13, D1//D2 or E1//E2	
	6.Tree Cover, regularly flooded: Mangrove	6 Tree Cover, regularly flooded: Mangrove	4*& A3, A12-13-14-15 and R3	
	>>>>-flooded forest types other than mangrove (swamp, peat swamp,) are not displayed at the global level but grouped under class (1)<<<<	1.3 Tree Cover, other, regularly flooded, closed	4*& A3, A12,A13+14	
		1.4 Tree Cover, other, regularly flooded, open	4*& A3, A13+15	
Shrub land type and Shrub-Tree Savannas types	7.Shrub Cover, closed-open, evergreen (with or without sparse tree layer)	7.- minimum same as global optional: > 7.1 without, 7.2 with sparse tree layer	2*& A4, D1-2, E1 and optional F2,F5	
	8.Shrub Cover, closed-open, deciduous (with or without sparse tree layer)	8.- minimum same as global optional: > 8.1 without, 8.2 with sparse tree layer	2*& A4, D1-2, E2 and optional F2,F5	

Continued

Grassland, Savannas, Health Pasture Tree Savanna type	Herbaceous Cover, closed-open	9.1 Herbaceous Cover, closed-open 9.11 natural; 9.12 pasture[1] 9.2 Herbaceous Cover, closed-open with sparse trees or shrubs (> sub-classes)	2*& A2-5-6, A10-11-12-13 2*& A6, A10-11-12-13 + user-label 'pasture' 2*& A2-5-6, F2, F5-6 2*& A3, A14-15-16 or 4*& A3, A16-17-18	· The global 'target legend' would consist of the 21 classes listed above - assuming that they can be consistently formed from the original LCCS classes. · At the (sub-) regional level the legends would be as detailed as consistently possible and as discussed in the regional GLC2000 groups. It is required that the classes can be integrated into the global scheme. Some sub-classes generally desired at this level are displayed above, however the regional working group may add others. If sub-classes cannot be formed consistently for a sub-region or region one would fall back to the global categories.
Steppe types	9.Sparse Herbaceous or sparse shrub cover	10.- minimum same as global -	2*& A2-5-6, A14-15-16 or 2*& A4, A14-15-16	
Tundra types	10. Lichens & Mosses	11 - minimum same as global -	2*& A7-8-9	
Wetland types	11.Regularly flooded shrub and/or herbaceous cover	12- minimum same as global -	4*& A4, D1-2, E1-2, F2,F5	· The original LCCS classes are built in each sub-region, region or data set independently and following the LCCS criteria and philosophy: original land cover classes are described to the detail possible. The 'target' legend above would be the result of aggregation of the original classes.
Bog type	12.Regularly flooded cover of mosses (and lichens)	13- minimum same as global -	4*& A2-5-6-8-9 or 4*&A7-10-11	
Croplands	13.Cultivated and managed areas	14.1- terrestrial	0*& A11,	If 'cultivated grassland' = 'pasture'

Continued

		14.11 Tree and shrub cover (perennial) (orchards, vineyards)	1*& A1-A2s	cannot be distinguished from natural grassland, it will be included in the natural class
		14.12 Herbaceous crops (annual), non-irrigated	1*& A3-4-5 (&D1)	
		14.13 Herbaceous crops (annual), irrigated	1*& A3-4-5 & D3	
		14.2- aquatic (flooded during cultivation period)	0*& A23	
Mosaic types Each component ≥"20% and ≤"80% First component	14.Tree cover/other natural vegetation	15- minimum same as global -	2*& A3 and A2-4-5-6 or C2, F2, F4-6 / 0004 or 4*& A3, A2-4-5-6-8-9 / 0004	
dominant	15.Cropland / Tree Cover	16- minimum same as global -	0*/ 2*& A3 or 0*/ 4*& A3	
	16.Cropland / Other natural vegetation (non-trees)	17- minimum same as global -	0*/ 2*& A2, 4-9 or 0*/ 4*& A2-11	
Barren & Desert	17.Bare Areas	18- minimum same as global -	6*	
Water, Snow and Ice	18.Water Bodies (natural & artificial)	19- minimum same as global -	8*& A1 or 0*& B27	
	19.Snow and Ice (natural & artificial)	20- minimum same as global -	8*& A2-3	
Urban	20.Artificial surfaces and associated areas	21- minimum same as global -	0*& B15	

7.0 IGBP LULC class definition

Land Cover Class	Definition
1. Evergreen Needle leaf Forests	Lands dominated by woody vegetation with a percent cover >60% and height exceeding 2 meters. Almost all trees remain green all year. Canopy is never without green foliage.
2. Deciduous Needle leaf Forests	Lands dominated by woody vegetation with a percent cover >60% and height exceeding 2 meters. Consists of seasonal, needle leaf tree communities with an annual cycle of leaf-on and leaf-off periods.
3. Evergreen Broadleaf Forests	Lands dominated by woody vegetation with a percent cover >60% and height exceeding 2 meters. Almost all trees and shrubs remain green all year. Canopy is never without green foliage.
4. Deciduous Broadleaf Forests	Lands dominated by woody vegetation with a percent cover >60% and height exceeding 2 meters. Consists of broadleaf tree communities with an annual cycle of leaf-on and leaf-off periods.
5. Mixed Forests	Lands dominated by woody vegetation with a percent cover >60% and height exceeding 2 meters. Consists of tree communities with interspersed mixtures or mosaics of the other four forest types. None of the forest types exceeds 60% of landscape.
6. Closed Shrub lands	Lands with woody vegetation less than 2 meters tall and with shrub canopy cover >60%. The shrub foliage can be either evergreen or deciduous.
7. Open Shrub lands	Lands with woody vegetation less than 2 meters tall and with shrub canopy cover between 10-60%. The shrub foliage can be either evergreen or deciduous.
8. Woody Savannas	Lands with herbaceous and other under story systems, and with forest canopy cover between 30-60%. The forest cover height exceeds 2 meters.
9. Savannas	Lands with herbaceous and other under story systems, and with forest canopy cover between 10-30%. The forest cover height exceeds 2 meters.
10. Grasslands	Lands with herbaceous types of cover. Tree and shrub cover is less than 10%.
11. Permanent Wetlands	Lands with a permanent mixture of water and herbaceous or woody vegetation. The vegetation can be present in either salt, brackish, or fresh water.
12. Croplands	Lands covered with temporary crops followed by harvest and a bare soil period (e.g., single and multiple cropping systems). Note than perennial woody crops will be classified as the appropriate forest or shrub land cover type.
13. Urban and Built-Up	Land covered by buildings and other man-made structures.
14. Cropland/Natural Vegetation Mosaics	Lands with a mosaic of croplands, forests, shrub land, and grasslands in which no one component comprises more than 60% of the landscape.
15. Snow and Ice	Lands under snow/ice cover.
16. Barren	Lands with exposed soil, sand, rocks, or snow and never have more than 10% vegetated cover during any time of the year.
17. Water Bodies	Oceans, seas, lakes, reservoirs, and rivers. Can be either fresh or salt-water bodies.

8.0 Anderson classification system for land use and land cover classification system for use with remote sensor data

Level I	Level II
1. Urban or Built-up Land	11. Residential.
	12 Commercial and Services.
	13. Industrial.
	14. Transportation, Communications, and Utilities.
	15. Industrial and Commercial complexes.
	16. Mixed Urban or Built-up Land.
	17. Other Urban or Built-up Land.
2. Agricultural Land	21. Cropland and Pasture.
	22. Orchards, Groves, Vineyards, Nurseries, and Ornamental Horticultural Areas.
	23. Confined Feeding Operations.
	24. Other Agricultural Land.
3. Rangeland	31. Herbaceous Rangeland.
	32. Shrub and Brush Rangeland.
	33. Mixed Rangeland.
4. Forest Land	41. Deciduous Forest Land.
	42. Evergreen Forest Land.
	43. Mixed Forest Land.
5. Water	51. Streams and Canals.
	52. Lakes.
	53. Reservoirs.
	54. Bays and Estuaries.
6. Wetland	61. Forested Wetland.
	62. Non-forested Wetland.
7. Barren Land	71. Dry Salt Flats.
	72. Beaches.
	73. Sandy Areas other than Beaches.
	74. Bare Exposed Rock.
	75. Strip Mines, Quarries, and Grave Pits
	76. Transitional Areas.
	77. Mixed Barren Land.
8. Tundra	81. Shrub and Brush Tundra.
	82. Herbaceous Tundra.
	83. Bare Ground Tundra.
	84. Wet Tundra.
	85. Mixed Tundra.
9. Perennial Snow or Ice	91. Perennial Snowfields.
	92. Glaciers.

8.1 ***Anderson sub-categorization for land use and land cover classification system for use with remote sensor data (one example).***

Level I	Level II	Level III
1. Urban or Built-up	11. Residential.	111. Single family Units.
		112. Multi-family Units.
		113. Group Quarters.
		114. Residential Hotels.
		115. Mobile Home Parks.
		116. Transient Lodgings.
		117. Other.

Reference

Anderson, James R., 1971, Land use classification schemes used in selected recent geographic applications of remote sensing: Photogramm. Eng., v. 37, no. 4, p. 379-387.

Anderson, James R., Hardy, Ernest E., and Roach, John T., 1972, A land-use classification system for use with remote-sensor data: U.S. Geol.
Survey Circ. 671, 16 p., refs.

Anderson, James R., Hardy, Ernest E., and Roach, and Witmer, R.E. 1976. A revision of the land use classification system as presented in U.S. Geological Survey Circular 671. Geological Survey Professional Paper 964. United States Government Printing Office, Washington: 1976.

Appendix 3:

Global Forest Cover (5 classes) and density (0-100 %)

1.0 Overview of the forest cover (5 classes)

Description:

The forest cover for the globe was mapped based on 1-km AVHRR data. Monthly composites of the 1995 images were used for the purpose. A decision tree approach involving NDVI and red band reflectances formed the basis of the first two classes: the closed forest (40% - 100% canopy cover), and open or fragmented forest (10 - 40% canopy cover). The USGS global land cover characteristics database was used to stratify and map the other 3 classes.

Accuracy:

Validated on the basis of existing reference data sets, the map is estimated to be 77 percent accurate for the first four classes (no reference data were available for water), and 86 percent accurate for the forest and nonforest classification.

Reference:

Defries, R., Hansen, M., Janetos, A., Loveland, T.R., Townshend, J., and 2000. A Global 1km Data Set of Percent Tree Cover Data Derived from Remote Sensing. Global Change Biology, v. 6, p. 247-254.

Download site:

http://glfc.umiacs.umd.edu/

Contact:

pdavis@umd.edu

Credits:

University of Maryland
USGS
FAO

1.1 Legend of forest classes

1. closed forest
2. open fragmented forest
3. other wooded land
4. other land cover
5. water

1.1.1 Header information of forest classes

Appendix forests 1a: Global Forest Density (0-100%)

2.0 Overview of the forest density (0-100%)

Description:

The forest cover for the globe was mapped based on 1-km AVHRR data. Monthly composites of the 1995 images were used for the purpose. A decision tree approach involving NDVI and red band reflectances formed the basis of the first two classes: the closed forest (40% - 100% canopy cover), and open or fragmented forest (10 - 40% canopy cover). The USGS global land cover characteristics database was used to stratify and map the other 3 classes.

Accuracy:

Validated on the basis of existing reference data sets, the map is estimated to be 77 percent accurate for the first four classes (no reference data were available for water), and 86 percent accurate for the forest and nonforest classification.

Reference:

Defries, R., Hansen, M., Janetos, A., Loveland, T.R., Townshend, J, and 2000. A Global 1km Data Set of Percent Tree Cover Data Derived from Remote Sensing. Global Change Biology, v. 6, p. 247-254.

Download site:

http://glfc.umiacs.umd.edu/

Contact:

pdavis@umd.edu

Credits:

University of Maryland
USGS
FAO

2.1 Legend of forest density

0 to 100 percent density, scaled.

2.2 Header information of forest classes

Appendix 4

Inter-sensor calibrations

B. IKONOS and ETM + NDVI using 4m pixels

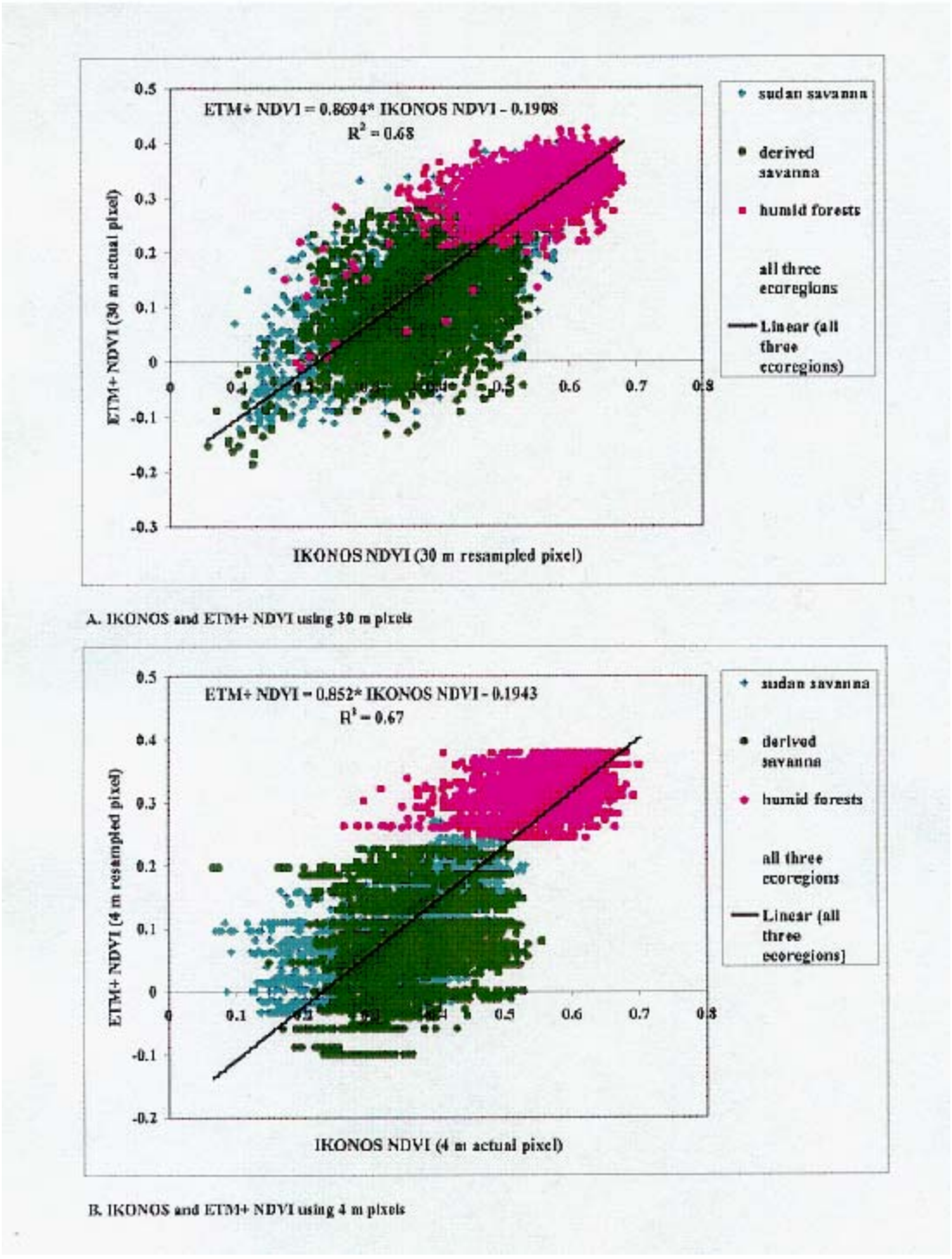

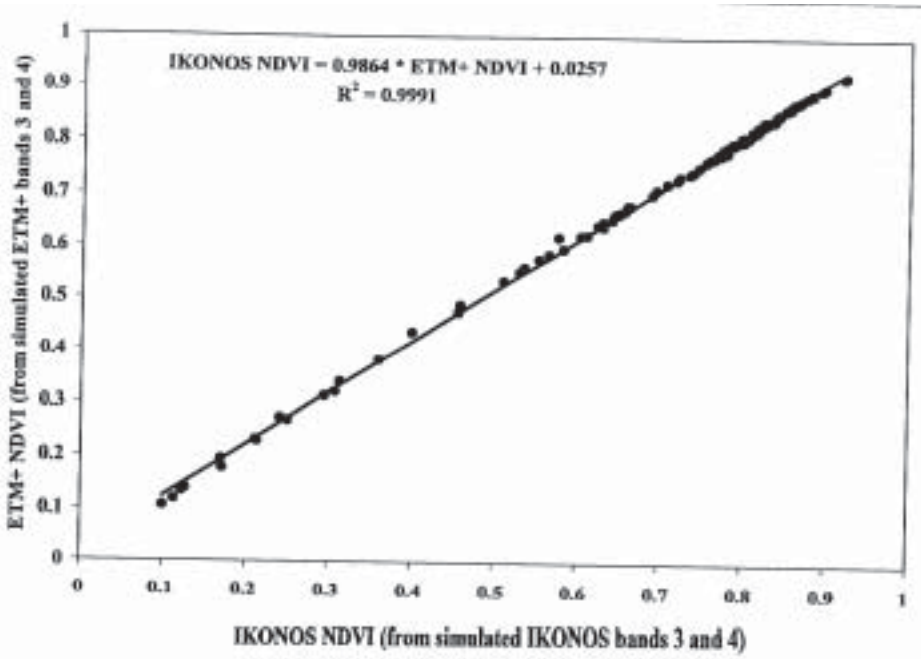
IKONOS NDVI = 0.9864 * ETM+ NDVI + 0.0257
R² = 0.9991
ETM+ NDVI (from simulated ETM+ bands 3 and 4)
IKONOS NDVI (from simulated IKONOS bands 3 and 4)
0
0.1
0.2
0.3
0.4
0.5
0.6
0.7
0.8
0.9
1

Appendix 5

Radiometric and Atmospheric corrections (normalization)

The radiometric and atmospheric corrections can be categorized into a 3 step process, as described below.

Step 1: Conversion from digital numbers (unit less) to radiance (W/m² Sr μm),

1.1 Basin-level datasets: MODIS 7-band Reflectance, AVHRR monthly and 10-day composites

These data come as apparent reflectance values that are scaled to 8 or 16-bit integer values. Move to step 3.

1.2 Sub-basin level datasets: ETM+, TM, ASTER, and ALI data

1.2.1 ETM+ digital numbers to radiance (W/m² Sr μm)

The Landsat-7 Enhanced Thematic Mapper plus (ETM+) 8-bit digital numbers (DN's) are converted to radiances using the following equation as illustrated for one image:

$$\text{Radiance } (W/m^2 \text{ Sr } \mu m) = \text{gain} * DN + \text{offset} \quad (5a)$$

which is also expressed as:

$$\text{Radiance } (W/m^2 \text{ Sr } \mu m) = ((LMAX-LMIN)/(QCALMAX-QCALMIN))(QCAL-QCALMIN) + LMIN \quad (5b)$$

where: QCALMIN = 1
QCALMAX = 255
QCAL = Digital Number

The LMINs and LMAXs are the spectral radiances for each band at digital numbers 1 and 255 (i.e QCALMIN, QCALMAX), respectively. The LMAX and LMIN values (in W/m² Sr μm)for the March 18, 2001 ETM+ image are: LMAX_BAND1 = 191.600; LMIN_BAND1 = -6.200; LMAX_BAND2 = 196.500; LMIN_BAND2 = -6.400; LMAX_BAND3 = 152.900; LMIN_BAND3 = -5.000; LMAX_BAND4 = 241.100; LMIN_BAND4 = -5.100; LMAX_BAND5 = 31.060; LMIN_BAND5 = -1.000; LMAX_BAND61 = 17.040; LMIN_BAND61 = 0.000; LMAX_BAND62 = 12.650; LMIN_BAND62 = 3.200; LMAX_BAND7 = 10.800; LMIN_BAND7 = -0.350; LMAX_BAND8 = 243.100; LMIN_BAND8 = -4.700.

Table #.. Sample calibration coefficients for Landsat-7 ETM+. See header files for specific values for your data.

Table 11.2 ETM+ Spectral Radiance Range

watts/(meter squared * ster * μm)

Band Number	Before July 1, 2000				After July 1, 2000			
	Low Gain		High Gain		Low Gain		High Gain	
	LMIN	LMAX	LMIN	LMAX	LMIN	LMAX	LMIN	LMAX
1	-6.2	297.5	-6.2	194.3	-6.2	293.7	-6.2	191.6
2	-6.0	303.4	-6.0	202.4	-6.4	300.9	-6.4	196.5
3	-4.5	235.5	-4.5	158.6	-5.0	234.4	-5.0	152.9
4	-4.5	235.0	-4.5	157.5	-5.1	241.1	-5.1	157.4
5	-1.0	47.70	-1.0	31.76	-1.0	47.57	-1.0	31.06
6	0.0	17.04	3.2	12.65	0.0	17.04	3.2	12.65
7	-0.35	16.60	-0.35	10.932	-0.35	16.54	-0.35	10.80
8	-5.0	244.00	-5.0	158.40	-4.7	243.1	-4.7	158.3

The following information is obtained from the header files:

1.2.2 TM digital numbers to radiance (W/m² Sr μm)

The Landsat-5 TM Spectral radiance is computed using the following equation:

$R_i = \alpha_i \, DN_i + \beta_i$ (4)

R_i = spectral radiance in W / $m^2 \mu m^1$

α_i = gain or slope in W / m^2 μm^1

β_i = bias or intercept in W / $m^2 \mu m^1$

DN_i = digital number of each pixel in TM bands

i = 1 to 5 and 7 (except the thermal band 6)

The α_i and β_i values are for the image are obtained from the header files.

1.2.3 ASTER digital numbers to radiance (W/m² Sr μm)

Radiance = (DN value -1) x Unit conversion coefficient

The unit conversion coefficient L_{ni} are:

VNIR and SWIR bands::

For TIR bands $$Lni = \frac{L\max i}{253}$$

$$Lni = \frac{L\max i}{4093}$$

Lni: the unit conversion coeffcient from DN to radiance of band i

Lmaxi: the maximum radiance of band i

Table #: Unit conversion coefficients for ASTER data

Band No.	Maximum radiance (W/(m² sr mm))			
	High gain	Normal gain	Low gain 1	Low gain 2
1	0.676	1.688	2.25	
2	0.708	1.415	1.89	
3N	0.423	0.862	1.15	N/A
3B	0.423	0.862	1.15	
4	0.1087	0.2174	0.290	0.290
5	0.0348	0.0696	0.0925	0.409
6	0.0313	0.0625	0.0830	0.390
7	0.0299	0.0597	0.0795	0.332
8	0.0209	0.0417	0.0556	0.245
9	0.0159	0.0318	0.0424	0.265
10		6.882 x 10-3		
11		6.780 x 10-3		
12	N/A	6.590 x 10-3	N/A	N/A
13		5.693 x 10-3		
14		5.225 x 10-3		

Table # Maximum input radiance for the various gain settings

Band #	Maximum Input Radiance [W/m²/sr/μm] (Lmax) High Gain	Maximum Input Radiance [W/m²/sr/μm] (Lmax) Normal Gain	Maximum Input Radiance [W/m²/sr/μm] (Lmax) Low Gain - 1	Maximum Input Radiance [W/m²/sr/μm] (Lmax) Low Gain - 2
1	170.8	427	569	N/A
2	179.0	358	477	N/A
3	106.8[1]	218	290	N/A
4	27.5	55.0	73.3	73.3
5	8.8	17.6	23.4	103.5
6	7.9	15.8	21.0	98.7
7	7.55	15.1	20.1	83.8
8	5.27	10.55	14.06	62.0
9	4.02	8.04	10.72	67.0
10		28.17*	N/A	N/A
11		27.75*		
12		26.97*		
13		23.30*		
14		21.38*		

Notes: The value will be slightly different when applying High Gain Conversion Coefficient. Apparent gain is 2.0412 as compared to the nominal gain value 2.

*Radiance of 370 K Blackbody

Table #: Radiance conversion coefficient for individual bands.

Band #	High gain	Normal gain	Low gain-1	Low gain-2
1	2.5	1.0	0.75	N/A
2	2.0	1.0	0.75	N/A
3	2.0	1.0	0.75	N/A
4	2.0	1.0	0.75	0.75 (NBR)
5	2.0	1.0	0.75	0.17 (NBR)
6	2.0	1.0	0.75	0.16 (NBR)
7	2.0	1.0	0.75	0.18 (NBR)
8	2.0	1.0	0.75	0.17 (NBR)
9	2.0	1.0	0.75	0.12 (NBR)
10-14	N/A	N/A	N/A	N/A

1.2.4 ALI digital numbers to radiance (mW/cm^2 Sr μm)

The digital numbers (DNs) of advanced land imager (ALI) represent 16-bit absolute radiances but are stored as a 16-bit integer with a scaling factor of 300. The ALI DNs are converted to radiances (mW/cm^2 Sr μm) using equation

$$\text{Radiance (mW/cm}^2\text{ Sr μm) L for ALI} = \frac{\text{Digital number}}{300} \quad (4)$$

1.3 Watershed-level datasets: IKONOS and Hyperion

1.3.1 IKONOS digital numbers to radiance (mW/cm^2-sr)

The 11-bit IKONOS digital numbers (DNs) are converted to radiance (mW/cm^2-sr) using equation

$$L_{i,j,k} = DN_{i,j,k} * [CalCoef_k]^{-1} \quad (3)$$

where:

i,j,k = IKONOS image pixel i,j in spectral band k

$L_{i,j,k}$ = in-band radiance at the sensor aperture (mW/cm^2-sr)

$CalCoef_k$ = In-Band Radiance Calibration Coefficient (mW/cm^2*sr-DN)

$DN_{i,j,k}$ = image product digital value (DN)

The Calibration coefficients ($CalCoef_k$) for post Febraury 22, 2001 IKONOS images were 728 (for band 1), 727 (band 2), 949 (band 3), and 843 (band 4). Since both IKONOS images used in this study are post February 22, 2001 the above $CalCoef_k$ were used.

1.3.2 Hyperion data to radiance (W/m^2 Sr μm)

The digital values (DNs) of the hyperion level 1 products are 16-bit radiances and are stored as 16-bit signed integer. The DNs are converted to radiances (W/m^2 Sr μm) using appropriate scaling factor which is 40 for visible and near infrared (VNIR) and 80 for Short Wave infrared (SWIR).

There are 50 VNIR hyperion bands that are calibrated. These start with band 8 (427.55 nm) and go upto band 58 (925.25 nm). Each band is about 10 nm wide.

$$\text{Radiance (W/m}^2\text{ Sr μm) L for VNIR bands} = \frac{\text{Digital number}}{40} \quad (1)$$

There are 146 SWIR hyperion bands that are calibrated and unique in wavelength. These start with band 79 (932.72 nm) and go upto band 224 (2395.53 nm). Each band is about 10 nm wide.

$$\text{Radiance (W/m}^2\text{ Sr μm) L for SWIR bands} = \frac{\text{Digital number}}{80} \quad (2)$$

Step 2: Conversion from to radiance (W/m² Sr μm) to apparent or at-satellite exo-atmospheric reflectance (percent)

2.1 Basin-level datasets: MODIS 7-band Reflectance, AVHRR monthly and 10-day composite data

These data come as apparent reflectance values that are scaled to 8 or 16-bit integer values. Move to step 3.

2.2 Subbasin level datasets: ETM+, TM, ASTER, and ALI data

A reduction in between-the-scene variability can be achieved through a normalization for solar irradiance by converting spectral radiance, as calculated above, to planetary reflectance or albedo (see Markam and Barker, 1985 and Markham and Barker, 1987). This combined surface and atmospheric reflectance of the Earth is computed with the following formula:

$$\rho_p = \frac{\pi * L_\lambda * d^2}{ESUN_\lambda * \cos \theta_s} \quad (6)$$

ρ = at-satellite exo-atmospheric reflectance (unitless)

L^p = radiance W / m^2 Sr^1 μm^1 or mW/cm^2 sr μm^1 or mW/cm^2 Sr μm

d^λ = earth to sun distance in astronomic units obtained based on acquisition date from standard tables (unitless) (see Markham and Barker, 1987)

$ESUN_\lambda$ = Mean solar exo-atmospheric irradiances (W / m^2 Sr^1 μm^1 or mW/cm^2 sr μm^1 or mW/cm^2 Sr μm) or solar flux data obtained from Neckel and Labs (1984) data. For IKONOS, ALI, and ETM+ bands see data in Table 2 derived from Neckel and Labs (1984).

θ_s = solar zenith angle in degrees (which is 90 degrees minus the sun elevation or sun angle when the scene was recorded as given in the image header file; see Table 1 for sun elevation data from header files of images or can be calculated based on latitude, longitude, and acquisition time).

Table 2a. Solar flux or exatmospheric irradiances (mW cm^{-2} μm^{-1}) for Landsat-5 TM wavebands (Markham and Barker, 1985). For other sensors see the plot below.

Band	Solar Flux or ex-atmospheric irradiances (mW cm^{-2} μm^{-1})
1	194.648
2	181.263
3	154.595
4	104.670
5	21.112
6	1.000
7	7.691

Table 2b. Solar flux or ex-atmospheric irradiances (mW cm^{-2} μm^{-1}) for Landsat-t ETM+ wavebands. For other sensors see the plot below.

ETM band #	irradiance (W m^{-2} µm^{-1})
1	1970
2	1843
3	1555
4	1047
5	227.1
7	80.530
8	1368

For band # 6

k1 666.09 W m^{-2} sr^{-1} µm^{-1}
k2 1282.71 temperature degree kelvin

Figure 1. Solar flux (mW cm-2μm-1) (Neckel and Labs, 1981).

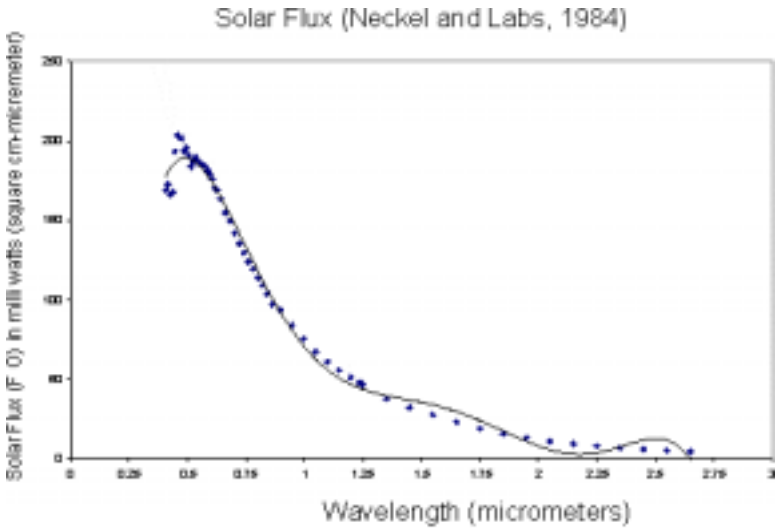

Table 11.4 Earth-Sun Distance in Astronomical Units

Julian day	Distance	Julian day	Distance	Julian day	Distance	Julian day	Distance	Julian day	Distance
1	.9832	74	.9945	152	1.0140	227	1.0128	305	.9925
15	.9836	91	.9993	166	1.0158	242	1.0092	319	.9892
32	.9853	106	1.0033	182	1.0167	258	1.0057	335	.9860
46	.9878	121	1.0076	196	1.0165	274	1.0011	349	.9843
60	.9909	135	1.0109	213	1.0149	288	.9972	365	.9833

2.3 Watershed-level datasets: IKONOS and Hyperion data

Same as in section 2.2.

Step 3: Atmospheric normalization for surface reflectance

Conversion from to apparent or at-satellite exo-atmospheric reflectance (percent) to surface reflectance (percent)

3.1 Basin-level datasets: MODIS 7-band Reflectance, AVHRR monthly and 10-day composite data

3.1.1 MODIS data Atmospheric normalization

Dynamic range of MODIS 7-band reflectance data is 11bit (2048 DNs). Data are stretched and provided as signed 16 bit integer. Scale factor of 100 is used to divide 16 bit DNs to get reflectance in percent. This is at-satellite exo-atmosperic reflectance (apparent reflectance). For time series MODIS images, use the following procedure for atmospheric corrections to obtain surface reflectance:

1. Select desert sites (time invariant locations);

2. Use 3 x 3 or 5 x 5 window to extract mean, minimum, maximum, and standard deviations of individual band reflectance for, say 2000-current period;

3. Determine the mean band reflectance for the entire period of 2000-current1 for this time invariant site (e.g., MODIS Terra or MODIS Aqua);

4. Calibration coefficient for any image = (mean band reflectance of time invariant site)/(measured band reflectance of the image in consideration for the same time invariant site)

5. Similarly compute calibration coeffcient for the entire period;

6. Use the calibration coefficient of each image to correct that particular image. Repeat the procedure for all images.

3.1.2 AVHRR 1981-2001 data atmospheric normalization

First calculate the apparent reflectance (at-satellite) from the scaled DNs using appropriate offset and gains in the NOAA AVHRR monthly and 10-day composites for the 1981-2001 period. The relevant equations are:
Apparent Reflectance = (Band 1 16-bit radiance – 10) * 0.002
Apparent Reflectance = (Band 1 16-bit radiance – 10) * 0.002
Apparent Reflectance =(Band 4 scaled DN in 16-bit + 31990) * 0.005
Apparent Reflectance =(Band 4 scaled DN in 16-bit + 31990) * 0.005
Surface Reflectance using split window technique: $Ts = T_4 + 3.3 (T_4 – T_5)$
NDVI = (SNDVI – 128) * 0.008

Then apply atmospheric normalization on all images use the following steps for NDVI data (apply similar procedure for individual band data as well).

1. Select desert sites (time invariant locations);

2. Use 3 x 3 or 5 x 5 window to extract mean, minimum, maximum, and standard deviations of NDVI for the 1981-2001 period;

3. Determine the mean NDVI for the entire period of 1981-2001 for this time invariant site (e.g., NOAA 7 to NOAA 14);

4. Calibration coefficient for any image = (mean NDVI of time invariant site)/(measured NDVI of the image in consideration for the same time invariant site)

5. Similarly compute calibration coeffcient for the entire period;

6. Use the calibration coefficient of each image to correct that particular image. Repeat the procedure for all images.

3.2 Subbasin level datasets: ETM+, TM, and ALI data

3.2.1 Simple dark-object subtraction technique (S-DOS)

S-DOS = simple dark object subtraction method = individual haze value extracted from the image by observing the histogram of each band and deducting the minimum haze value. This often leads to over correction.

1. look into histogram of all bands

2. in haze effected data the visible bands have high starting values relative to NIR and MIR bands

3. note the MINIMUM value of all bands

4. deduct each band from its MINIMUM DN value

5. what we get is new DN values for each band without haze effected DNs

6. this helps in multidate comparisons where one image is haze effected and the other is not.

3.2.2 Improved dark-object subtraction technique (I-DOS)

I-DOS = (relative haze) * (normalized gain x) + (offset x)

Where, relative haze = relative haze value = (starting haze value for band 1) – (offset band 1) * factor for each band.

This, scene-based atmospheric scattering correction is done using Chavez modified dark-object subtraction technique. Especially in arid and semi-arid regions most atmospheric affects are due to scattering of light by gas molecules and aerosols. Chavez technique is based on the theory that the degree of scattering is strongly wavelength-dependent: it affects blue wavelengths much more than red and infrared wavelengths. The Chavez procedure uses a number of relative scattering models for different atmospheric conditions, as follows:

Atmospheric conditions	Relative scattering model
Very clear	$\lambda^{-4.0}$
Clear	$\lambda^{-2.0}$
Moderate	$\lambda^{-1.0}$
Hazy	$\lambda^{-0.7}$
Very Hazy	$\lambda^{-0.5}$

The method is well suited for the study areas which are predominantly in semi-arid or arid regions. Rayleigh relative scattering model of $\lambda^{-4.0}$ is used when there are “very clear” images. The method involves selecting a starting haze value (SHV) by plotting and observing the histograms of band 1 where atmospheric effects are most pronounced . The Chavez model then calculates haze affected band values for other bands. The haze affected band values of each band are then deducted from the original band values. The theory here is that the digital numbers or reflectance over perfect “dark objects” (e.g., unpolluted deep water bodies), for example, should remain unchanged from time period 1 to time period 2 if not for atmospheric effects.

3.2.3 Radiometric approach of darkest and brightest objects

Radiometric approach of selecting brightest and darkest objects and calibrating.
Target areas of time invariant dark objects (typically deep water) and bright objects (high albedo soils or concrete) are identified and a linear relationship between satellite response over multiple acquisition dates are developed for normalization of atmospheric objects. Developed by before extracting any information, atmospheric affects were normalized for 3 study images. Regression analysis was attempted resulting in regression equations for each band (Table 3c). However, this method suffered from great difficulty in determining a “perfect” bright object over a decade long duration.

Figure #. Process of choosing the starting haze value (SHV), preferably for band 1.

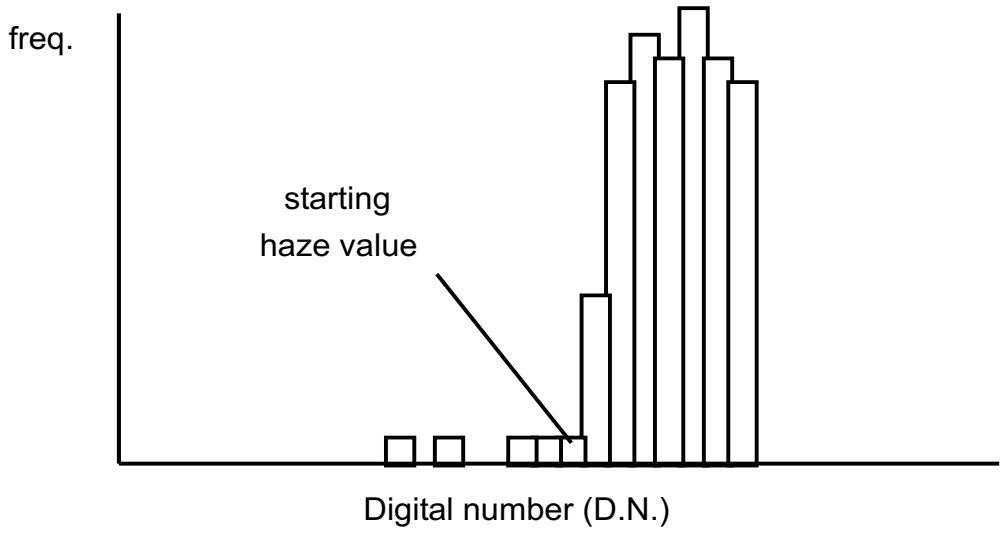

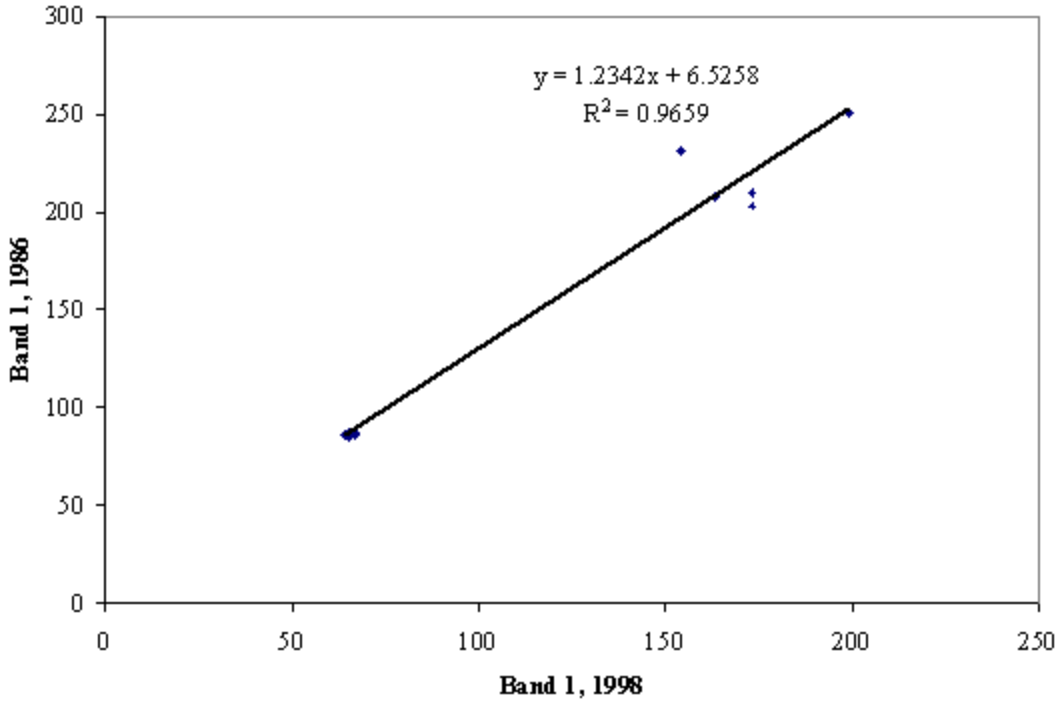

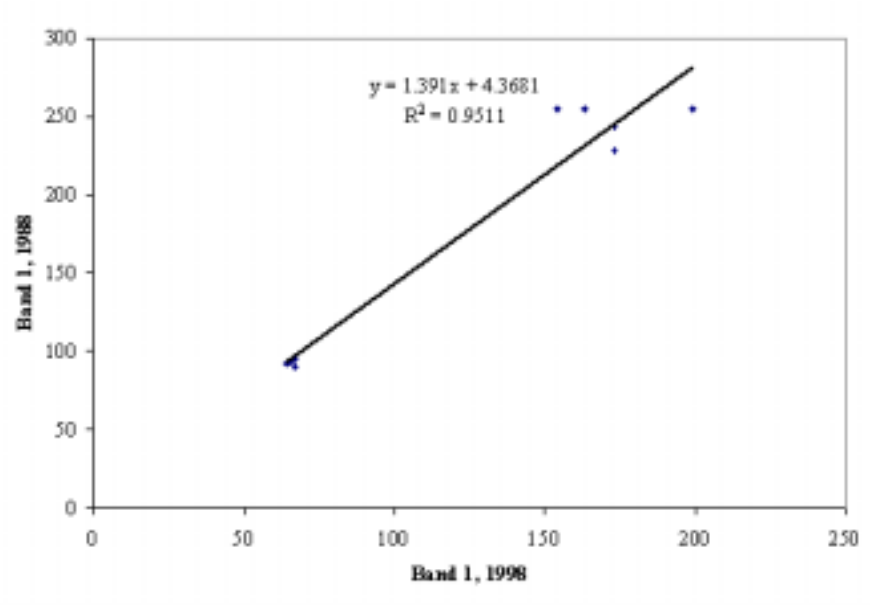

3.2.4 6-S Model

If detailed climatic data for the region is available, this approach can be attempted.

3.3 Watershed-level datasets: IKONOS and Hyperion data

Same as in section 3.2.

4.0 Temperature from ETM+ thermal data

ETM+ Band 6 imagery can also be converted from spectral radiance (as described above) to a more physically useful variable. This is the effective at-satellite temperatures of the viewed Earth-atmosphere system under an assumption of unity emmissivity and using pre-launch calibration constants listed in Table 11.5. The conversion formula is:

T = Effective at-satellite temperature in Kelvin
K2 = Calibration constant 2 (1282.71 temperature degree kelvin)
K1 = Calibration constant 1 (666.09 W m^{-2} sr^{-1} μm^{-1})
L = Spectral radiance in watts/(meter squared * ster * μm)

$$T = \frac{K_2}{\text{Ln}((K_1 / L_\lambda) + 1))}$$

Kelvin (K): for thermodynamic temperature. (Metric countries legally use degrees celcius [°C], which measure the same [one degree celsius = one degree kelvin] but start at a different level of the same scale [0 K = -273.15 °C] [0 °C = 273.15 K] [100 °C = 373.15 K])

Thereby, a 300 degree kelvin is 26.85 degree celcius.

3.0 References

Markham, B.L, and Barker, J.L., 1987, Radiometric properties of U.S. processed Landsat MSS data. Remote Sensing of Environment, 22:39-71.

Markham, B.L, and Barker, J.L., 1985, Spectral characterization of the LANDSAT Thematic Mapper sensors. International Journal of Remote sensing, 6(5):697-716.

Neckel, H., and Labs, D., 1981, Improved data of solar spectral irradiance from 0.33 to 1.25 m m. Solar Physics, 74:231-240.

Neckel, H., and Labs, D., 1984, The solar radiation between 3300 and 12500 A, Solar Physics, 90:205-258.

EO-1 Hyperion and ALI

http://eo1.gsfc.nasa.gov/miscPages/home.html
http://eo1.usgs.gov/
http://eo1.usgs.gov/dataproducts/faq.asp
http://edcdaac.usgs.gov/landsat7/

Landsat-7 ETM+

http://ltpwww.gsfc.nasa.gov/IAS/handbook/handbook_toc.html
http://edcsns17.cr.usgs.gov/EarthExplorer/
Sun elevation angle calculation
http://www.srrb.noaa.gov/highlights/sunrise/azel.html

Reference:

http://ltpwww.gsfc.nasa.gov/IAS/handbook/handbook_htmls/chapter11/chapter11.html
http://ltpwww.gsfc.nasa.gov/IAS/handbook/handbook_toc.html

References

Anderson, J. R. 1971. Land use classification schemes used in selected recent geographic applications of remote sensing: Photogram. Eng., v. 37, no. 4, p. 379-387.

Anderson, J. R.; Hardy, E. E.; and Roach, J. T. 1972. A land-use classification system for use with remote-sensor data: U.S. Geol. Survey Circ. 671, 16 p., refs.

Anderson, J. R.; Hardy, E. E.; Roach, J. T.; and Witmer, R.E. 1976. A revision of the land use classification system as presented in U.S. Geological Survey Circular 671. Geological Survey Professional Paper 964. United States Government Printing Office, Washington: 1976..

Anderson, J.D.; Jensen, K. H.; Refsgaard, J. C.; and Rasmussen, K., 2002. Use of remotely sensed precipitation and leaf area index in a distributed hydrological model. Journal of Hydrology 264 (2002) 34–50.

Barker-Schaaf, C.; Friedl, M. A.; Gopal, S.; Woodcock, C.; Muchoney, D.; and Strahler, A.H. 2000. A note on procedures used for accuracy assessment in land cover maps derived from AVHRR data. International Journal of Remote Sensing, 21, 1073– 1077.

Bauer, M. E.; Burk, T. E.; Coppin, P. R.; Ek, A. R.. Lime, S. D.; Walters, D. K.; and Walsh, T. A.1994. Satellite inventory of Minnesota forest resources. Photogrammetric Engineering and Remote Sensing, 60, 287– 298.

Bayr, K. J.; DiGirolamo, N. E.; Hall, D.K.; Riggs, G. A.; and Salomonson, V.V. 2002. MODIS snow-cover products. Remote Sensing of Environment 83, 181–194.

Bell, C.; Balogh, M.; Congalton, R. G.; Green, K.; Milliken, J. A.; and Ottman, R. 1998.

Mapping and monitoring agricultural crops and other land cover in the Lower Colorado river basin. Photogrammetric Engineering and Remote Sensing, 64, 1107– 1112.

Belward, A.; Baret, F.; Justice, C.; Lewis, P.; Morisette, J.; and Privette, J. 2000. Developments in the 'validation' of satellite sensor products for the study of the land surface. International Journal of Remote Sensing, 21, 3383– 3390.

Belward, A.; Estes, J.; Justice, C.; Loveland, T.; Scepan, J.; Strahler, A.; and Townshend, J. 1999. The Way Forward, Photogrammetric Engineering and Remote Sensing, v. 65, no. 9, p. 1,089-1,093.

Belward, A. S.; and Loveland, T. R.; 1997. The IGBP-DIS Global 1 km Land Cover Data Set, DISCover First Results. International Journal of Remote Sensing, v. 18, no. 5, p. 3,289-3,295.

Borak, J.; Friedl, M.; Gopal, S.; Hyman, A.; Lambin, E.; Moody, A.; Muchoney, D.; Strahler, A.; and Townshend, J. 1996, MODIS L and Cover Product Algorithm Theoretical Basis Document (AT BD), V 4.1 (Boston: Boston University Center for Remote Sensing).

Borak, J.; Friedl, M.; Gopal, S.; Lambin, E.; Moody; A. Muchoney; D.; and Strahler, A. MODIS Land Cover Product Algorithm Theoretical Basis Document (ATBD). Version 5.0. MODIS Land Cover and Land-Cover Change Team, Boston University.

Borak, J.; Lambin, E.; Friedl, M.; Gopal, S.; Moody, A.; Muchoney, D.; and Strahler, A. 2003. MODIS Land Cover Product Algorithm Theoretical Basis Document (ATBD). Version 5.0. MODIS Land Cover and Land-Cover Change Team, Boston University.

Bowers, T. L.; and Rowan, L. C. 1996. Remote mineralogic and lithologic mapping of the Ice River Alkaline Complex, British Columbia, Canada using AVIRIS data. Photogrammetric Engineering and Remote Sensing, 62, 1379– 1385.

Brodley, C. E.; and Friedl, M. A. 1997. Decision Tree Classification of Land Cover from Remotely Sensed Data. Remote Sensing of Environment. v. 61, no. 3, p. 399-407.

Brown, J. F.; Loveland, T .R.; Merchant, J. W.; Reed, B. C.; and Ohlen, D.O. 1993. Using Multisource Data in Global Land Characterization: Concepts, Requirements, and Methods, Photogrammetric Enginneering and Remote Sensing, v. 59, no. 6, p. 977-987.

Brown, J. F.; and Loveland, T. R. 1999. Impacts of Land Cover Legends on Global Land Cover Patterns, In Proceedings of the ASPRS Annual Conference, Portland, Oregon, May, 1999, p. 509-519. (CD-ROM).

Brown, J. F.; Loveland, T. R.; Ohlen, D. O.; and Zhu, Z. (1999). The global land-cover characteristics database: the user's perspective. Photogrammetric Engineering and Remote Sensing, 65, 1069–1074.

Brodley, C. E.; and Friedl, M. A. 1997. Decision tree classification of land cover from remotely sensed data. Remote Sensing of Environment 61:399–409.

Brodley, C.; Friedl, M. A.; and Strahler, A. 1999, Maximizing land cover classi. Cation accuracies produced by decision trees at continental to global scales. IEEE Transactions on Geoscience and Remote Sensing, 37, 969–977.

Brown, J. F.; Loveland, T. R.; Ohlen, D. O.; and Zhu, Z. 1999. The global land-cover characteristics database: the user's perspective. Photogrammetric Engineering and Remote Sensing, 65, 1069–1074.

Brown, J. F.; Loveland, T. R.; Merchant, J. W.; Ohlen, D. O.; Reed, B.C.; Zhu, J.; and Yang, L. 2000. Development of a Global Land Cover Characteristics Database and IGBP DIS Cover from 1-km AVHRR Data. International Journal of Remote Sensing, v. 21, no. 6/7, p. 1,303-1,330.

Chapin, F. S. III.; Diaz, S.; Eviner, V. T.; Hooper, D. U.; Hobbie, S. E.; Lavorel, S.; Mack, M. C.; Naylor, R. L.; Reynolds, H. L.; Sala, O. E.; Vitousek, P. M.; and Zavaleta, E. S. 2000. Consequences of changing biodiversity. Nature, 405, 234–242.

Chen, H.; Daughtry, C.; Fang, H.; Liang, S.; Morisette, J.; Strahler, A.; Shuey,. Schaaf,, C.J.;Walthall, C. 2002. Validating MODIS land surface reflectance and albedo products: methods and preliminary results, Remote Sensing of Environment 83 (2002) 149–162.

Congalton, R. G. 1994. Accuracy assessment of remotely sensed data: future needs and directions. In: Proceedings of Pecora 12 land information from space-based systems (pp. 383– 388). Bethesda: ASPRS.

Congalton, R. G.; Balogh, M.; Bell, C.; Green, K.; Milliken, J. A.; and Ottman, R. 1998. Mapping and monitoring agricultural crops and other land cover in the Lower Colorado river basin. Photogrammetric Engineering and Remote Sensing, 64, 1107– 1112.

Congalton, R. G.; and Green, K. 1999. Assessing the accuracy of remotely sensed data: principles and practices. Boca Raton: Lewis Publishers.

Congalton, R. G.; and Plourde, L. C. 2000. Sampling methodology, sample placement, and other important factors in assessing the accuracy of remotely sensed forest maps. In: G. B. M. Heuvelink, M. J. P. M.

Curran, P. J. (Eds.) and Foody, G. M. Environmental remote sensing from regional to global scales (pp. 84– 110). Chichester: Wiley.

Davis, R.; Lorenzini, M.; Waller, E.; and Zhu, Z. 1999. Forest Cover Mapping for the Forest Resources Assessment 2000 of the Food and Agriculture Organization. In Proceedings of the ASPRS Annual Conference, Portland, Oregon, May 1999, p. 520-525. (CD-ROM).

Dawson, R. W.; Tao, S.; and Li, B. 2002. Relations between AVHRR NDVI and ecoclimatic parameters in China. Int. j. remote sensing, vol. 23, no. 5, 989–999.

DeFries, R.; Hanson, M.; and Townshend, J. 1995. Global discrimination of land cover types from metrics derived from AVHRR pathfinder data. Remote Sensing of Environment 54:209–222.

DeFries, R.; Hanson, M.; Sohlberg, R.; and Townshend J. 1998. Global land cover classifications at 8-km spatial resolutions: The use of training data derived from landsat imagery in decision tree classifiers. International Journal of Remote Sensing, 19(6):3141-3168.

DeFries, R. S.; and Los, S. O. 1999. Implications of Land-Cover Misclassification for Parameter Estimates in Global Land-Surface Models: An Example from the Simple Bioshpere Model (SiB2). Photogrammetric Engineering and Remote Sensing, v. 65, no. 9, p. 1,083-1,088.

DeFries, R. S.; and Townshend, J. R. G. 1994. Global land cover: comparison of ground-based data sets to classifications with AVHRR data. In:

Defries, R.; Hansen, M.; Janetos, A.; Loveland, T. R.; and Townshend, J. 2000. A Global 1km Data Set of Percent Tree Cover Data Derived from Remote Sensing. Global Change Biology, v. 6, p. 247-254.

DiMiceli, C.; DeFries, R.; Huang, C.; Hansen, M.; Sohlberg, R.; Townshend, J. R. G.; and Zhan, X. 2000. The 250 m global land cover change product from the Moderate Resolution Imaging Spectroradiometer of NASA's Earth Observing System. International Journal of Remote Sensing, 21(6 and 7), 1433– 1460.

Didan, K.; Ferreira, L. G., Gao.; X., Huete; A., Miura, T.; and Rodriguez, E.P. 2002. Overview of the radiometric and biophysical performance of the MODIS vegetation indices. Remote Sensing of Environment, 83: 195–212.

Douglas, I. 1999. Hydrological investigations of forest disturbance and land cover impacts in South-East Asia: a review. Philosophical Transactions of the Royal Society of London, Series B, 354, 1725-1738.

Ehrlich, D.; and Lambin, E. F. 1996a. The surface temperature-vegetation index space for land cover and land-cover change analysis. International Journal of Remote Sensing 17(3): 463–487.

Enclona, E. A.; Thenkabail, P. S..; Celis, D.; Diekmann, J. 2002. Wheat yield prediction from IKONOS data using after-harvest yields and field-sensor measured yields. International Journal of Remote Sensing. (in press. Accepted for publication).

Estes, J. E.; and Loveland, T.R. 1999. Toward the Use of Remote Sensing and Other Data to Delineate Functional Types in Terrestrial and Aquatic Systems. In Scaling of Trace Gas Fluxes between Terrestrial and Aquatic Ecosystems and the Atmosphere, L. Bouwman, editor. Amsterdam, Elsevier Science Press, p. 123-150.

Estes, J. E.; Loveland, T. R.; and Scepan, J. 1999. Introduction: Special Issue on Global Land Cover Mapping and Validation. Photogrammetric Engineering and Remote Sensing, v. 65, no. 9, p. 1011-1011.

Foody, G. M. 1999. The continuum of classification fuzziness in thematic mapping. Photogrammetric Engineering and Remote Sensing, 65, 443– 451.

Foody, G. M. 2000a. Mapping land cover from remotely sensed data with a softened feedforward neural network classification. Journal of Intelligent and Robotic Systems, 29, 433– 449.

Foody, G. M.(2001a). Monitoring the magnitude of lan-cover change around the southern limits of the Sahara. Photogrammetric Engineering and Remote Sensing, 67, 841-847.

Foody, G. M. 2002. Status of land cover classification accuracy assessment. Remote Sensing of Environment 80 (2002) 185–201 189.

Friedl, M. A.; and. Brodley, C. E. 1997. Decision tree classification of land cover from remotely sensed data. Remote Sensing of Environment 61:399–409. Malingreau, J. -P., C. J. Tucker and N. Laporte, 1989. AVHRR for monitoring global tropical deforestation. International Journal of Remote Sensing 10:855–867.

Friedl, M. A.; Brodley, C.; and Strahler, A. 1999. Maximizing land cover classification accuracies produced by decision trees at continental to global scales. IEEE Transactions on Geoscience and Remote Sensing, 37, 969–977.

Friedl, M. A.; Woodcock, C.; Gopal, S.; Muchoney, D.; Strahler, A. H.; and Barker-Schaaf, C. 2000. A note on procedures used for accuracy assessment in land cover maps derived from AVHRR data. International Journal of Remote Sensing, 21, 1073– 1077.

Friedl, M. A.; Gao, F.; Huete, A.; Hodges, J. C. F.; Reed, B. C.; Strahler, A. H., Schaaf, C.B.; Zhang, X. 2003. Monitoring vegetation phenology using MODIS. Remote Sensing of Environment, 84, 471–475.

Goff, T. E.; Holben, B. N.; and Tucker, C. J. 1984. Intensive forest clearing in Rondonia, Brazil, as detected by satellite remote sensing. Remote Sensing of Environment 15:255–261.

Gopal, S.; and Woodcock, C. 1994. Theory and methods for accuracy assessment of thematic maps using fuzzy sets. Photogrammetric Engineering and Remote Sensing, 60, 81–188.

Hall, D. K.; Riggs, G. A.: and Salomonson, V. V. 1995. Development of methods for mapping global snow cover using Moderate Resolution Imaging Spectroradiometer data. Remote Sensing of Environment, 54, 127-14

Hall, D. K.; Riggs, G. A.; Salomonson, V.V.; DiGirolamo, N.E.; and Bayr, K.J. 2002. MODIS snow-cover products. Remote Sensing of Environment 83, 181–194.

Han, X.; defrays, R.; Townshend, J. R. G.; DiMiceli, C.; Hansen, M.; Huang, C.; and Sohlberg, R. 2000. The 250 m global land cover change product from the Moderate Resolution Imaging Spectroradiometer of NASA's Earth Observing System. International Journal of Remote Sensing, 21(6 and 7), 1433– 1460.

Hansen, M. C.; Menz, G.; and Scepan, J. 1999. The DISCover validation image interpretation process. Photogrammetric Engineering and Remote Sensing, 65, 1075– 1081.

Hansen, M.; and Reed, B. C. 2000. A Comparison of the IGBP DISCover and University of Maryland Global Land Cover Products. International Journal of Remote Sensing, v. 21, no. 6/7, p. 1,365-1,374.

Huete, A. 1999. A light aircraft radiometric package for MODL and Quick Airborne Looks (MQUALS). Earth Observations, 11, 22-25. (NASA/GSFC).

Huete, A.; Didan, K.; Miura, T.; Rodriguez, E. P.; Gao, X.; and Ferreira, L. G. 2002. Overview of the radiometric and biophysical performance of the MODIS vegetation indices. Remote Sensing of Environment 83 (2002) 195-213.

Ichii, K.; Kawabata, A.; Yamaguchi, Y. 2002. Global correlation analysis for NDVI and climatic variables and NDVI trends: 1982–1990. int. j. remote sensing, 2002, vol. 23, no. 18, 3873–3878.

Jakubauskas, M. E.; Kastens, J. H., Legates, D. R. 2002. Crop identification using harmonic analysis of time-series AVHRR NDVI data. Computers and Electronics in Agriculture 37: 127-139.

Jackson, T. J.; Kustas, W. P.; Rango, A.; Ritchie, J. C.; and Schmugge, T .J. 2002. Remote sensing in hydrology. Advances in Water Resources, 25: 1367–1385

Janssen, L.L.F.; and F. J. M. Van Der Wel. 1994. Accracy Assessment of Satellite Derived Land Cover Data: A Review. Photogrammetic Engineering Remote Sensing, Vol. 60, No. 4, pp. 419-426.

Justice, C; Belward, A.; Morisette, J.; Lewis, P.; Privette, J.; and Baret, F. 2000. Developments in the 'validation' of satellite sensor products for the study of the land surface. International Journal of Remote Sensing, 21, 3383– 3390.

Justice, C.O.; Morisette, J. T.; Privette, J. L. 2002. A framework for the validation of MODIS Land products. Remote Sensing of Environment 83 (2002) 77–96.

Justice, C. O.; Townshend, J. R..G. 2002. Towards operational monitoring of terrestrial systems by moderate-resolution remote sensing. Remote Sensing of Environment 83 (2002) 351–359.

Kogan, F. N. 1995. Droughts of the late 1980s in the United States as derived from NOAA polar orbiting satellite data. Bull. Am. Meteorol. Soc. 76:655–668.

Kogan, F. 1997. Global drought watch from space. Bull. Am. Meteorol. Soc. 78:621–636.

Kogan, F. N. 2000. Global drought detection and impact assessment form space. In Drought: A Global Assessment (D. A. Wilhite, Ed.), Vol. 1, Hazard and Disaster Series, Routledge, London and New York, pp. 196–210.

Liang, S.; Fang, H.; Chen, H.; Shuey, C. J.; Walthall, C.; Daughtry, C.; Morisette, J.; Schaaf, J.; and Strahler, A. 2002. Validating MODIS land surface reflectance and albedo products: methods and preliminary results, Remote Sensing of Environment 83 (2002) 149–162.

Lambin, E. F.; and Strahler A. H. 1994. Indicators of land-cover change for changevector analysis in multitemporal space at coarse spatial scales. International Journal of Remote Sensing 15:2099–2119.

Lambin, E. F.; and D. Ehrlich 1996. The surface temperature-vegetation index space for land cover and land-cover change analysis. International Journal of Remote Sensing 17(3):463–487.

Landgrebe, D.; and Safavian, S. R. 1991.A survey of decision tree classifier methodology. IEEE Transactions on Systems, Man, and Cybernetics 21:660–674.

Lawrence, R. L.; and Ripple, W. J. 1998. Comparisons among vegetation indices and bandwise regression in a highly disturbed, heterogeneous landscape: Mount St. Helens, Washington. Remote Sensing of Environment, 64, 91–102.

Loveland, T. R.; Pierce, L. L.; and Running, S.W. 1994. A Vegetation Classification Logic Based on Remote Sensing for Use in Global Biogeochemical Models, Ambio, v. 23, n. 1, p. 77-81.

Loveland, T. R.; Zhu, Z.; Ohlen, D.O.; Brown, J. F.; Reed, B.C.; and Yang, L. 1999. An Analysis of the IGBP Global Land-Cover Characterization Process. Photogrammetric Engineering and Remote Sensing, v. 65, no. 9, p. 1021-1032.

Loveland, T. R.; Reed, B. C.; Brown, J. F.; Ohlen, D. O.; Zhu, Z.; Yang, L.; and Merchant, J. W. 2000. Development of a global land cover characteristics database and IGBP DISCover from 1km AVHRR data. International Journal of Remote Sensing, 21, 1303– 1330.

Malingreau, J. P.; C. J. Tucker and N. Laporte, 1989. AVHRR for monitoring global tropical deforestation. International Journal of Remote Sensing 10:855–867.

Maxwell, S. K., Hoffer, R. M.; Chapman, P. L. 2002. AVHRR channel selection for land cover classification. int. j. remote sensing, 23(23):5061–5073.

Merchant, J.W.; Yang, L; and Yang, W. 1994. Validation of continental scale accuracy of land cover data bases developed from AVHRR data. In: Proceedings of Pecora 12 land information from space-based systems (pp. 63-72). Bethesda:ASPRS.

Morisette, J. T.; Privette, J. L.; and Justice, C.O. 2002. A framework for the validation of MODIS Land products. Remote Sensing of Environment 83 (2002) 77–96.

Nelson, C.S.; and Cunningham, J.D. 2002. The national polar-orbiting operational environmental satellite system future U.S. environmental observing system. American Meteorological Society 82nd Annual Meeting Sixth Symposium on Integrated Observing Systems (January 15, 2002).

Nemani, R.; and Running, S.W. 1997. Land Cover Characterization Using Multitemporal Red, Near-IR, and Thermal-IR Data from NOAA/AVHRR. Ecological Applications, v. 7, no. 1, p. 79-90.

Nouvellon, Y.; Moran, M.S.; Seen, D.L.; Bryant, R.;Rambal, S.; Nia, W.; Begueb, A.; Chehbounid, A.; William, E.; Emmericha, Heilmana, P.; and Qi. J. 2001. Coupling a grassland ecosystem model with Landsat imagery for a 10-year simulation of carbon and water budgets. Remote Sensing of Environment. 78(1-2): 131-149.

Olson, J. S. 1994. Global Ecosystem Framework: Definitions. USGS EROS Data Center Internal Report, Sioux Falls, SD, USA 37 p.

Olson, J. S. 1994. Global Ecosystem Framework: Translation Strategy. USGS EROS Data Center Internal Report, 39 p.

Penner, J.E. 1994. Atmospheric chemistry and air quality. In: W.B. Meyer, B.L. Turner II (Eds.), Changes in land use and land cover: a global perspective (pp. 175-209). Cambridge: Cambridge University Press.

Safavian, S. R.; and D. Landgrebe. 1991, A survey of decision tree classifier methodology. IEEE Transactions on Systems, Man, and Cybernetics 21:660–674.

Scepan, J.; Menz, G.; and Hansen, M. C. 1999. The DISCover validation image interpretation process. Photogrammetric Engineering and Remote Sensing, 65, 1075– 1081.

Schmugge, T. J.; Kustas, W. P.; Ritchie, J. C.; Jackson, T. J.; Rango, A. 2002. Remote sensing in hydrology. Advances in Water Resources, 25: 1367–1385.

Singh, A. 1989. Digital change detection techniques using remotely-sensed data. International Journal of Remote Sensing, 10, 989-1003. Environment, 70, 16-28.

Skole, D. L. 1994. Data on global land-cover change: acquisition, assessment and analysis. In W. B. Meyer, and B. L. Turner II (Eds.), Changes in land use and land cover: a global perspective (pp. 437–471). Cambridge: Cambridge University Press.

Smith, R.B.; Foster, J.; Kouchoukas, N.; Gluhosky, P.A.; Young, R.; and De Pauw, E. 1999. Spatial analysis of Climate, Landscape, and Hydrology in the Middle East: Modeling and Remote Sensing. Yale University Press, New Haven, USA.

Strahler, A.; Townshend, J.; Muchoney, D.; Borak, J.; Friedl, M.; Gopal, S.; Hyman, A.; Moody, A.; and Lambin, E. 1999, MODIS L and Cover Product Algorithm Theoretical Basis Document (AT BD), V 4.1 (Boston: Boston University Center for Remote Sensing).

Townshend, J. R. G.; Justice, C. O. 2002. Towards operational monitoring of terrestrial systems by moderate-resolution remote sensing. Remote Sensing of Environment 83 (2002) 351–359.

Thenkabail, P.S.; and Nolte, C. 1995. Mapping and Characterising Inland Valley Agroeco-systems of West and Central Africa: A Methdology Integrating Remote Sensing, Global Positioning System, and Ground_truth Data in a Geographic Information Systems Framework. RCMD Monograph No. 16, International Institute of Tropical Agriculture, Ibadan, Nigeria. 62pp.

Thenkabail, P.S. 1999. Characterisation of the alternative to slash-and-burn benchmark research area representing the Congolese rainforests of Africa using near-real-time SPOT HRV data. International Journal of Remote Sensing, 20(5): 839-877.

Thenkabail, P.S. 2002. Optimal hyperspectral narrowbands for discriminating agricultural crops. Remote Sensing Reviews, 20(4): 257-291.

Thenkabail, P.S.; Smith, R.B.; and De Pauw, E. 2000a. Hyperspectral vegetation indices and their relationships with agricultural crop characteristics. Remote Sensing of Environment, 71: 158-182.

Thenkabail P.S.; Nolte, C.; and Lyon, J.G. 2000b. Remote sensing and GIS modeling for selection of benchmark research area in the inland valley agroecosystems of West and Central Africa. Photogrammetric Engineering and Remote Sensing, Africa Applications Special Issue, 66(6):755-768.

Thenkabail, P.S.; Smith, R.B.; and De Pauw, E. 2002. Evaluation of narrowband and broadband vegetation indices for determining optimal hyperspectral wavebands for agricultural crop characterization. Photogrammetric Engineering and Remote Sensing, 68(6): 607-621

Thenkabail, P.S.; Enclona, A.; Ashton, M.S.; Legg, C.; and Minko Jean De Dieu. 2003. Hyperion, IKONOS, ALI, and ETM+ sensors in the study of African rainforests. Remote Sensing of Environment. In review.

Tucker, C. J.; Holben, B. N.; and Goff, T. E. 1984. Intensive forest clearing in Rondonia, Brazil, as detected by satellite remote sensing. Remote Sensing of Environment 15:255–261.

Vogelmann, J.E.; Helder, D.; Morfitt, R.; Choate, M.J.; Merchant, J.W.; and Bulley, H. 2001.

Effects of Landsat 5 Thematic Mapper and Landsat 7 Enhanced Thematic Mapper Plus radiometric and geometric calibrations and corrections on landscape characterization. Remote Sensing of Environment. 78(1-2):55-70.

Waller, E.; and Zhu, Z. 1999. Estimating Subpixel Forest Cover With 1-km Satellite Data. In Proceedings of the Pecora 14 Conference, Demonstrating the Value of Satellite Imagery, Denver, Colorado, December, 1999, p. 419-426 (CR-ROM).

Wen, C.G.; and Tateishi, R. 2001. 30-second degree grid land cover classi. cation of Asia. int. j. remote sensing, 2001, vol. 22, no. 18, 3845–3854.

Woodcock, C.E.; and Gopal, S. 2000. Fuzzy set theory and thematic maps: accuracy assessment and area estimation. International Journal of Geogrphical Information Science, 14, 153-172.

Zhang, X.; Friedl, M. A.; Schaaf, C. B.; Strahler, A. H.; Hodges, J. C. F.; Gao, F.; Reed, B.C.; and Huete, A. 2003. Monitoring vegetation phenology using MODIS. Remote Sensing of Environment, 84, 471–475.